The role of putative prion-like protein, CPEB2, in translation and long-term memory

By

Blake Ebner

Submitted to the graduate degree program in Molecular and Integrative Physiology and the Graduate Faculty of the University of Kansas in partial fulfillment of the requirements for the degree of Doctor of Philosophy

_____
Co-Chair/Advisor: Dr. Kausik Si

_____
Co-Chair: Dr. John Wood

_____
Dr. Russel Swerdlow

_____
Dr. Hiroshi Nishimune

_____
Dr. Timothy Fields

Date Defended: May 11, 2018

The Dissertation Committee for Blake Ebner certifies that this is the approved version of the following dissertation:

The role of putative prion-like protein, CPEB2, in translation and long-term memory

_____

Co-Chair: Dr. Kausik Si

_____

Co-Chair: Dr. John Wood

Date Approved: May 11, 2018

Abstract

CPEB proteins are a family of four mRNA-binding protein paralogs that regulate the synthesis of proteins required for a number of important cellular process. CPEB proteins act by binding to the CPE elements present on the 3'UTR of target mRNAs. One process regulated by CPEB is synaptic plasticity and long-term memory. A feature of the some CPEB members is their sequence similarity to a unique class of proteins, known as prion-like proteins that use distinct conformation states to regulate their function. It has been hypothesized that mammalian CPEB proteins employ a similar mechanism to induce the stable changes in synaptic activity required for memory maintenance. Previous studies implicated the CPEB family member, CPEB2, in synaptic plasticity and long-term memory. However, the function of the CPEB2 prion-like sequence is still unknown and this thesis evaluates the function of CPEB2 prion-like sequence in translation regulation and memory. The initial experiments demonstrate CPEB2 forms SDS-resistant oligomers in neurons. We generated an isoform specific CPEB2 knockout mouse that removed exon 1 and the prion-like sequence. We tested the ability of this knockout mice to form oligomeric structures, regulate translation, and form long-lasting memory. The results show that the CPEB2 isoform containing the prion-like sequence regulates expression of key memory molecules, and is required for synaptic plasticity and memory.

Acknowledgments

First, I want to give a whole hearted thank you to my advisor, Dr. Kausik Si for letting me train in an outstanding laboratory and for giving me exceptional mentoring. Thank you, Dr. Si.

Second, I want to thank my committee members, Dr. Hiroshi Nishimune, Dr. Timothy Fields, Dr. Russel Swerdlow, Dr. John Wood, and Dr. Jerry Workman for the excellent guidance and feedback they gave me all through my graduate training. Thank you all.

Third, I want to thank all the colleagues who were crucial to my thesis project. In particular, I want to thank our collaborators, Dr. Ana Covelo Fernndez and Dr. Alfonso Araque for studying the electrophysiology in our mouse model. A special thank you to Mary Huff for her expert assistance in studying our mouse model in CFC and OPT and to Mathew Christensen for all his expert cloning. Thank you both.

Fourth, I want to thank my colleagues of the Si lab for the stimulating and dynamic environment that was always a pleasure to be a part of. Thank you all.

And last but not least, I want to thank my wise, beautiful and smart wife for her unwavering support, encouragement and love. She, along with my family, have fortified and sustained me with their resolute and persistent loving support. Thank you dear wife, and thank you dear family.

Table of Contents

List of Figures

Chapter 1: General Introduction

Introduction

Memory is the ability of organisms to retain and use acquired information. A fundamental goal of neuroscience is to understand the mechanisms underlying memory. In 1885, Hermann Ebbinghauss proposed that there are two different types of memories, short-term memories (STM) and long-term memories (LTM) (Ebbinghaus, 1885). Since this initial hypothesis, we have learned that these two distinct types of memories involve a complex cellular machinery responsible for interpreting environmental and internal stimuli and weighing the necessity of storing and maintaining this information. Central to our understanding has been establishing that neurons and their connections to other neurons, synapses, are the cellular location where memories are stored. Like memory, the strength of synapses can be increased or decreased, referred to as synaptic plasticity. Decades of work have established that synaptic plasticity is fundamental to memory, however, many unanswered questions still remain. One highly active area of research is how synaptic plasticity can encode different types of memory, such as short and long-term memory. The focus of this thesis, are the mechanisms required for memory consolidation, that is, the transition from short term to long term memory.

Synaptic Plasticity

Neurons communicate with each-other through synapses, structure in which the axon terminal of a presynaptic neuron connects to the dendritic of a postsynaptic neuron. The most common type of synapse is a chemical synapse. Chemical synapses are composed of a

presynaptic axon terminal, synaptic cleft, and a post-synaptic spine. The presynaptic axon terminal, or synaptic bouton, contains neurotransmitters enclosed in synaptic vesicles. Communication across the synapses occurs through the process of synaptic transmission. There are two major classes of synaptic transmission, excitatory and inhibitory. This thesis focuses on excitatory transmission. Excitatory synaptic transmission occurs when the presynaptic neuron is activated and upon reaching its threshold potential generates an action potential, a self-sustaining wave of electrochemical membrane depolarization. The action potential travels along the axon of the presynaptic cell and invades the axon terminal at the synapse. With the depolarization of the invading action potential, the synaptic vesicles fuse to presynaptic membrane and release their neurotransmitters into the synaptic cleft. Once released into the synaptic cleft, the neurotransmitters bind to the membrane receptors on the postsynaptic spine or nearby dendrites. In excitatory chemical transmission, the neurotransmitters bind to ligand-gated ion channels resulting in opening of the channels and an influx of ions into the postsynaptic cell. The ions depolarize the local transmembrane potential and result in excitatory postsynaptic potential (EPSP). With a sufficiently large or with successive EPSPs, the probability increases that a post-synaptic neuron fires an action potential

Synaptic strength is not fixed. Synaptic strength can be modulated through a mechanism known as synaptic plasticity. Synaptic plasticity is a widely studied phenomenon and is considered to be one of the most fundamental mechanisms underlying both learning and memory formation. Synaptic plasticity can modulate the strength of synapses for both short (short-term plasticity) or long periods of time (long-term plasticity). For long-term plasticity, there are two distinct types of synaptic plasticity, synaptic potentiation (LTP) and long-term depression (LTD) (Mayford, Siegelbaum, & Kandel, 2012). Each results in long-lasting changes at the synapse and

alters its response to subsequent stimuli. Following LTP, an excitatory synapse responds with greater activation to the same presynaptic input. LTP has two phases. The first, early phase LTP (E-LTP), is induced by depolarization of the post-synaptic membrane. The depolarization results in the unblocking of the N-methyl D-aspartate receptor (NMDA) and allows Ca^{2+} entry through the NMDA channel (Kumar, 2011). The influx of intracellular Ca^{2+} activates a number of kinases that induce local, short-term changes in the synapse primarily through the activation of Ca^{2+}/calmodulin dependent protein kinase (CaMKII), protein kinase C (PKC), and tyrosine kinase (Kandel, Dudai, & Mayford, 2014). When activated during E-LTP, CAMKII and PKC phosphorylate AMPA receptors (α-amino-3-hydroxy-5-methyl-4-isoxazolepropionic acid) that increase the likelihood of AMPA receptors opening and/or initiate the insertion of additional AMPA receptors into the synaptic membrane (Boehm, Ehrlich, Hsieh, & Malinow, 2006; Lisman, Malenka, Nicoll, & Malinow, 1997). Both of these changes result in a larger post-synaptic response to the same synaptic input. AMPA receptors are one of the main excitatory glutamatergic receptors, and when their activity is enhanced via CAMKII or PKC phosphorylation or increased in number, the synapse will generate a larger post-synaptic response.

The second phase, late LTP (L-LTP), is initiated by persistent activation of post-synaptic kinases initially activated during E-LTP (Kumar, 2011). For the transition from early to late LTP to occur, the levels of synaptic cAMP must increase and cAMP-dependent protein kinase A (PKA) must be activated. Once activated, PKA phosphorylates p42 Mitogen-Activated Protein Kinase (MAPK). Both PKA and MAPK translocate to the cell nucleus where they either directly (PKA) or indirectly (MAPK) activate the transcription factor cAMP response element-binding protein (CREB) (Bacskai et al., 1993; Martin, Michael, et al., 1997). CREB phosphorylation

induces the transcription a subset of genes required for formation long-term potentiation and memory. Of the large number of genes CREB regulates, three are critical for stabilizing LTP: c-fos, activity regulated cytoskeleton-associated protein (Arc), and brain-derived neurotrophic factor (BDNF) (West, Griffith, & Greenberg, 2002). Activation of these genes results in the synthesis of synaptic components required for strengthening synapses, promoting synaptic growth, and inducing the formation of new synapses (Alberini & Kandel, 2014; Miyamoto, 2006).

Local Protein Synthesis

Short-term plasticity depends on rapid but easily reversible post-translational modifications in the synapse. However, long-term plasticity requires both transcription and translation. Identification that CREB dependent-transcription regulated long-term plasticity correlated with previous findings that demonstrated protein synthesis is required for the formation of L-LTP (U. Frey, Krug, Reymann, & Matthies, 1988; Krug, Lossner, & Ott, 1984). For example, in rat brain hippocampal slices, adding the protein synthesis inhibitor, anisomycin, throughout LTP induction blocks LTP formation (U. Frey et al., 1988). Further experiments explored which phases of LTP are dependent on transcription and translation by adding protein synthesis or transcription inhibitors during LTP. From these experiments, it emerged that protein synthesis is required for E-LTP and L-LTP, but transcription is only necessary for L-LTP. These studies established two phases of plasticity: an early phase dependent on protein synthesis and a late phase dependent on protein synthesis and transcription. Memory also requires protein

synthesis, as memory formation can be blocked by injection of protein synthesis inhibitors are injected into mouse hippocampus and temporal cortex (Flexner, Flexner, & Stellar, 1963).

How does protein synthesis regulate the formation of long-term potentiation and memory? An answer to this question came about from experiments demonstrating that L-LTP could be elicited by local application of brain-derived neurotrophic factor (BDNF) or neurotropin-3 (NT3), protein synthesis-dependent neurotropic growth factors (Kang & Schuman, 1996). These observations indicate that local L-LTP can be experimentally induced at the dendrites and/or synapse with these compounds. The LTP produced by BDNF and NT3 was similar to that induced by cAMP analogs, the established transcriptional CREB pathway, implying similar mechanisms of actions. However, additional experiments determined the precise location of the protein synthesis critical for L-LTP induction. Kang and Schuman demonstrated that LTP can be induced in synapses and dendrites physically isolated from the soma (Kang & Schuman, 1996). This LTP still requires protein synthesis. Martin et al used a system of a sensory neuron with a bifurcated axon projecting to two motor neurons that were physically separated. Local LTP is induced in a single branch by application of five serotonin pulses. If protein synthesis inhibitors are applied only to the induced branch, L-LTP formation is blocked (Martin, Casadio, et al., 1997). Both experiments support the concept that the synthesis of macromolecules required for L-LTP occurs in either the activated synapse or supporting dendrite. Because both ribosomes and mRNA are present in dendrites and synapses (Fass & Steward, 1983; Steward & Fass, 1983; Steward & Levy, 1982), this cellular machinery is likely responsible for regulating synaptic plasticity and long-term memory.

Synapse Specific Activation and "Synaptic Tags"

Induction of L-LTP requires persistent post-synaptic depolarization, activation of several kinases, a transcriptional cascade in the nucleus, and local protein synthesis. Nevertheless, it is well known that L-LTP occurs specifically at the originally activated synapse. This led to the hypothesis that neurons have a mechanism of marking or recognizing the synapse that requires the local protein synthesis. This concept of a "synaptic tag" was first tested by Frey and Morris using rat hippocampal slices (U. Frey & Morris, 1997). These investigators observed that if LTP is induced in one set of synapses, a subthreshold stimulus provided within a certain time window, that by itself would not produce LTP, can induce LTP in a separate set of synapses in the same dendritic compartment. LTP formation at either set of synapses can be inhibited if protein synthesis inhibitors are added before either stimulation. However, a novel finding was discovered when protein synthesis inhibitors were added after a 35-minute delay to same set of excitatory synapse on pyramidal neurons. The delayed addition of protein synthesis inhibitors did not prevent the induction of L-LTP to the first set of synapses. With protein synthesis completely inhibited, a separate synapse in the same cell was activated with a reduced stimulus that normally would induce only E-LTP. Intriguingly, in the absence of protein synthesis, the synapse subjected to reduced stimulation also established L-LTP. This suggests that the proteins synthesized in response to the first input, allows formation of L-LTP by the second input (S. Frey, Morris, & Petrides, 1997; Kelleher, Govindarajan, & Tonegawa, 2004). This supports the hypothesis that the weak stimulation generates a local "synaptic tag" capable of recruiting the needed synaptic plasticity proteins to induce L-LTP at the second synapse.

The synaptic tag phenomenon was also investigated in *Aplysia,* using a neuron with a bifurcating axon and two synapses. In this system, applying five puffs of serotonin to one of the synapses induces L-LTP and a single puff induces E-LTP (Martin, Casadio, et al., 1997). When five puffs of serotonin are applied to a synapse on one branch and one puff to the synapse on the separate branch of the same neurons, L-LTP is induced at both synapses. As observed in slice cultured hippocampal neurons, activation of local synaptic "tags" are sufficient to induce L-LTP. However, in the *Aplysia* experiment the synapses are separated by approximately 500 μm on different axonal branches and suggests the mRNAs produced by transcription are transported to every synapse in a neuron where the mRNAs remain dormant until a "synaptic tag" is activated.

The process of synaptic tagging is temporally complex. Casadio and Kandel established that marking the synapse is a two-phase process, similar to LTP, by repeating the branching axon experiments in *Aplysia*, but using an extended timeline. In the presence of protein synthesis inhibitors, L-LTP can be established at 3-4 hours post-induction at the second synapse, however L-LTP cannot maintained at 72 hours (Casadio et al., 1999). This suggests that during the first "induction" the synapse is tagged and allows plastic changes to occur. This early, protein-synthesis independent phase is likely due to the recruitment of pre-made proteins to the synapse. The later phase involves a second protein synthesis-dependent tag required for the maintenance of L-LTP. Therefore, synaptic tag function involves two steps for the induction and maintenance of LTP: 1) the tag resides in the synapse and synaptic activation captures essential pre-made synaptic plasticity proteins, and 2) the tag resides in the synapse and synaptic activation regulates the translation of locally retained mRNAs required for the maintenance of plasticity. To determine the nature of the protein synthesis-dependent tags, researchers worked to identify candidate proteins that regulate protein synthesis outside the nucleus.

Cytoplasmic Polyadenylation Binding Proteins

Local protein synthesis-dependent LTP and protein synthesis-dependent "synaptic tags" require mRNA translation in neuronal dendrites and synapses. This requires two important components: 1) local collections of mRNA, and 2) translation of specific dormant mRNAs at the synapse. Before addressing synaptic translation, it is useful to review how mRNA translation is regulated inside the cell. At the global level, ribosomes or mRNA binding protein can promote or inhibit translation. In addition to protein, non-coding RNA , such as microRNA can also regulates translation. The mechanisms include inducing cleavage of mRNA, destabilizing mRNA, or directly interfering with mRNA translation.

Increasing protein translation can also involve altering the mRNA level, by enhancing or reducing the stability of a transcript. The mRNA level can be regulated in the nucleus as a part of quality control. This occurs predominantly inside the nucleus, where generated mRNAs undergo splicing, 5' cap formation, and polyadenylation. RNA splicing involves a series of reactions to remove the intronic sequences to generate a mature messenger RNA from a nascent precursor messenger RNA. Subsequently, the 5' capping of the mature mRNA adds a 7-methlguanylate cap to the 5' end. The key functions of the 5' cap is to promote the nuclear export of the mRNA, protect the mRNA inside the cytoplasm, and promote translation by binding to eukaryotic translation initiation factor 4F complex, which recruits the 40S ribosome to the transcript. In the cytoplasm, where translation takes place, mRNA stability is control by the 3' and 5' untranslated regions.

A key mechanism in mRNA transport, stability and translation is polyadenylation that modifies the 3' tail of mRNA by adding multiple adenosine monophosphates. The poly(A) tail is a critical regulator of nuclear export, mRNA stability, and translation (Sachs, Sarnow, & Hentze, 1997). The poly(A) tail consist of A repeats that can be up to 200 nucleotides long and are part of the 3' UTR regulation of protein translation. Intriguingly, polyadenylation could be a mechanism the cell uses to alter the stability and translational activity of particular mRNAs in a stimulus-dependent manner (Richter, 1999; Salles, Lieberfarb, Wreden, Gergen, & Strickland, 1994). While generalized polyadenylation occurs inside the nucleus and is critical for nuclear export and stability, specific transcripts contain an additional sequence in the 3' UTR that allows for further regulation. This is a U-rich sequence with the consensus structure of UUUUUUAU, known as cytoplasmic polyadenylation element (CPE), and was first identified in the *Xenopus* oocyte (McGrew, Dworkin-Rastl, Dworkin, & Richter, 1989).

The function of CPEs was first described in detail by McGrew et al., who removed the CPE from 3' UTR of the gene G10 in *Xenopus*, and found that, unlike wild-type, the mutant transcript was not polyadenylated or expressed. (McGrew et al., 1989). This work established that CPEs are critical for gene expression by inducing cytoplasmic polyadenylation and thereby promoting translation. Later studies demonstrated how CPEs are used to bi-directionally control translation of cytoplasmic dormant mRNAs during oocytes maturation in a hormone-stimulus dependent manner. CPE sequence is bound by the protein, cytoplasmic polyadenylation element binding protein (CPEB1) and CPSF (cleavage and polyadenylation specificity factor), and together they transport transcripts to the cytoplasm (Lin, Evans, Shen, Xing, & Richter, 2010). Inside the cytoplasm, CPEB1 bound to CPE forms a complex with CPSF, cytoplasmic poly(A) polymerase Gld-2, a scaffolding protein Symplekin, and deadenylating enzyme poly(A)

ribonuclease (PARN) (Barnard, Ryan, Manley, & Richter, 2004; J. H. Kim & Richter, 2006; Villalba, Coll, & Gebauer, 2011). This RNA-binding complex can either repress or activate translation dependent upon phosphorylation of CPEB1. In the complex's basal and repressed state, CPEB1 is dephosphorylated and PARN binds to CPEB1 and continually deadenylates and silences the transcript. mRNAs bound to unphosphorylated CPEB1 bind Maskin, which interacts with eukaryotic factor 4E (eIF4E) and inhibits formation of the translation initiation complex, also silencing the transcript (Minshall, Reiter, Weil, & Standart, 2007; Stebbins-Boaz, Cao, de Moor, Mendez, & Richter, 1999). As the oocyte begins to age, progesterone is released and induces CPEB1 phosphorylation. This results in 1) increasing interaction between CPEB1 and CPSF, 2) dissociating PARN from the RNA-binding complex, and 3) reducing the affinity between CPEB1 and Maskin by removing its inhibitory constraint (Cao & Richter, 2002; J. H. Kim & Richter, 2006; Mendez, Murthy, Ryan, Manley, & Richter, 2000; Stebbins-Boaz et al., 1999). As a result, the activated complex enables the polyadenylation of the mRNA by Gld-2 (Barnard et al., 2004). These findings established a regulatory mechanism inside the cell in which CPEB1's activation state regulated the stability and translation of CPE genes. These findings also provided a potential means by which expression of mRNAs in other tissues could be controlled, including in synapses.

CPEB in the Nervous System Regulates Synaptic Growth and Synaptic Plasticity:

Although CPEB1 was discovered in oocytes, an initial study showed that in the mouse brain, CPEB1 is expressed in synapses and binds to and regulates mRNAs containing CPEs in their 3' UTR (L. Wu et al., 1998). As a consequence of CPEB1's unique role as an activator and

repressor of cytoplasmic translation and the requirement of neurons for local mRNA translation, it was hypothesized that CPEB1 may regulate synaptic protein translation. One of the mRNA transcripts regulated by CPEB1 is Ca^{2+} /calmodulin-dependent protein kinase II (CaMKII), a kinase necessary for synaptic plasticity and the formation of long-term memory (Giese, Fedorov, Filipkowski, & Silva, 1998). When synapses are stimulated with glutamate, Aurora kinase phosphorylates CPEB1 and induces polyadenylation of CaMKII (Huang, Jung, Sarkissian, & Richter, 2002). This work and others demonstrated CPEB1-mediated polyadenylation controls translation in an activity-dependent manner in mammals (Drisaldi et al., 2015; Huang, Kan, Lin, & Richter, 2006; Lai et al., 2016; Lu, Yeh, & Huang, 2017; Turimella et al., 2015). The CPEB-like protein in *Apylsia*, apCPEB, can be induced by synaptic activity (Si, Giustetto, et al., 2003). Similar to CPEB1 in mammals, activated apCPEB polyadenylates CPE containing mRNAs at the synapse. In *Drosophila Melanogaster*, the CPEB orthologue, Orb2, binds to a number of targets required for growth and synapse formation including: 1) neuroligin, a postsynaptic adhesion component, 2) synaptobrevin, a protein required for synaptic vesicle exocytosis, and 3) tequila, a serine protease that reorganizes synapses (Mastushita-Sakai, White-Grindley, Samuelson, Seidel, & Si, 2010). Using a cell-based translational assay, it was shown that these three targets are translationally regulated by Orb2, further establishing that synaptic growth is regulated by CPEB.

Therefore, CPEB1 is activated in a stimulus dependent-manner, it regulates translation at synapses, and a subset of CPEB1 targets are related to synaptic plasticity. This raised the possibility that CPEB is essential for synaptic plasticity. To address this question, Si et al., examined in detail the role of apCPEB in *Aplysia*, using the bifurcated axon model. When serotonin puffs are applied selectively to synapses on an isolated branch, apCPEB becomes

activated and F-actin is polyadenylated (Si, Giustetto, et al., 2003). Interestingly, when transcriptional or translational inhibitors are added during the stimulation, apCPEB activation is independent of transcription, but requires protein synthesis. To show that activation of apCPEB is necessary for L-LTP, apCPEB expression was inhibited by applying an antisense oligonucleotide to apCPEB. When apCPEB is inhibited, stimulation can induce E-LTP but not stable L-LTP. To understand when apCPEB is critical for synaptic plasticity, apCPEB was inhibited during the two stages of L-LTP; 1) the stabilization stage consisting of the first 72 hours after LTP induction requiring local synaptic protein synthesis, and 2) the maintenance stage consisting of the post 72 hours requiring local synaptic growth (Miniaci et al., 2008). Inhibiting apCPEB after 24 hours or 72 hours blocked the stabilization of L-LTP and synaptic growth. Therefore, CPEB translational regulation appears critical for both the stabilization and maintaining the growth of local synapses.

CPEB in Mammals and its Role in Long-Term Memory

Most studies detailing CPEB function use model organisms and systems amendable to studying individual synapses. However, given the hypothesized fundamental role for CPEB in synaptic plasticity, the next question was whether or not CPEB is critical for the formation of long-term memory? To address this, question researchers turned to murine models. Four different CPEB family members, CPEB 1-4, have been identified in mammals. Based on amino acid sequence similarity, the four members are divided into two groups: CPEB1 and CPEB2-4 (Theis, Si, & Kandel, 2003). Each CPEB has an N-terminal regulatory domain followed by two C-terminal RNA recognition motifs and a zinc finger (ZnF). CPEB1 has been the species of the

most intensive study as detailed above. Relatively less is known about CPEB2-4. However, due to CPEB1 and apCPEB role in synaptic plasticity, recent efforts have focused on understanding the function of the other family members. The goal of these mammalian studies is to determine if CPEB1-4 are critical for long-term memory. The main approach has been to generate knockout mice of each family member and assess synaptic plasticity and long-term memory formation. Detailed below is what we have learned from these studies by gene.

CPEB1:

The first gene to be removed from the mouse genome was CPEB1. Surprisingly, these mice exhibit only a modest reduction in some forms of LTP (Alarcon et al., 2004). CPEB1 knockout (CPEB1 KO) mice form normal long-term memories, but do show impairments in memory extinction (Berger-Sweeney, Zearfoss, & Richter, 2006). These results were somewhat paradoxical to the other forms of mammalian CPEB and *Drosophila* CPEB, in which manipulation of results in more dramatic deficits in LTP and long-term memory (discussed below). Interestingly, CPEB1 likely regulates global changes inside the neurons. In CPEB1 KO mice, growth hormone levels are dramatically decreased in the nervous system (Zearfoss, Alarcon, Trifilieff, Kandel, & Richter, 2008). Growth hormone induces LTP in hippocampal slices (Mahmoud & Grover, 2006). While growth hormone is not a CPEB1 target, a significant transcription factor c-jun, is a CPEB1 target and c-jun regulates growth hormone expression. These observations demonstrate that CPEB1 has multiple actions that include transcription changes and long-term synaptic changes. Thus, it has been suggested that CPEB1 regulate synaptic plasticity differently than the other family members.

CPEB2:

CPEB2 was discovered in mouse germ cells. It shares the most homology with CPEB3 and CPEB4 (Kurihara et al., 2003). Expressed in the brain (Hagele, Kuhn, Boning, & Katschinski, 2009; Theis et al., 2003), CPEB2 interacts with previously identified mRNAs containing CPE elements including B-catenin and CAMKII. This suggests CPEB2 functions as a regulator of translation (Turimella et al., 2015). Another study generated a CPEB2 Cre recombinase global knockout (CPEB2 KO) by flanking exons 3-5 with LoxP sites. Of the entire CPEB family, only CPEB2 KO mice die shortly after birth when CPEB2 is removed from all tissues (Lai et al., 2016). At the prenatal stage, CPEB2 KO mice have hyper-activation of parasympathetic cholinergic neurons that results in fatal bronchoconstriction. These mice also reported to have increased levels of choline acetyltransferase (ChAT), the enzyme responsible for the synthesis of neurotransmitter acetycholine. The increase in ChAT correlates with the hyper-activation of cholinergic neurons. Further, it was demonstrated CPEB2 binds to and represses the translation of ChAT in a Neuro-2a neuroblastoma cell line. This result was supported by an RNA immunoprecipitation experiment that revealed ChAT mRNA binds to CPEB2 protein (Lai et al., 2016). Together these findings suggest CPEB2 acts as a translational repressor in the parasympathetic nervous system. However, because the global knockout of CPEB2 is lethal in the perinatal stage, it is not possible to assess synaptic plasticity or behavior in these animals.

To address the role of CPEB2 in plasticity and memory, an alternative approach restricted the excision of CPEB2 by expressing Cre recombinase only in excitatory neurons of the cerebral cortex, amygdala, and hippocampus (Lu et al., 2017). The restricted excision CPEB2 conditional knockout (CPEB2 cKO) results in normal development but impaired long-term potentiation and

disrupted long-term memory. The CPEB2 cKO also exhibit a significant increase in the number of immature spines and a decrease in surface expression of AMPARs. The authors associated the decrease in AMPARs with an increased expression of the GRIP-associated protein 1 (GRASP1). GRASP1 regulates the endosomal recycling of AMPARs receptors through its association with glutamate receptor-interacting protein 1 (GRIP1) by coupling the GRASP1-GRIP1 complex to endosomes (Hoogenraad et al., 2010). CPEB2 was shown to regulate the translation of GRASP1, using a firefly luciferase reporter assay in which firefly 3'UTR was replaced with the 3'UTR of GRASP1. Firefly luciferase levels increase when expressed in the presence of CPEB2 relative to GFP (Lu et al., 2017). This study established CPEB2 as a translation regulator required for long-term plasticity and long-term memory.

CPEB3:

CPEB3 is second most studied CPEB family member behind CPEB1. Early studies demonstrated that CPEB3 expression is upregulated in both the mouse hippocampus and cultured hippocampal neurons after stimulation, establishing CPEB3 as a strong candidate for the activity-dependent synaptic tag (Fioriti et al., 2015; Theis et al., 2003). Likewise, CPEB3 shares a number of sequence similarities with apCPEB, as discussed below. Two approaches have been used to remove CPEB3 from the mouse genome. The first approach generated a global knockout. Surprisingly, these mice displayed normal synaptic plasticity and actually performed better in memory-related tasks (Chao et al., 2013). The second, more precise approach, selectively removed CPEB3 in the forebrain (the cortex, amygdala, and hippocampus). With this approach, a more dramatic phenotype was observed. Using this CPEB3 cKO model, researchers found impaired memory formation using three distinct long-term memory paradigms.

Interestingly, reducing CPEB3 expression during long-memory consolidation (after the long-term memory was established) resulted in the animals being unable to maintain a previously formed memory (Fioriti et al., 2015). Late phase long-term potentiation was also reduced in upon CPEB3 conditional knockout. Both of these deficits could be rescued be providing exogenous CPEB3 via transducing viruses encoding CPEB3. The molecular circuit responsible for these deficits was explored, focusing on the expression of two previous identified CPEB3 targets, AMPA receptors subunits GluA1 and GluA2 (Huang et al., 2006; Pavlopoulos et al., 2011). The protein levels of both GluA1 and GluA2 were significantly increased in the hippocampus of the CPEB3 conditional knockout. In accord with CPEB3 regulating translation and not the transcription of its targets, the mRNA levels of GluA1 and GluA2 were not significantly different from wild-type animals. Together these results demonstrate that CPEB3 acts as a translational regulator and is required for LTP and for maintenance of memory.

CPEB4:

The final member of the mammalian CPEB family, CPEB4, is also expressed in neurons (Theis et al., 2003). Similar to CPEB1,CPEB4 induces polyadenylation and translation in Xenopus oocytes (Novoa, Gallego, Ferreira, & Mendez, 2010). However, no overt phenotype is evident with complete removal of the CPEB4 gene in mice (Tsai et al., 2013). Also, CPEB4 KO mice have normal synaptic plasticity and memory. These findings suggest CPEB4 is the only CPEB family member not required for plasticity and learning. However, the phenotype for conditional removal of CPEB4 is unknown.

CPEB is a Synaptic Mark and has Prion-Like Properties

Studies in mice, *Drosophila*, and *Aplysia* demonstrate CPEB activity is induced by neuronal activity, is necessary for L-LTP, induces synaptic growth, and is dependent on translation. These are the features of a synaptic tag required for L-LTP maintenance, leading to the hypothesis that members of the CPEB protein family act in this role. To explore this possibility, Si and Kandel found that when a single puff of serotonin is applied to a synapse, apCPEB expression increases three to four-fold, but the increase is restricted to stimulated synapse (Si, Giustetto, et al., 2003). This activity-dependent, local increase, which results in the maintenance of L-LTP, implicates that apCPEB functions as a synaptic tag. apCPEB maintains L-LTP by inducing the translational proteins required for long lasting synaptic potentiation.

Interestingly, apCPEB contains domains that are highly similar with group of prion proteins in yeast, known as prion-like domains. Originally discovered by Stanley Prusiner, the prion protein (PrP) is unique as both the toxic agent and the infectious particle causing a group of mammalian neurodegenerative disorders, the transmissible spongiform encephalopathies (TSE) (Prusiner, 1982). Unlike other infectious diseases in which a virus or bacterium produces toxic proteins or disrupts normal physiological processes, neurodegeneration in TSEs occurs when the normal cellular prion protein (PrP^{C}) undergoes a structural conformation change into scrapie prion protein (PrP^{Sc}) (Prusiner, 1998). While the pathogenic mechanism is still being explored, it is clear that the conformational shift to PrP^{Sc} imparts a highly-stable β-sheet rich structure to the protein that enables the formation of higher-order oligomers (Pan et al., 1993). PrP^{Sc} oligomers are protease resistant variants that generate insoluble amyloid aggregates responsible for disease (Oesch et al., 1985; Telling et al., 1996). Of particular relevance for this thesis, once

established, PrP^{Sc} acts as a seed to convert non-pathogenic monomers of PrP^{C} to PrP^{Sc} (Prusiner, 1998). Using this process of continual self-renewal, PrP^{Sc} is maintained inside the cell. Originally considered only a pathogenic mechanism, yeast proteins were found to have prion-like properties. Yeast prion proteins share with PrP the capability to form distinct conformations. The prion state conformation converts the non-prion state to the prion state (Derkatch, Chernoff, Kushnirov, Inge-Vechtomov, & Liebman, 1996). Yeast use this conformational switching to rapidly alter protein function in response to environmental stress (Derkatch, Bradley, Zhou, Chernoff, & Liebman, 1997). Yeast prions are passed from cytoplasm of the mother to the daughter cells to generate stable phenotypic changes in their offspring (Ganusova et al., 2006; Mathur, Taneja, Sun, & Liebman, 2010).

Si and Kandel were intrigued why a synaptic protein responsible for regulating a long-lasting cellular process had a prion-like domain enriched with polar glutamine and asparagine residues. This led to the hypothesis that apCPEB uses a prion-like conformation as a mechanism to establish and maintain a synaptic tag (Si, Lindquist, & Kandel, 2003). Using immunofluorescence and electron microscopy, it was shown that apCPEB forms oligomeric structures in sensory neurons. Since thioflavin T(ThT) binds to β-sheet portions of amyloid proteins, a ThT binding assay can be used to determine the oligomeric composition of apCPEB (Si, Choi, White-Grindley, Majumdar, & Kandel, 2010). After complete denaturing and refolding the protein, apCPEB strongly binds ThT but only when oligomeric structures begin to appear. These and other data suggest apCPEB has amyloid-like features (Raveendra et al., 2013). Furthermore, apCPEB oligomers share other properties of functional prion-like proteins such as: 1) oligomers are assemblies of apCPEB monomers, 2) oligomers are self-sustaining by

recruiting additional apCPEB monomers to the assembly, and 3) apCPEB oligomers are formed in response to extracellular stimuli, in this instance serotonin.

The role of apCPEB oligomers in synaptic plasticity still remained to be determined. In particular, can neurons still form LTP? To answer this question, the oligomer apCPEB was removed by injecting an antibody that selectively recognized the oligomer. Neurons lacking oligomeric apCPEB, form but cannot maintain LTP (Si et al., 2010), implying that the function of this higher-order structure is to sustain synaptic potentiation.

Prion-Like Proteins in Memory

The findings that apCPEB has prion-like properties and undergoes oligomerization with neuronal stimulation raises the intriguing possibility that cells utilize these self-sustaining, higher order assemblies to stabilize and maintain synaptic potentiation. Depending on the context, CPEB-proteins can act as translational repressor or activator. These observations provide a possible model in which activity-dependent stimulation converts CPEB proteins from a translational repressor in the monomeric state to a self-sustaining prion-like protein capable of maintaining LTP, thus preserving long-term memory. Alternatively, activity-dependent stimulation and CPEB oligomeric conversion may act to inactivate a repressor, thereby permitting the translation of mRNAs required for synaptic plasticity and memory.

Two recent studies, explore the possibility that Orb2 in Drosophila and CPEB3 in mice function to regulate long-term memory by amylogenic conversion. In Drosophila, Orb2 contains amino acid domains similar to other prion-like proteins (Keleman, Kruttner, Alenius, & Dickson, 2007; Kruttner et al., 2012; Majumdar et al., 2012). If this domain is removed or if Orb2

oligomerization is inhibited by mutating a residue critical for the conversion, the transgenic flies are unable to form long-term memory (Keleman et al., 2007; Majumdar et al., 2012). The functional role of oligomerization was further established by purifying monomeric and oligomeric Orb2, followed by evaluating how these two different conformational states affect translation *in vitro* (Khan et al., 2015). Adding monomeric Orb2 represses its translational targets and adding oligomeric Orb2 enhances the same translational targets. In addition, the effects on poly(A) elongation were examined, finding that the monomer reduces the poly(A) tail whereas oligomeric Orb2 elongates the poly(A) tail (Khan et al., 2015). These actions likely occur through conformational-dependent interactions. Co-immunoprecipitation demonstrates that the Orb2 monomer directly interacts with a complex responsible for de-adenylating poly(A) tail and the oligomer interacts with the complex responsible for poly-adenylating. Therefore, bi-directional translational control by Orb2 is regulated by its conformational state.

In the vertebrate nervous system, CPEB3 may have a similar role in synaptic plasticity as apCPEB in *Apylsia* and Orb2 in Drosophila. CPEB3 forms aggregates after behavioral training and CPEB3 contains a prion-like domain in the N-terminal of the protein (Fioriti et al., 2015). When the N-terminal prion-like domain is removed and transfected into cells, CPEB3 fails to form oligomers (Fioriti et al., 2015). To determine if CPEB3 oligomerization is critical for the formation of long-term memory, wild-type or N-terminal lacking CPEB3 expressing viruses were introduced into hippocampal neurons of CPEB3 knockout mice (which cannot form long-term memory). The transduced WT CPEB3 rescues the memory phenotype, but N-terminal lacking CPEB3 does not. Likewise, transducing N-terminal lacking CPEB3, does not rescue the LTP deficit observed in CPEB3 null mice. These results suggest that the oligomerization of CPEB3 is critical for long-term potentiation and the maintenance of long-term memory.

Our understanding of functional prion-like proteins in normal physiology is in its infancy. Only a small number of prion-like proteins have been explored in all taxa and few of those studies have focused on mammals. The goal of my thesis is to determine if other mammalian CPEB family members function similar to apCPEB, CPEB3, and Orb2 in regulating synaptic plasticity and the formation of long-term memory. In addressing this question, this thesis seeks to determine if prion-like proteins are more abundant and critical than previously thought. To this end, the thesis first examines if other members of the CPEB family (CPEB1, 2, and 4) share prion-like domains with other known prion proteins. We identified the most "prion-like" of the CPEB family member based on sequence homology. This led to the hypothesis that CPEB2 plays a central role in synaptic plasticity and long-term memory.

To test this hypothesis, the thesis first examines if CPEB2 forms higher-order structures as observed for apCPEB, CPEB3, and Orb2. Once we determined CPEB2 assembles into oligomeric species, we sought to selectively inhibit CPEB2 oligomers from developing. The strategy involved generating a mouse model that expresses a truncated form of CPEB2 without its prion domain by modifying the endogenous mouse locus. Using this mouse model, I assayed the ability of non-oligomeric CPEB2 mice to form long-term memories and synaptic plasticity.

Chapter 2: CPEB2 is a putative prion-like protein and forms higher-order oligomers in neurons

CPEB2 is rich with "low-complexity" and "prion-like" sequences

The finding that prion-like domains allow proteins to adopt different physical states and function prompted us to interrogate how prevalent such proteins are in the nervous system and whether they influence normal function of the nervous system. Prion-like domain often have specific characteristic that includes amino acid composition, structural features. To identify prion-like motifs we employed two bioinformatic tools to compare the whole mammalian proteome as well as sequences of individual members of the mammalian CPEB family. The first tool, the SEQ algorithm, scores the amount of low-complexity based on the primary protein sequence (Wootton & Federhen, 1996). Sequences with high "low-complexity" scores contain a large number of repeats consisting of either motifs or single amino acids. Prion-like domains are a subset of these "low-complexity" domains (Harrison & Shorter, 2017). The second tool we used was Prion-Like Amino Acid Composition analysis (PLAAC), which scores protein sequences based upon the degree of homology with known prion-like proteins (Lancaster, Nutter-Upham, Lindquist, & King, 2014).

We used the sequences of the predominant isoforms of the mouse CPEB family members to perform the analysis. CPEB2 had the highest degree of low-complexity sequence (0.32) (Fig 2.1A). In comparison, CPEB3 had a low-complexity score of 0.17. CPEB3's score was similar to CPEB4 at 0.145. CPEB1 had the lowest score at 0.06. When we scored the CPEB proteins for prion-like sequences using PLAAC, CPEB2 had the highest prion-like score (20.0). CPEB3

scored a close second (19.4) (Fig 2.1B). CPEB4 had a mid-range score (9.5). CPEB1 had a negative score. These results agree with previous findings that CPEB2-4 are in a super-group and are distinct from CPEB1 (Huang et al., 2006). Our analysis suggests CPEB2 contains prion-like sequences. This has also been demonstrated for CPEB3 (Drisaldi et al., 2015; Fioriti et al., 2015; Stephan et al., 2015). Prion-like domains are rich in glutamine (Q) and asparagine residues (N). To further investigate CPEB sequences for features consistent with prion-like regions, we next examined the number of Q and N residues in the different proteins. The total amino acid composition of CPEB2 and CPEB4 is similarly rich in Q and N residues relative to CPEB3 (9.7%, 10.8%, and 11.4% respectively) (Fig 2.1C).

CPEB1 has a lower percentage of Q and N residues (6.2%). Finally, we used the same analyses to compare the low-complexity scores and prion-like domains for members of the mouse CPEB family relative to all sequences in the mouse proteome. We calculated the low-complexity score and prion-like scores for all sequences in the proteome. CPEB2-4 clustered to the right with a remarkably high low-complexity compared to the entire proteome, yet the complexity of CPEB1 is similar to the entire proteome (Fig 2.1D). When the prion-like sequences in the CPEB family are compared to the entire mouse proteome, CPEB2-4 exhibit a higher prion-like like score than 95% of the proteome (Fig 2.1E), with CPEB-2 having the highest score. This prompted us to further explore CPEB-2. Even though a similar argument could be made for CPEB4, we did not consider it further in light of previous studies reporting CPEB4 deletion had no effect on synaptic plasticity or long-term memory. Therefore, of the remaining members of the CPEB family in the mouse, we thought CPEB2 was the strongest candidate for further study.

Figure 2.1

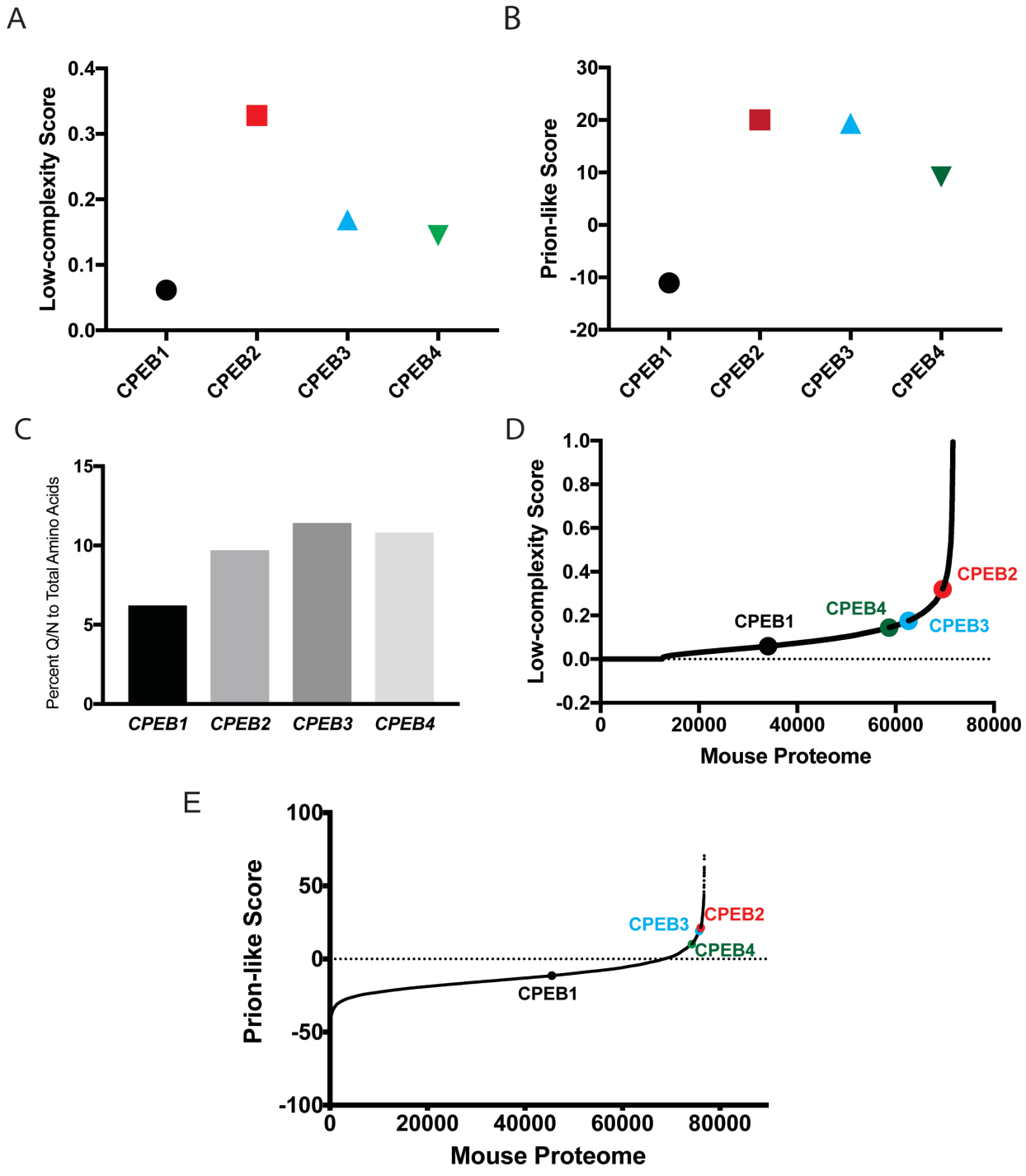
A
Low-complexity Score
0.4
0.3
0.2
0.1
0.0
CPEB1
CPEB2
CPEB3
CPEB4
B
Prion-like Score
30
20
10
0
-10
-20
CPEB1
CPEB2
CPEB3
CPEB4
C
Percent Q/N to Total Amino Acids
15
10
5
0
CPEB1
CPEB2
CPEB3
CPEB4
D
Low-complexity Score
1.0
0.8
0.6
0.4
0.2
0.0
-0.2
CPEB1
CPEB4
CPEB2
CPEB3
0
20000
40000
60000
80000
Mouse Proteome
E
Prion-like Score
100
50
0
-50
-100
CPEB3
CPEB2
CPEB4
CPEB1
0
20000
40000
60000
80000
Mouse Proteome

Figure 2.1 Characterization of the Low-Complexity and Prion-Sequences of CPEB family. Amino acid sequence of full-length CPEB isoforms was evaluated by bioinformatics for low-complexity and prion-like sequences. **(A)**. CPEB2 isoforms are least complex. SEQ analysis of degree of low-complexity sequence in individual CPEB isoforms. A higher low-complexity score indicates less varied sequence. **(B)**. CPEB2 isoforms are most prion-like. CPEB1-4 sequence prion-like score by PLAAC analysis. Higher Prion-like score in indicates greater sequence homology with known yeast prion-like proteins. **(C)**. Percent of glutamine (Q) and asparagine (N) residues to total amino acids of CPEB1-4. **(D)**. Mouse proteome SEQ analysis of low-complexity sequence. Each dot represents gene from proteome, CPEB1-4 families highlighted in color. Sequences were sorted by lowest to highest low-complexity. **(E)**. Mouse proteome PLAAC analysis of Prion-like score. Each dot represents gene from proteome, CPEB1-4 families highlighted in color. Sequences were sorted by lowest to highest prion-like score. Mouse reference proteome: UP000000589.

CPEB2 forms higher-order structures in cultured cells and neurons

Having established that the amino acid sequence of CPEB2 has similar sequence properties to the amylogenic CPEB3, the next step was to test whether CPEB2 shares features of prion-like proteins, in particular, the ability to, form stable oligomeric or disorganized aggregated structures. As a first step to assess whether CPEB2 aggregates in cells, a N-terminal GFP-tagged CPEB2 driven by the mammalian promoter CMV was transfected into HEK293T cells. We used fluorescence microscopy to visualize GFP-CPEB2 transfected cells. We found CPEB2 formed aggregated puncta of differing sizes which were broadly distributed throughout the cytoplasm of HEK293T cells (Fig 2.2A). We also analyzed lysates from CPEB2-GFP transfected cells by SDS-page western blot to assay the nature of the CPEB2 aggregates. CPEB2 was visualized by immunoblotting with an antibody against GFP. We found CPEB2 was present at the expected molecular weight of 150kD (CPEB2 110kD including GFP 27kD). Unexpectedly, a band of a much larger molecular weight (>200kD) with an underlying "smear" was also visualized on the blot. It should be emphasized that we prepared the protein lysates under denaturing conditions suggesting CPEB2 likely forms highly stable oligomers.

After observing CPEB2 aggregation in an immortalized mammalian cell line, we next investigated CPEB2 localization and whether it forms aggregates in primary neuron cultures. The first step was to isolate and culture hippocampal neurons from post-natal day 18 (p18). *In-vitro*, hippocampal neurons are phenotypically similar to pyramidal neurons and develop axons, dendrites, and spines that form synaptic connections (Kaech & Banker, 2006). Once the cultures reached maturity, we transfected them with the same GFP-tagged CPEB2 construct in the previous experiments. We used MAP2K immunostaining to differentiate transfected neurons

from transfected glia. Similar to the expression in HEK293T cells, fluorescence microscopy revealed large positive CPEB2 punctae throughout the neurons (Fig 2.2C, D). Of interest, small CPEB2 punctae were also present in neurites (Fig 2.2D – red arrows). These results illustrate that when overexpressed, CPEB2 aggregates in cultured neurons and the aggregates are located in the dendrites, and likely near the synaptic sites.

Figure 2.2

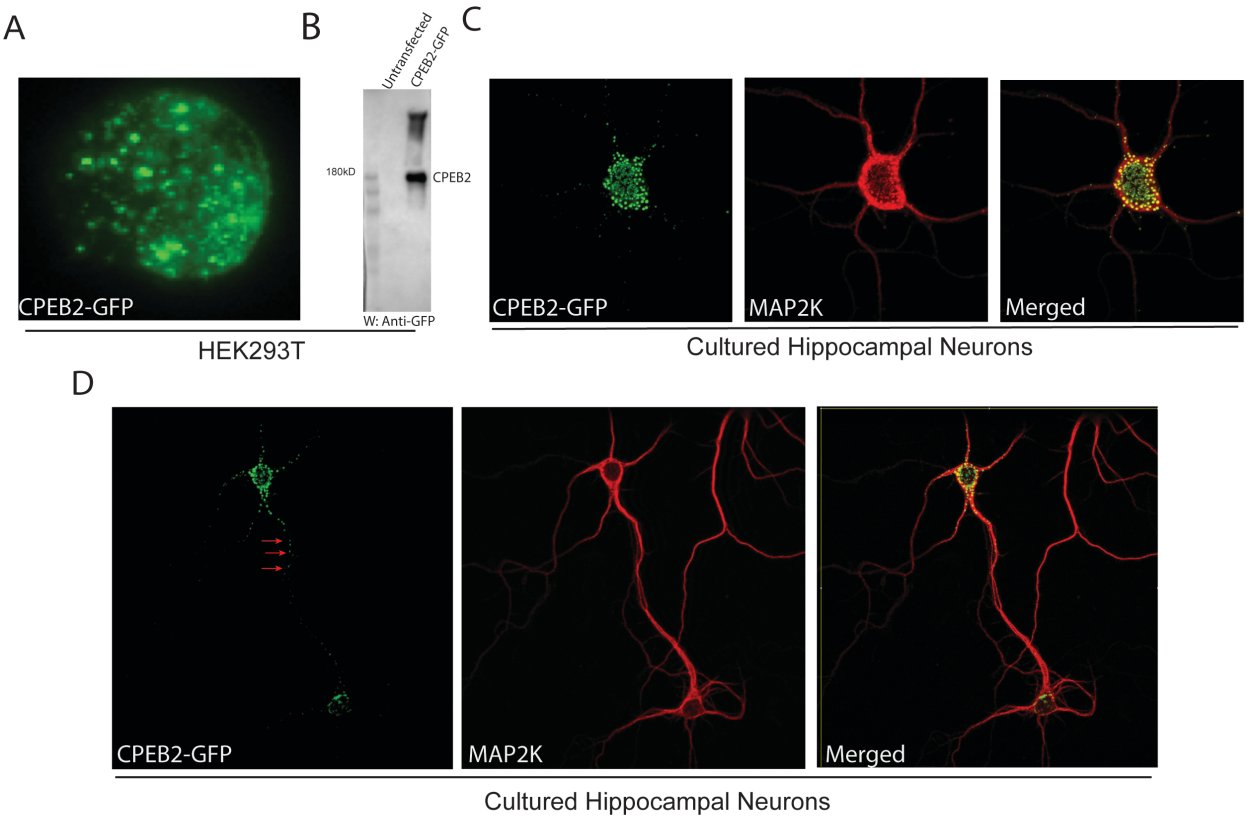

Figure 2.2 Subcellular localization and aggregation properties of transfected CPEB2-GFP in HEK293T cells and cultured hippocampal neurons. Transfected CPEB2-GFP forms aggregated puncta and higher-ordered oligomers in HEK293T cells. In cultured hippocampal neurons, transfected CPEB2-GFP positive puncta are present in cytoplasm and neurites. **(A)** Fluorescence from expressed CPEB2-GFP in HEK293T cells. **(B)** Western blot of non-transfected and CPEB2-GFP transfected HEK293T cell lysates, probed with anti-GFP antibody. Notice there is a large oligomeric smear of CPEB2. **(C)** and **(D)** Fluorescence expression of CPEB2-GFP in hippocampal neurons (green). The cultures were counter-stained with MAP2K to label hippocampal neurons (red). Number of neurons (n) assessed for each genotype: wild-type n = 30 and CPEB2 $PD^{-/-}$ n = 25.

Generation of CPEB2 isoform specific knock out

The sequence analysis and cell-based studies outlined above suggested that CPEB2 has the ability to form stable aggregates when ectopically expressed. Therefore, we sought to determine whether endogenous CPEB2 displays oligomeric properties and whether those properties are critical for synaptic plasticity and long-term memory. To test this end we generated a mouse model in which the ability of CPEB2 to oligomerize was disrupted.

For the first phase of this experiment, we used PLAAC analysis to identify the sequence location of CPEB2 prion-like domain. In mice, the *Cpeb2* gene has 12 exons and encode three distinguishable protein encoding-transcripts varying between 110 and 30 kD (CPEB2-201,-202,-204) (Fig 2.4A). We identified a probable prion-like domain in the C-terminal portion of the exon 1 of CPEB-201 and CPEB-204 (Fig 2.3B). After identifying the sequence harboring the prion-like domain, we devised a knockout strategy to generate the *Cpeb2* gene with exon 1 deleted. We targeted two guide RNAs against the 5' and 3' intronic regions of exon 1. They were delivered with CRISPR-CAS9 into the mouse embryo (Fig 2.3C). The aim was to induce double stranded breaks at both guide RNA loci, followed by non-homologous end joining of the cut chromosome in order to remove the exon 1 of *Cpeb2* and with it the prion-like domain (Fig 2.3C). Even though this approach removes the first start codon, another in-frame methionine is still present at the 5' end of exon 2. We anticipated that the in-frame methionine of exon 2 could generate a truncated CPEB2 protein lacking the prion-like domain (Fig 2.3C).

The pups produced after pronuclear injection and embryo implantation were screened by PCR and sequencing for transgenic founders in which exon 1 was removed. We identified a line that completely lacked exon 1 and the prion-like domain (CPEB2 PD). We used a heterozygous

CPEB2 PD mating strategy to obtained wild-type, heterozygous, and homozygous mice at the expected Mendelian ratios (Fig 2.3D). The homozygous CPEB2 PD mice did not exhibit obvious physical defects and remained in excellent health for at least a year (data not shown). The normal viability and expected Mendelian ratios of the offspring of the CPEB2 PD model suggest, in contrast to the full knockout, that a vital form of CPEB2 was being produced. To this end, to determine if additional truncated transcripts were present, we isolated mRNA transcripts from the brain and analyzed the various forms of CPEB2 mRNA expression by reverse transcription-coupled PCR (RT-PCR). For this assay, we used forward primers from CPEB2 exons 1, 2, and 3 with reverse primers to regions of the C-terminal exons. CPEB2 PD mice specifically lack transcripts containing the exon 1 (Fig 2.3E). However, these mice contain transcripts of exon 2 and exon 3 that are similar in size to the wild-type mice CPEB2-202 transcripts (Fig 2.3E). Given that CPEB2 PD animals lack exon 1 and its annotated start codon entirely; these results suggest that an alternative start codon located in exon 2 produced these mRNAs.

Figure 2.3

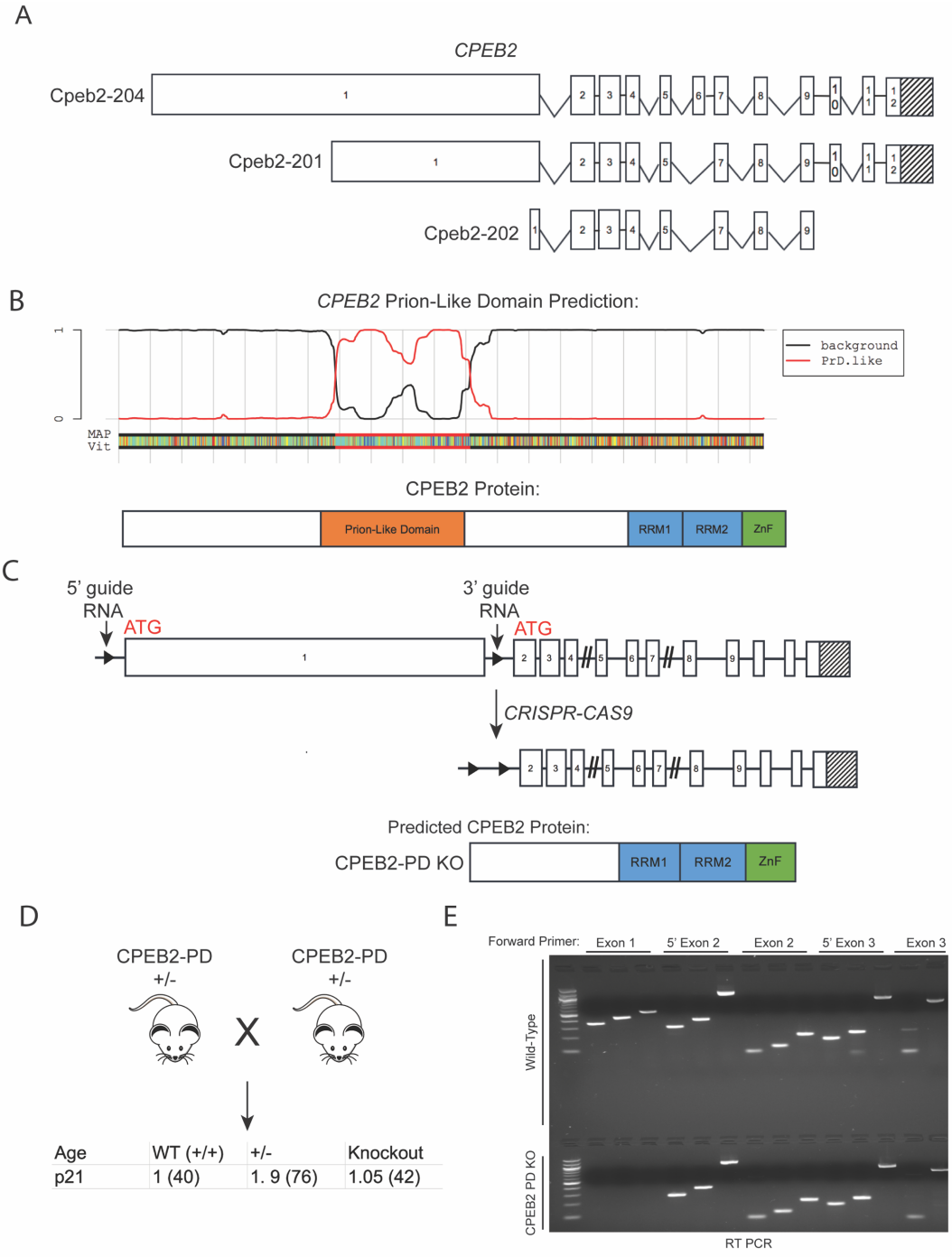
A
CPEB2
Cpeb2-204
Cpeb2-201
Cpeb2-202
B
CPEB2 Prion-Like Domain Prediction:
background
PrD.like
MAP
Vit
CPEB2 Protein:
Prion-Like Domain
RRM1
RRM2
ZnF
C
5' guide RNA
ATG
3' guide RNA
ATG
CRISPR-CAS9
Predicted CPEB2 Protein:
CPEB2-PD KO
RRM1
RRM2
ZnF
D
CPEB2-PD +/-
CPEB2-PD +/-
X
Age | WT (+/+) | +/- | Knockout
p21 | 1 (40) | 1. 9 (76) | 1.05 (42)
E
Forward Primer:
Exon 1
5' Exon 2
Exon 2
5' Exon 3
Exon 3
Wild-Type
CPEB2 PD KO
RT PCR

Figure 2.3 Generation of CPEB2 PD$^{-/-}$ mouse model. (A) Schematic of Cpeb2-201, Cpeb2-202, Cpeb2-204 isoforms. Cpeb2-204 and Cpeb2-201 contain first exon. **(B)** CPEB2 has predicted prion-like domain in exon 1. Top: Output format of PLAAC prion-like prediction algorithm for Cpeb2-204. Orange trace is predicted probability of individual amino acid belonging to prion-like domain region (PRD). Black trace is probability the sequence is not prion-like. Bottom: schematic of Cpeb2-204 protein aligned to prion-like prediction. Shown in color are CPEB2 protein domains: prion-like domain in orange, RNA recognition motifs 1 and 2 in blue (RRM), and zinc finger domain in green (ZnF). **(C)** Top: strategy for the generation of the CPEB2 PD$^{-/-}$ mice. Guide RNAs were targeted intronic regions flanking exon 1 of *Cpeb2*. Guide RNAs and CAS9 protein were introduced into the pronucleus by microinjection to selectively excise exon 1 of *Cpeb2*. Bottom: predicted truncated CPEB2 protein lacking exon 1 and prion-like domain. **(D)** Normal distribution ratios of WT, heterozygous, and homozygous CPEB2 PD$^{-/-}$ mice produced from heterozygous CPEB2 PD$^{+/-}$ mating. Numbers in parenthesis denote the number of mice in each genotype. **(E)** Reverse transcription coupled PCR analysis (RT-PCR) demonstrated loss of transcripts containing exon 1 in CPEB2 PD$^{-/-}$ mice. RNA isolated from brains was reverse-transcribed and PCR-amplified for Cpeb2 using forward primers designed in exons 1, 2, and 3 and reverse primers designed against multiple C-terminal exons junctions. No difference was observed in the transcripts containing exon 2 or 3 between wild-type and CPEB2 PD$^{-/-}$ mice.

The next experiments investigated the level of the full-length CPEB2 (CPEB2-204) protein (which contains exon 1) in CPEB2 PD animals. We processed lysates from wild-type, heterozygous CPEB2 $PD^{+/-}$, and homozygous CPEB2 $PD^{-/-}$ mouse brains for western blots. We used a CPEB2 specific antibody that recognizes the C-terminal portion of CPEB2 common to all CPEB2 protein variants. In brain lysates prepared from wild-type mice at p5 and 405p, the affinity-purified CPEB2 antibody detects an 115kD weight protein that corresponds to full length CPEB2-204 (Fig 2.4A). In lysates prepared from CPEB2 $PD^{-/-}$ mice no proteins were detected at 115kD (Fig 2.4A). The 115kD is observed in *CPEB2* $PD^{+/-}$ mice at lower levels (Fig 2.4A). These results illustrate that full length CPEB2 isoform is not expressed in *CPEB2* $PD^{-/-}$. Additionally, 35kD band is detected (Fig 2.4A) in CPEB2 $PD^{-/-}$ samples and is also detected in wild type controls. This band likely represents the smallest isoform of CPEB2 (31 kD), CPEB2-202 that lacks the majority of exon 1.

We isolated hippocampal neurons from wild-type and *CPEB2* $PD^{-/-}$ mice to better understand the expression and distribution of endogenous CPEB2 protein *in vivo*. We stained them with CPEB2 specific antibody for detection by immunofluorescence and observed diffuse endogenous CPEB2 throughout the neurons. When compared to wild type, immunodetection of endogenous CPEB2 in CPEB2 $PD^{-/-}$ was clearly diminished. Considering that the antibody used is against C-terminus of CPEB2, the residual immunofluorescence detected here may represent truncated CPEB2-protein. Taken together, these data suggest the CPEB2 PD mouse model lacks the full-length CPEB2 protein but expresses a truncated CPEB2-like isoform.

Figure 2.4

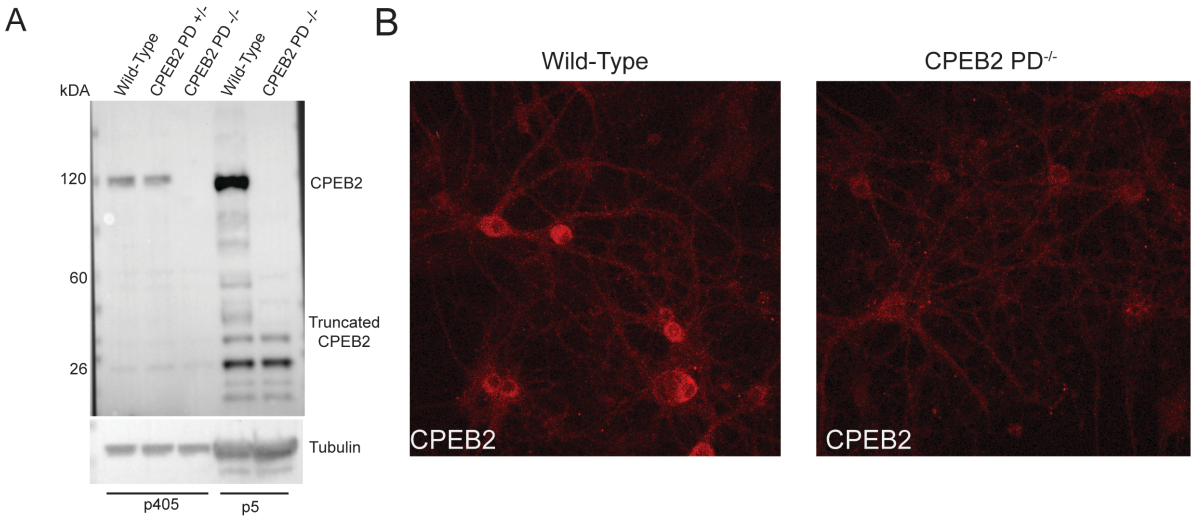

Figure 2.4 Characterization of CPEB2 expression in CPEB2 PD$^{-/-}$ mouse model. CPEB2 PD$^{-/-}$ mice lack expression of full-length CPEB2. **(A)** Western blot analysis of CPEB2 expression in brains from wild-type, CPEB2 PD$^{+/-}$, and CPEB2 PD$^{-/-}$ mice at p5 and 405 days of age. CPEB2 was detected with affinity-purified CPEB2 antibody. Full-length CPEB2 is absent in CPEB2 PD$^{-/-}$ mice and a smaller protein correlating to the truncated CPEB2 protein is at 35kD at p5. A protein corresponding to smallest CPEB2 isoform (31kD), Cpeb2-202, is observed in wild-type mice at p5. **(B)** CPEB2 immunofluorescent expression is diminished in CPEB2 PD$^{-/-}$ neurons. Immunofluorescent confocal images taken at 60x of wild-type and CPEB2 PD$^{-/-}$ cultured hippocampal neurons immunostained with CPEB2 antibody.

CPEB2 forms higher-order structures in vivo

Supplied with both a prion-domain lacking CPEB2 mouse model and an antibody specific to CPEB2 we were able to reliably asses the formation of CPEB2 oligomers *in vivo*. We fractioned by size, brain lysates from wild-type and CPEB2 PD$^{-/-}$ to perform this analysis. We followed a protocol that uses a series of centrifugations to isolate increasingly heavier components of the cell (Fig 2.5A). CPEB2 is an RNA binding protein and potentially found in large stable RNA-protein complexes. To control for this, brain lysates were pretreated with the nuclease, benzonase. Benzonases degrade all forms of DNA and RNA and, as a result,

dissociate proteins from RNA-protein complexes. At the end of the centrifugation steps, immunodetection determined the amount of CPEB2 in each fraction using the CPEB2 specific antibody. In wild-type mice, full length and oligomeric CPEB2 were present in each fraction (Fig 2.5B). In the CPEB2 $PD^{-/-}$ lysates, neither full length nor oligomeric CPEB2 expression was observed (Fig 2.5B). However, because SDS-PAGE has several confounding factors when used to analyze high-order structures, including pore-size limitation, we also employed SDD-agarose (SDD-AGE) gel analysis. SDD-AGE gels have significantly larger pore size and enable visualization of large SDS-resistant oligomers. SDD-AGE gels are routinely used to resolve mammalian amyloidogenic aggregates (Bagriantsev, Kushnirov, & Liebman, 2006). In the semi-denaturing conditions of SDD-AGE, prions and prion-like proteins oligomers are maintained, while disordered aggregates disassemble (Kryndushkin, Alexandrov, Ter-Avanesyan, & Kushnirov, 2003).

Wild type fractions run in SDD-AGE showed both a monomeric CPEB2 band and large molecular weight-smears, suggesting CPEB2 formed amyloid-like oligomers (Fig 2.5C). There was no evidence of CPEB2 monomers or oligomers in the fractions from the CPEB2 $PD^{-/-}$. To further assess the nature of the oligomers, medium weight S2 fractions from both wild-type and *CPEB2* $PD^{-/-}$ were treated with increasing concentrations of the reducing agent dithiothreitol (DTT). In wild-type mice, CPEB2 oligomers were resistant to the 5mM DTT and 2% SDS (Fig 2.5D).

Figure 2.5

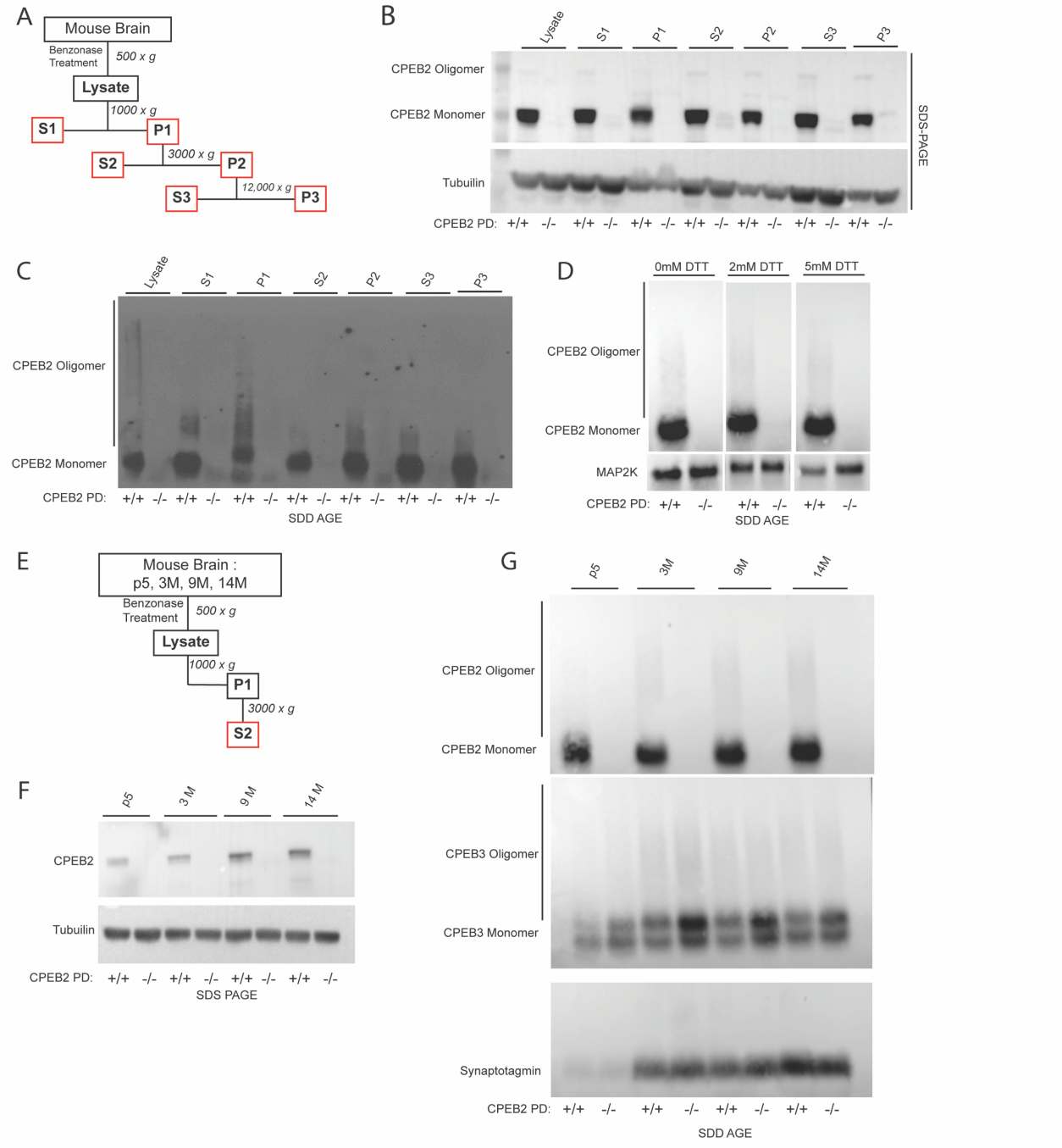
A
Mouse Brain
Benzonase Treatment
500 x g
Lysate
1000 x g
S1
P1
3000 x g
S2
P2
12,000 x g
S3
P3
B
Lysate
S1
P1
S2
P2
S3
P3
CPEB2 Oligomer
CPEB2 Monomer
Tubuilin
SDS-PAGE
CPEB2 PD: +/+ -/- +/+ -/- +/+ -/- +/+ -/- +/+ -/- +/+ -/- +/+ -/-
C
Lysate
S1
P1
S2
P2
S3
P3
CPEB2 Oligomer
CPEB2 Monomer
CPEB2 PD: +/+ -/- +/+ -/- +/+ -/- +/+ -/- +/+ -/- +/+ -/- +/+ -/-
SDD AGE
D
0mM DTT
2mM DTT
5mM DTT
CPEB2 Oligomer
CPEB2 Monomer
MAP2K
CPEB2 PD: +/+ -/- +/+ -/- +/+ -/-
SDD AGE
E
Mouse Brain : p5, 3M, 9M, 14M
Benzonase Treatment
500 x g
Lysate
1000 x g
P1
3000 x g
S2
F
p5
3 M
9 M
14 M
CPEB2
Tubuilin
CPEB2 PD: +/+ -/- +/+ -/- +/+ -/- +/+ -/-
SDS PAGE
G
p5
3M
9M
14M
CPEB2 Oligomer
CPEB2 Monomer
CPEB3 Oligomer
CPEB3 Monomer
Synaptotagmin
CPEB2 PD: +/+ -/- +/+ -/- +/+ -/- +/+ -/-
SDD AGE

Figure 2.5 CPEB2 forms oligomeric structures *in vivo.* **(A)** Schematic diagram of the brain lysate fractionation procedure using several differential centrifugation steps. Six distinct fractions of increasing heavier components were isolated. Fractions assayed by western blots and SDD-AGE are shown in red (Blots: B-D). **(B)** Western blots of the different cellular fractions show monomeric and oligomeric CPEB2 in each fraction from wild-type mice. Neither monomeric nor oligomeric CPEB2 is present in CPEB2 $PD^{-/-}$ mice. **(C)** SDD-AGE analysis for CPEB2 oligomers in cellular fractions from wild-type and CPEB2 $PD^{-/-}$ mice. Smear of SDS-resistant oligomeric CPEB2 is observed in wild-type mice but not CPEB2 $PD^{-/-}$ fractions. **(D)** SDD-AGE analysis determining CPEB2 oligomer stability in S2 fractions treated with increasing concentration of DTT. CPEB2 oligomers were resistant to reduction by DTT. **(E)** Schematic of procedure for isolating brain lysates from animals at p5, 3 months, 9 months, and 14 months. S2 fraction was assayed by western blot and SDS-AGE (Blots: F-G) **(F)** Western blots of S2 lysates. CPEB2 protein is expressed at each time point in wild-type mice. **(G)** SDD-AGE analysis of CPEB2 oligomers at each age. SDS-resistant oligomer CPEB2 is present in lysates of wild-type mice at 3, 9, and 14 months of age. CPEB3 oligomers are found in wild-type and CPEB2 $PD^{-/-}$ mice. No oligomers were observed in the non-prionogenic synaptotagmin in either genotype.

Since DTT reduces proteins and prevents intramolecular and intermolecular disulfide bonds, these results suggest CPEB2 linkages are either not readily reducible or not necessary for maintenance of SDS-resistant CPEB2 oligomers. To determine whether CPEB2 oligomers are transiently present at a particular stage or present throughout the mouse's lifespan, western blot analysis was used to first confirm CPEB2 expression in brain lysates prepared from a variety of times points (Fig 2.5E). We found CPEB2 present throughout the different aged animals (Fig 2.5F). Next, we assayed the CPEB2 oligomers in these lysates using SDD-AGE (Fig 2.5G). The CPEB2 oligomers are detected in 4, 9, and 14 months old in wild-type mice (Fig 2.5G). Again, no oligomers were detected in CPEB2 $PD^{-/-}$ mice (Fig 2.5G). As an additional control, we assessed if either the known prion-like protein, CPEB3, or a non-prion synaptic protein, synaptotagmin, form oligomeric smears in this assay. As previously observed, CPEB3 forms oligomers (Fioriti et al., 2015; Turimella et al., 2015), but synaptotagmin does not (Fig 2.5 Appendix 3: Regulation of Amyloidogenic Oligomerization of Drosophila Orb2 Protein G). In summary, these results demonstrate that CPEB2 forms SDS-resistant oligomers in the brain throughout the mouse's lifespan and these oligomers display some of the properties expected of prion-like proteins.

Discussion

This chapter provides data that suggest CPEB2 may be a prion-like a protein.

CPEB2-4 super family is rich in prion-like sequences:

To identify whether additional members of the CPEB family harbor prion-like domain, the amino acid sequences of CPEB proteins were assayed for low-complexity regions and prion-like sequences found in prion-like proteins. The analysis revealed that CPEB2-4 have regions containing little amino acid diversity and share sequence homology with other prion-like proteins. Of the family members, CPEB2 has the highest low-complexity scores and highest degree of homology with other known prion-like proteins. This suggests CPEB2 is a potential prion-like protein. The algorithm to screen for prion-like sequence is based on the amino acids found in 28 yeast proteins that have distinct conformational shapes or that form amyloid structures (Lancaster et al., 2014). Importantly, this technique is used to identify prion-like sequences in mammalian proteins (H. J. Kim et al., 2013; King, Gitler, & Shorter, 2012). Therefore, the sequences of CPEB2-4 are highly rich in amino acids found in proteins with prion-like features. In particular, CPEB2 strongly meets these criteria.

To determine if these features are unique to the CPEB family, we analyzed the degree of low-complexity and prion-like sequences in the entire genome and show CPEB2-4 are rich with low-complexity sequences relative to the genome. Low-complexity regions are relatively abundant in the genome (Golding, 1999). Their functions are still relatively unknown. Prion-like domains are low complexity sequences comprised of polar amino acids (glutamine, asparagine, typrsine, and serine) (Alberti, Halfmann, King, Kapila, & Lindquist, 2009; L. Li &

Lindquist, 2000; Michelitsch & Weissman, 2000). Previous studies demonstrate that CPEB3 contains a prion-like domain that promotes amyloid aggregation (Drisaldi et al., 2015; Fioriti et al., 2015; Stephan et al., 2015). Additionally, when expressed in the nervous system, the N-terminal low-complexity region of CPEB4 forms nucleolar aggregates (Shin, Salameh, & Richter, 2016). Given these conclusions, we hypothesized that the low-complexity of CPEB2-4 is associated with the presence of their prion-like sequences. Supporting this hypothesis, CPEB2-4 prion-like prediction scores are higher than 95% of the genome. In addition, the low-complexity regions of CPEB2-4 are predominantly in exon 1, which is in agreement with our own and others' PLAAC analysis. (Appendix 1) (Fioriti et al., 2015; Shin et al., 2016). The CPEB2-4 exon 1 share relatively low-homology, but the prion-like sequence of CPEB2-4 is found in exon 1 (Appendix 1). Interestingly, a disproportionate number of human RNA-binding proteins, such as CPEB, contain prion-like domains (Harrison & Shorter, 2017). Clues to the role of prion-like domain in RNA-binding proteins come from studies demonstrating that upon cellular or environmental stress a number of RNA-binding proteins with prion-like domains are recruited into stress granules (Anderson & Kedersha, 2008; Y. R. Li, King, Shorter, & Gitler, 2013). Stress granules are cytoplasmic structures consisting of the translational machinery and mRNAs that serve to repress translation of unnecessary proteins, in order to devote more cellular resources toward production of more critical proteins required for survival (Harrison & Shorter, 2017). Thus, these domains are essential for protein-protein interactions to function correctly in response to environmental stimuli. Likewise, in apCPEB and CPEB3, these domains also promote aggregation upon neuronal stimulation (Fioriti et al., 2015; Si et al., 2010). However, neither oligomeric CPEB3 nor apCPEB localize stress granules. Instead of repressing translation, CPEB is associated with active translation. Therefore, considering that these

domains have been preserved in both CPEB2 and CPEB4, the prion-like sequence similarities between CPEB2-4 superfamily raises the possibility that CPEB2 and CPEB4 require their prion-like domain in order to function.

CPEB2 PD$^{-/-}$ is an isoform specific knockout

We focused on CPEB2 due to its prion-like amino acid sequence properties and its role in synaptic plasticity and long-term memory (Lu et al., 2017). We generated a CPEB2 knockout mouse lacking the prion-like domain to further characterize the prion-like properties of CPEB2. After identifying that a putative prion-domain resides in the exon 1 of CPEB2, a CPEB2 prion-domain knockout was generated by removing exon 1 from the endogenous mouse locus using CRISPR-CAS9. Initial characterization of the *CPEB2 PD$^{-/-}$* model showed successful removal of exon 1 from the mouse genome. Importantly, in *CPEB2 PD$^{-/-}$* mice, CPEB2 transcripts containing the exon 1 were absent but, transcripts containing the exon 2 and exon 3 were present. Additionally, CPEB2 PD$^{-/-}$ mice did not express the full-length CPEB2 protein. We generated and used an antibody targeted against the C-terminal portion to assay the CPEB2 protein. Considering that CPEB2 PD$^{-/-}$ mice still contain this region and transcribe CPEB2 transcripts containing exon 2, we reasoned that our knockout is isoform specific and would express a truncated version of the CPEB2 protein. The data support this hypothesis. In wild-type animals we observed a protein corresponding to the smallest CPEB2 isoform (CPEB2-202), which correlates to the predicted truncated CPEB2 protein observed in the knockout. These two proteins are of comparable size, given that the smallest isoform contains only 16 amino acids of the first exon. These findings indicate that the CPEB2 PD$^{-/-}$ model is a CPEB2 isoform specific

knockout. Other functional and structural domains identified in CPEB2 (two RNA recognition motifs and a zinc finger) reside in the distal C-terminal portion (Fig 2.3B, C) (Turimella et al., 2015). As described above, the complete CPEB2 knockout mouse model in which exons 3-5 are deleted is lethal in the prenatal and early postnatal period. In that case no protein or truncated protein is produced (Lai et al., 2016). We hypothesized that a truncated CPEB2 protein containing the functional and structural domains may maintain the essential CPEB2 functions required to generate a viable animal. We observed that CPEB2 $PD^{-/-}$ animals are viable and only express a CPEB2 truncated protein. Taken together these results indicate that the truncated *CPEB2* $PD^{-/-}$ model maintains a CPEB2 truncated form with functional domains in the C-terminus that is sufficient for CPEB2 functions in early development.

CPEB2 as a putative prion-like protein

The next experiments addressed whether CPEB2 shares features with other prion-like proteins. First, we established that CPEB2 forms large aggregates in tissue culture cells and hippocampal primary cell cultures. When overexpressed, large CPEB2 aggregates form in tissue culture cell and primary hippocampal neurons. Next, we used CPEB2 $PD^{-/-}$ mice to test if CPEB2 forms oligomeric structures *in vivo*. The results showed high molecular weight oligomers are present in wild-type mice but not in CPEB2 $PD^{-/-}$ mice. Likewise, when wild-type brain lysates were examined by SDD-AGE, a smear of SDS-resistant high molecular weight CPEB2 was detected. Our CPEB2 isoform specific knockout did not form these structures. In addition to being SDS-resistant, the CPEB2 oligomer was resistant to reducing conditions with increasing concentrations of DTT and was present throughout the lifespan of the mouse. The

presence of high molecular weight CPEB2 oligomers is intriguing for two reasons. First, this finding demonstrates CPEB2 forms large oligomers *in-vivo*. Second, it establishes that similar to CPEB3, CPEB2 is another mammalian CPEB family member capable of forming SDS-resistant oligomers. The full-length CPEB2 shares features with prion-like proteins including, 1) forming high molecular weight structures, and 2) the oligomers being resistant to reducing detergents. However, it remains to be determined whether CPEB2 meets the other two criteria important for establishing its identity as a functional prion, 1) formation of fibers, and 2) ability to convert monomeric CPEB2 to the aggregate form. Regardless of the classification, we demonstrated that the formation of the oligomeric CPEB2 is imparted by exon 1 containing the prion-like domain. Consistent with the results shown here, removing the N-terminal portion of CPEB3, which contains it prion-like domain, reduces the formation of the prion-like oligomeric CPEB3 (Stephan et al., 2015). Likewise, the LTP and long-term memory deficit observed in the CPEB3 cKO mice can be rescued by transducing full-length CPEB3. But, they cannot be rescued by CPEB3 lacking the N terminus. In the remaining chapters, we explore the effect of removing the CPEB2's exon 1 and its prion-like domain on CPEB2-dependent translation, synaptic plasticity and long-term memory.

Chapter 3: CPEB2's role in translation

CPEB2 associates with translating ribosomes

The formation of long term-memory requires stimulus-dependent synthesis of new proteins by neurons, from existing but dormant mRNA or from newly transcribed mRNAs. In mouse forebrain, CPEB2 effects the formation of long-term memory, likely by acting as a translational regulator of key mRNAs. Selective loss of CPEB2 in the forebrain affects the formation of long-term memory and the regulation of the translation of target genes in (Lai et al., 2016; Lu et al., 2017; Turimella et al., 2015). Further, CPEB2 in the nervous system acts both as a translational repressor and as an activator (Lai et al., 2016; Lu et al., 2017). Previous studies analyzed CPEB2 translational effects on a small subset of genes, which limits generalization. We sought to gain a more unbiased and fundamental understanding of CPEB2-dependent translation regulation by first exploring which phase of translation CPEB2 is present.

To better understand the role of CPEB2 in translation, we used polysome profiling which separates ribosomes according to their translational status. Polysome profiling also allows us to discriminate ribosomes that are actively elongating mRNA (Chasse, Boulben, Costache, Cormier, & Morales, 2017) from ribosomes that are not engaged in translation and therefore can serve as an indicator of overall translation status of the cell. Additionally, following the separation of ribosomes, the proteins and mRNAs associated with the different types of ribosomes can be indentified. For example, translating ribosomes associate with the translational machinery, translational activators, and other translational regulators (Chasse et al., 2017). Typically, translation repressors are found with dissociated ribosomes and untranslated mRNAs.

Polysome profiling enabled us to determine if CPEB2 associated with ribosomes. Further, using this technique, we could identify if CPEB2 associates with either untranslating or translating ribosomes,

Polysome profiling begins with arresting translation and immobilizing the ribosome onto the mRNA by treating brain lysates with the protein synthesis inhibitor, cycloheximide. Translationally active ribosomes form groups of multiple 80S ribosomes or chains of ribosomes (polysomes), and are separated from ribosomal subunits not undergoing translation by a sucrose gradient. Following centrifugation, the gradient is fractionated and the amount of RNA in each fraction quantified using an absorbance wavelength of 260 nm (A_{260}). The mRNA transcripts being highly translated are bound by two or more 80S ribosomes and reside in the heaviest sucrose fractions (polysome fractions) (Fig 3-1A). Conversely, single ribosomal subunits and free mRNAs are present in the lighter fractions (Fig 3-1A). Following sucrose gradient separation, proteins present in the translating or non-translating fractions can then be assayed by western blot. Using this technique, we asked which fractions contained CPEB2 to determine the role, if any, of CPEB2 in the three main phases of translation.

Figure 3.1

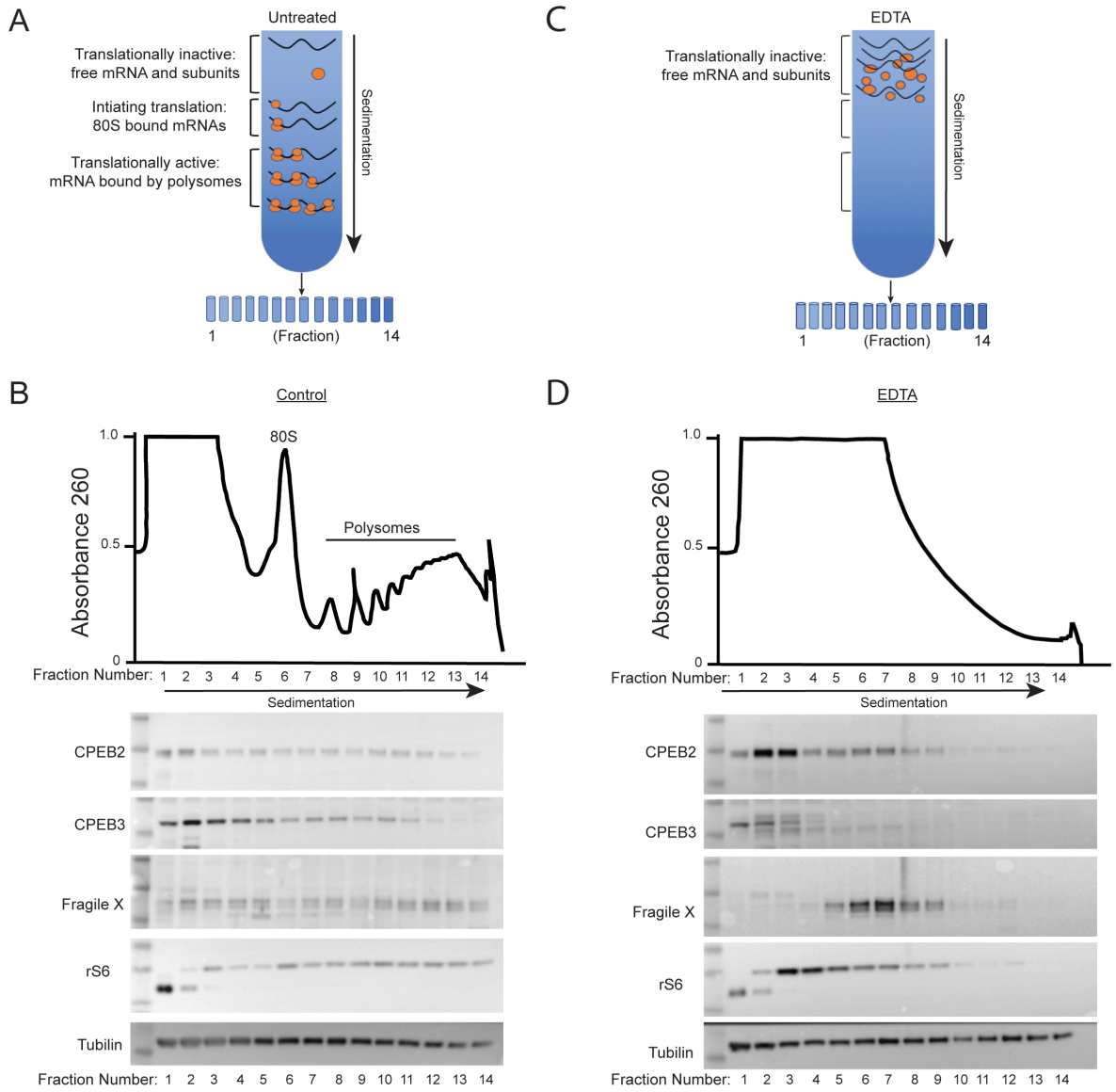

Figure 3.1 CPEB2 associates with polyribosomes. Polysome profiling conducted on lysates prepared from brain cortices of 3 month old wild-type mice. **(A)** and **(C)** Cartoon showing sedimentations patterns of the mRNAs during different translational phases in each type of sucrose gradient. (**B)** and **(D)** *Top panel:* RNA absorption profile of 7-47% (w/w) sucrose gradient at 260 nm absorbance. 80s ribosomal and polysome peaks are indicated. *Bottom panel:* western blots show distribution of CPEB2, CPEB3, Fragile X, 40S ribosomal subunit S6(RS6) and tubulin in relation to absorption profile. Fraction numbers are indicated underneath; faction 1 is lightest and 14 is heaviest. In (**B)** polysome profiling on untreated lysates shows CPEB2 co-sediments with the polyribosomes in fractions 8-14. In **(D)** EDTA treated lysates RNA absorption profile shows loss of polyribosome peaks due to dissociation of ribosomes. In absence of polyribosomes, CPEB2 sediments to earlier fractions.

Whole brain lysates from 3 month old wild-type mice were analyzed by polysome profiling. The lysates were fractionated as described above. A typical RNA profile from these experiments includes a large 80S ribosomal complex represented by a high level of A_{260} absorbance peak in fractions 5 and 6 (Fig. 3-1B). The multiple small peaks in fractions 8-14 correspond to the polysomes, with each successive peak corresponding to an additional ribosome per transcript (Fig. 3-1B). Following quality-control profiling, the samples were run on western blot to assay levels of individual proteins found in each fraction. The blots were probed for the 40S ribosomal subunit S6 (rS6) to determine the distribution of 40S, 60S, and 80S ribosomal subunits.

As shown by the western blots, the light fractions (1-4), which is primarily composed of free mRNA or small RNP-complexes contains low amounts of ribosomes, including 40S ribosomes (Fig. 3-1B: lower panel). The fractions corresponding to the ribosomal 80s complexes and polysomes have increased levels of rS6 since they contain both 40s and 60S ribosomes (Fig. 3-1B: lower panel, fractions 6-14). Interestingly, CPEB2 was found in the polysome fractions associated with elongating mRNAs (fractions 8-14). CPEB3 which activates translation, and Fragile X mental retardation protein (FMRP), which associates with elongating mRNAs, were used as controls and were also found in these fractions (Fig. 3-1B: lower panel). These results suggest CPEB2 is in a complex with mRNA actively undergoing translation.

To confirm whether CPEB2 associates with mRNAs undergoing translation, we first dissociated 80S ribosomes in the solution and then measured CPEB2 distribution. To sequester the Mg^{2+} required for ribosomal stability, the lysates were treated with 30 mM EDTA, and we used a sucrose gradient containing 10 mM EDTA. This results in dissociation of the translating 80S ribosomal subunits to 40S and 60S subunits and release of the translating mRNA and

translational regulators (Fig 3-1C). As shown in the figure, after EDTA treatment there are no 80S ribosome or polysome peaks seen by A_{260} (Fig 3-1D) and all the mRNAs sediment in the earlier fractions because they weigh significantly less without the ribosomes. As a consequence of dissociating the ribosomes, proteins bound to the polysomes or their mRNA also shift to the earlier fractions. Dissociation of ribosome subunits in the lysate is a key control to differentiate the heavy fraction proteins that complex with mRNA undergoing translation from those that do not.

We subjected wild-type brain lysates to this protocol and found, as predicted, ribosome levels increase in the earlier, lower weight fractions and decrease in the later, higher weight fractions, as indicated by absorbance of the ribosomal RNA at A_{260} (Fig 3-1B, top). The shift of ribosomal protein S6 toward the earlier fractions illustrates how this ribosome dissociation condition shifts their distribution from high weight to lower weight fractions (Fig 3-1B: lower panel, fractions 1-7). In this case, the polysome mRNA binding protein, FRMP, also shows a similar shift toward the earlier fractions. Tubulin, which does not bind mRNAs or the ribosomal complex, does not shift. Following EDTA treatment, CPEB2 levels demonstrate a loss of CPEB2 protein in the polysome fractions and an increase in earlier fractions. These results suggest that CPEB2 binds to mRNA transcripts that are being actively translated and imply CPEB2's functions to regulate mRNAs undergoing translation.

CPEB2 acts as a translational repressor

The previous results established CPEB2 interacts with mRNAs undergoing translation. One possibility is that CPEB2 bound to polysomes acts as a translational activator, like Orb2, by

promoting polyadenylation (Khan et al., 2015). However, two studies to date have provided evidence on CPEB2 acting as both a translational repressor (of choline acetyltransferase in the peripheral nervous system) and a translational activator (of GRASP1 in the hippocampus) (Lai et al., 2016; Lu et al., 2017). To reconcile these seemingly conflicting observations, one hypothesis is that different CPEB2 isoforms or CPEB2 oligomers have different regulatory effects on translation. To address this hypothesis, we investigated whether the translational targets of CPEB2 are up- or down- regulated in the isoform specific CPEB $PD^{-/-}$ mouse model.

In neurons, CPEB2 binds to mRNAs encoding β-catenin, CaMKII, protein kinase α, synapse-associated protein 97, and GRASP1 (Lu et al., 2017; Turimella et al., 2015). Putative targets have also been identified by the presence of CPE motifs in their 3' UTRs, including mRNAs encoding GluR1 and EPH receptor A4, (Turimella et al., 2015). We reasoned that if CPEB2 acts as a translational regulator *in vivo*, then levels of CPEB2 target proteins would be dysregulated in CPEB2 $PD^{-/-}$ mice. To test this hypothesis, western blots were prepared with whole brains lysates from P5 of wild type and CPEB2 $PD^{-/-}$ mice. As a first step, we examined the levels of the GRASP1 protein, which is decreased in hippocampal cultured neurons of the full-CPEB2 knockout mouse (Lu et al., 2017). However, GRASP1 protein levels were not significantly different in CPEB2 $PD^{-/-}$ p5 brains lysates when compared to wild-type controls, (Fig 3-2A,B).

Figure 3.2

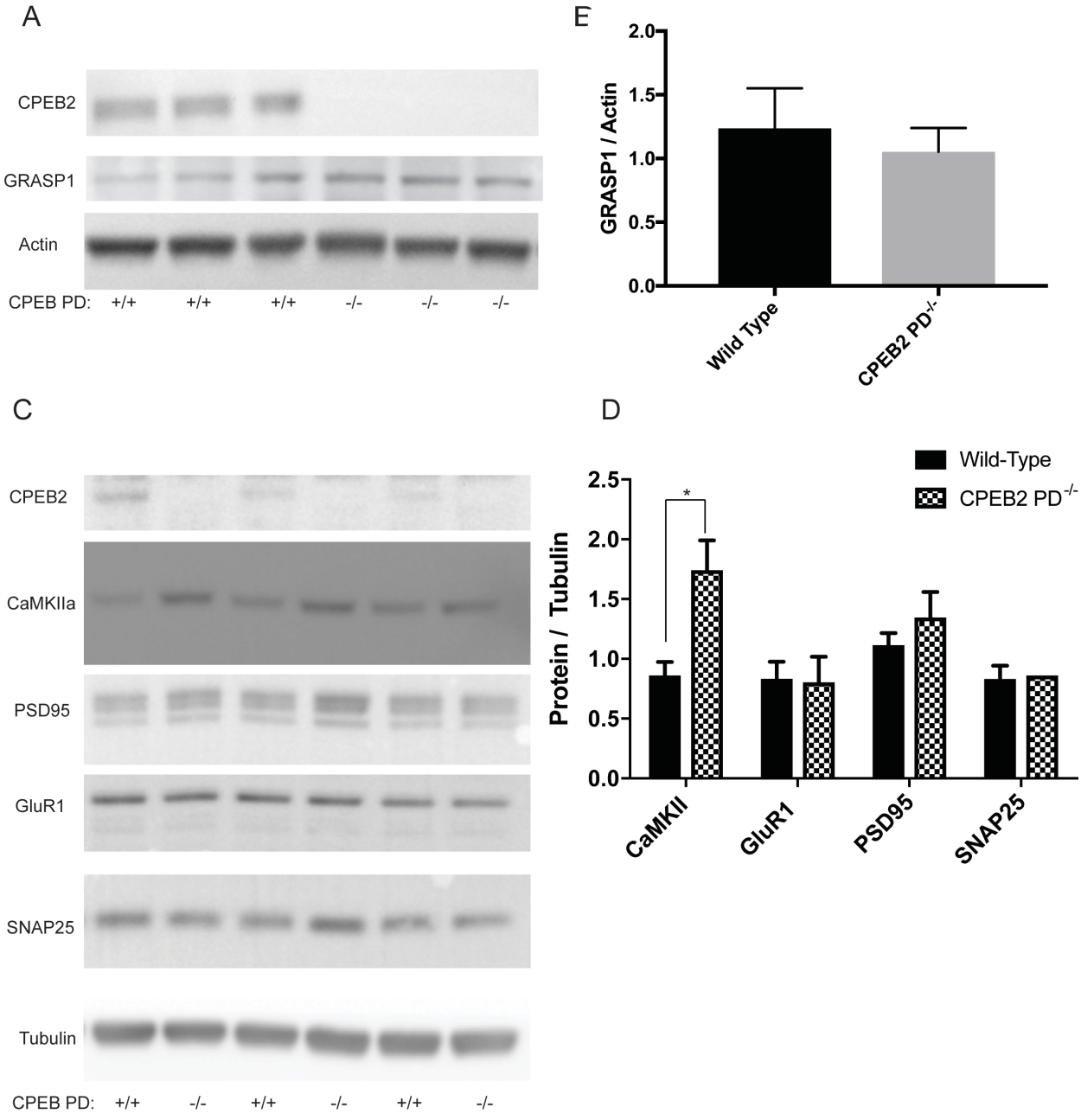

Figure 3.2 Increased protein levels of CPEB2 target, CaMKIIa, in brains of CPEB2 PD$^{-/-}$ mice. Western blots of whole brain lysates were used to evaluate levels of CPEB2 target proteins (n=3) for each target in wild-type and CPEB2 PD$^{-/-}$ **(A)** Western blot densitometry analysis shows no change in the expression of CPEB2 target, GRASP1, between wild-type and CPEB2 PD$^{-/-}$ animals at p5 (quantified in **B**). **(C)** CaMKIIa expression is increased in CPEB2 PD$^{-/-}$ mice. No change was observed between CPE (PSD95, GLUR1) and non-CPE (SNAP25, Tubulin) proteins levels in wild-type and CPEB2 PD$^{-/-}$ mice (quantified in **D**). Data are represented as mean ± SEM. Statistics: (B) Student's t-test (D) Two-way ANOVA, Bonferroni post hoc test, * $p < 0.05$.

To further examine how in CPEB2 PD$^{-/-}$ mice, loss of exon 1 alters the expression of proteins potentially regulated by CPEB2, the above samples were then probed for a series of proteins, including CaMKIIa (CPEB2 binds CAMKIIa mRNA), GluR1 (putative CPEB2 target), PSD95 (a CPEB3 target), and SNAP25 or synaptotagmin (synaptic proteins not associated with CPEB2) (Chao et al., 2013; Turimella et al., 2015). CaMKIIa expression is increased in the CPEB2 PD$^{-/-}$ relative to wild-type mice. The levels of PSD95, GlurR1, SNAP25 were unchanged between wild-type and CPEB2 PD$^{-/-}$ lysates (Fig 3-2C, D). These results demonstrate that mice lacking exon 1 of CPEB2, specifically increases the expression of CaMKIIa. This is an intriguing finding as CaMKIIa expression is required for hippocampal LTP and hippocampal based long-term memory (Silva, Stevens, Tonegawa, & Wang, 1992). This finding prompted the next question: is CaMKIIa expression also dysregulated in the hippocampus, a brain structure critical for the formation of long-term memory?

To address this question, hippocampi were dissected from p30 wild-type and CPEB2 PD$^{-/-}$ mice. Lysates were probed for CaMKIIa, GluR1, synaptotagmin, SNAP25, and tubulin. Like the findings in whole-brain lysates, the CPEB2 PD$^{-/-}$ hippocampal lysates demonstrated an increase in CaMKII protein relative to wild-type mice (Fig 3-3A, B). GluR1, synaptotagmin, and SNAP25 levels were unchanged from wild-type. Together, these observations suggest that CPEB2 either directly or indirectly acts as a translational repressor of CAMKIIa in whole brain and hippocampus. Moreover, GRASP1, a protein with dysregulated expression in the global CPEB2 knockout, was not affected in our model. Comparing the translation changes in complete CPEB2 knockout, with those in our model, allow identification of mRNA that are regulated by the prion-like variants of CPEB2.

Figure 3.3

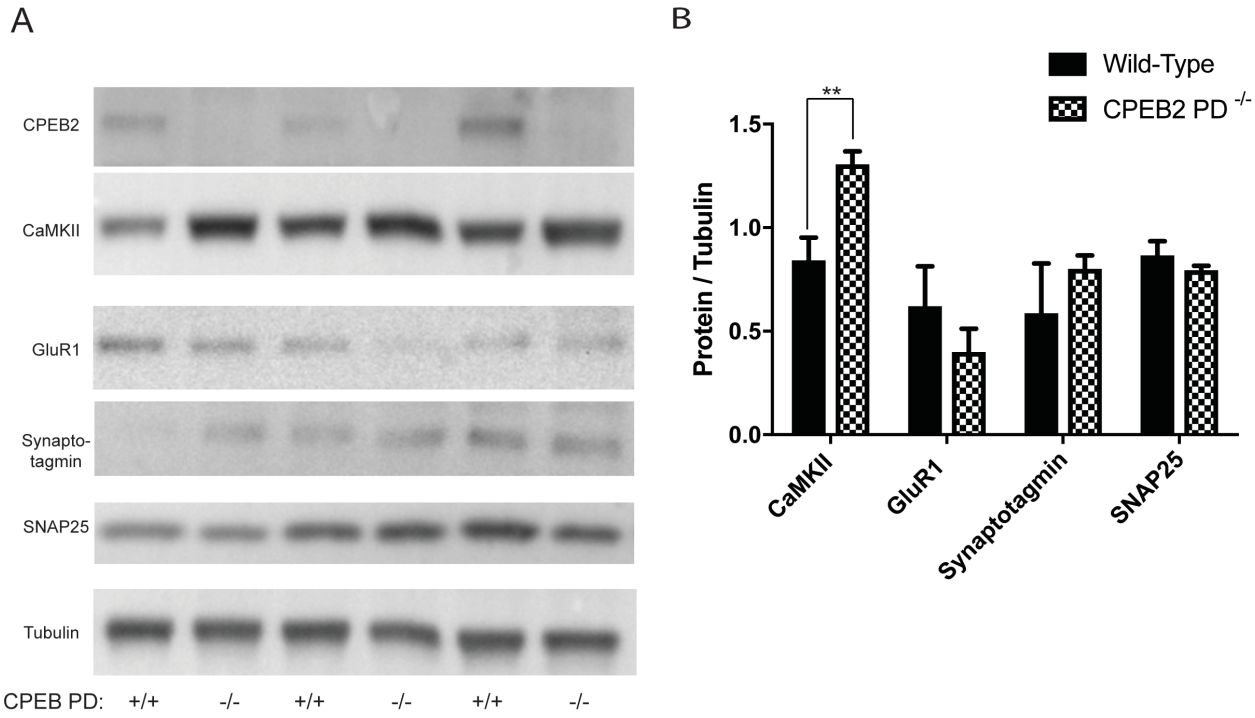

Figure 3.3 Increased protein levels of CPEB2 target, CaMKIIa, in the hippocampus of CPEB2 PD$^{-/-}$ mice. Lysates prepared from dissected hippocampus were used in western blots to evaluate levels of CPEB2 target proteins (n=3) for each target in wild-type and CPEB2 PD$^{-/-}$ **(A)** Western blot densitometry analysis shows increased expression in CaMKIIa in CPEB2 PD$^{-/-}$ animals at p30 (quantified in **B**). Data are represented as mean ± SEM. Two-way ANOVA, Bonferroni post hoc test, ** $p < 0.005$.

CPEB2 localizes to synapses

The current model suggests that CPEB proteins act as synaptic marks by inducing spatially targeted translational-dependent changes to the synapse. The results outlined above demonstrate that CPEB2 interacts with translating mRNAs and that the CPEB2 isoform containing the prion-like domain likely represses translation. However, for CPEB2 to act as a synaptic regulator, it must be localized at the synapse. Although in Chapter 2, we demonstrate using immunofluorescence that GFP-tagged CPEB2 is present in the dendrites of hippocampal

neurons (Fig 2-2D), it has not been determined whether CPEB2 is located at the synapse. The next experiment evaluated the subcellular distribution of CPEB2 in neurons, to resolve if CPEB2 is found in the synapse.

Typically, this approach would entail labeling the synapses and CPEB2 by indirect-immunofluorescent in brain sections and examining for co-localization. However, due to the fact the CPEB2 specific antibody performs poorly in immunofluorescence detection of endogenous CPEB2 (Fig 2-4B), we turned to synaptosome purification to biochemically isolate synapses from brain tissue. When brain tissue is homogenized in an isotonic solution, the pre- and post-synaptic components are sheared away from the axons and dendrites. Once in solution, the isolated membranes re-seal to form synaptosomes (Whittaker, Michaelson, & Kirkland, 1964). Synaptosomes have a distinct density from other cellular compartments and can be isolated by differential centrifugation through a sucrose gradient. Purified synaptosomes retain the pre- and postsynaptic components and mimic functionally intact synapses (Whittaker, 1993). Therefore, synaptosome preparations can be used to reliably investigate synaptic composition.

Brain lysates from three-month-old of wild-type and CPEB2 $PD^{-/-}$ were used to purify synaptosomes. Four different fractions were isolated sequentially with the following subcellular components: 1) cytosol and membranes, 2) nucleus, 3) cytosol and light membranes, and 4) synaptosomes further purified to synaptic plasma membrane (SPM) (Fig 3.4A). After separation, we used western blotting to examine the proteins present in each subcellular compartment. GLUR1, an AMPA receptor subunit located exclusively in synapses, was examined as a positive control of purified synaptic components in SPM. Indeed, GLUR1 levels were rich in the SPM fraction (Fig 3.4B). Tubulin, normally present throughout the cell, was found in every fraction. The transcription factor CREB, a positive control for nuclear proteins,

was enriched in the nuclear fraction. Regarding CPEB2 protein, full-length protein was detected equally in all fractions in wild-type mice (including the SPM) (Fig 3.4B). These results are consistent with the *in vitro* experiments described in Chapter 2 (Fig 2.2 B, C), in which GFP-CPEB2 transfected primary neural cultures is broadly expressed, including in both the dendritic and axonal projections. The synaptosomes preparations presented here demonstrate endogenous CPEB2 is also located in synapses.

Figure 3.4

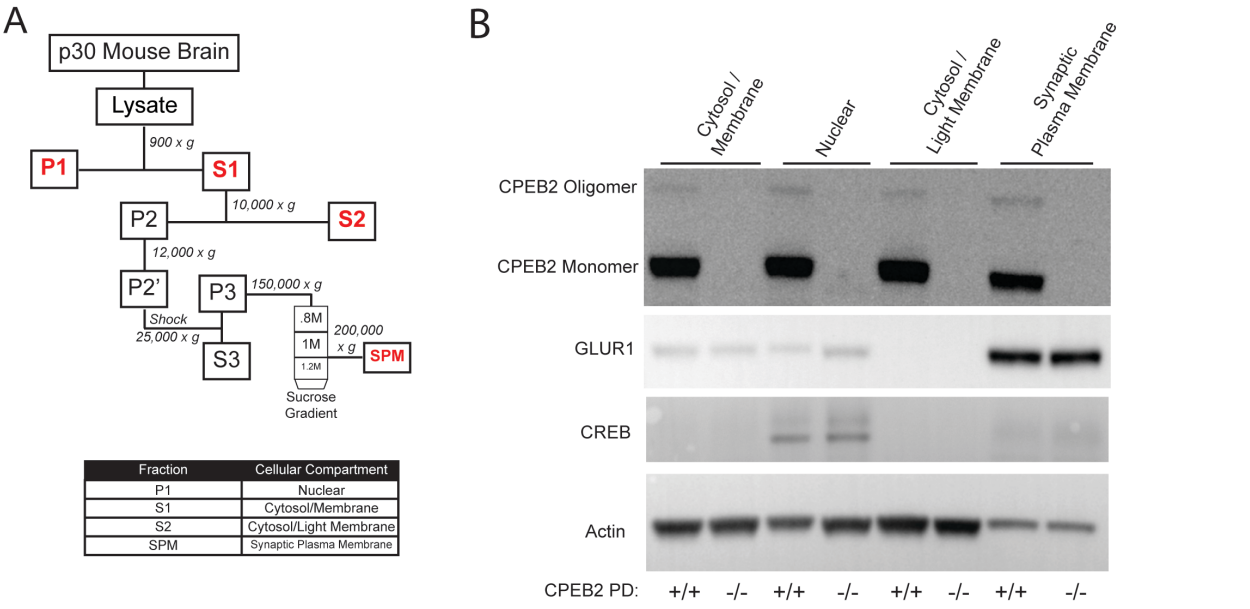

Figure 3.4 CPEB2 is detected in synaptic fractions. Preparation of synaptic membranes from wild-type and CPEB2 PD$^{-/-}$ brains. **(A)** Diagram of synaptosome purifications protocol used to isolate distinct cellular fractions. Fractions in red were used for SDS-PAGE analysis. Table indicates cellular compartments in each fraction. **(B)** CPEB2 purifies with synaptic plasma membrane. Western blot of cellular compartment fractions. Immunoblotted for CPEB2 and subcellular markers of the different cellular compartments: GluR1 (synaptic plasma membrane), CREB (nuclear), and actin (loading control). GluR1 is exclusively in the synaptic plasma membrane, indicating successful isolation of the synaptic plasma membrane. Monomeric and oligomeric CPEB2 is present in all fractions including synaptic plasma membrane from wild-type brains.

Discussion

CPEB2 as a translational regulator

CPEB2 is an RNA-binding protein hypothesized to regulate translation by binding to the 3' UTR of mRNAs. In this chapter, we establish by polysome profiling that CPEB2 exists in mRNA fractions undergoing all stages of translation. Interestingly, CPEB2 is present in fractions containing polysome bound RNAs. By using control gradients in which ribosomes are dissociated, the results show that CPEB2 is absent from the polysome fractions that contain mRNAs bound to multiple ribosomes. The association of CPEB2 with mRNAs that are being actively translated, suggests CPEB2 acts as a translational regulator. Does CPEB2 repress or activate these transcripts? Generally, proteins that interact with polysomes and their associated mRNA are translational activators or elongation inhibitors that act to stall the translational machinery (Chen & Huang, 2012; Darnell et al., 2011). Intriguingly, CPEB2 is proposed to be an elongation inhibitor. This hypothesis originates from *in vitro* studies demonstrating that CPEB2 binds to the hypoxia-inducible factor-1α (HIF-1α) mRNA in Neuro-2a cell lysates (Chen & Huang, 2012). In Neuro-2a cells cultured under normoxic conditions, the longest CPEB2 isoform binds to elongating HIF-1α mRNA and eukaryotic elongation factor 2 (eEF2). When bound to CPEB2, eEF2 stalls the translation of HIF-1α by inhibiting the GTP hydrolysis required for translocation of the ribosome. However, under hypoxic conditions, CPEB2 dissociates from the HIF-1α mRNA and removes eEF2 repression. This novel form of regulating elongating mRNAs has been proposed to be a mechanism that rapidly alters translational activity in response to environmental stimuli. If true, actively translating mRNAs or mRNAs stalled during

elongation would both be present in the polysome fractions. Our results extend these observations by showing *in vivo* that CPEB2 binds to mRNA associated with polysomes.

To determine if CPEB2 acts as a repressor or activator, we should consider these findings in conjunction with our analysis of CPEB2 targets expression. Examination of CPEB2 targets in the CPEB2 $PD^{-/-}$ model found that CAMKIIa expression is increased in the brain and hippocampus. Although we cannot conclude that CAMKIIa translation is directly regulated by CPEB2 because we did not establish this *in vitro*, other groups have demonstrated CPEB2 binds to CAMKIIa mRNA *in vitro* (Turimella et al., 2015). If indeed CPEB2 does act as translational regulator of CAMKIIa, our results would suggest the full length CPEB2 protein acts as a translational inhibitor. In conjunction with CPEB2 being present in the polysome, CPEB2 may regulate the expression of CAMKIIa by acting to stall translation.

However, CPEB2 also activates the translation of GRASP1. Previously it was shown that in cultured neurons grown from the restricted CPEB2 knockout, the protein levels of GRASP1 are decreased (Lu et al., 2017). We did not observe a change in GRASP1 protein *in vivo*. Likewise, in the forebrain restricted removal of CPEB2, no changes were observed in CaMKIIa expression (Lu et al., 2017). However, we assayed protein levels *in vivo*, while Lu et al., assayed protein levels in cultured hippocampal neurons. From our own experience using hippocampal neurons, CAMKIIa protein levels are even more pronounced, but we did not examine GRASP1 using this approach. It is difficult to reconcile these findings, since the LTP and memory deficit in the forebrain restricted CPEB2 knock can be rescued by viral transduction of GRASP1 into the hippocampus (Lu et al., 2017). Further studies examining GRASP1 expression in the CPEB2 $PD^{-/-}$ *in vitro* would help elucidate these differences.

CPEB1 and CPEB3 in mice, and Orb2/CPEB in *Drosophila* act as both translational activators and translational repressors. As discussed in the introduction, CPEB1 acts as a translational activator or repressor dependent on its phosphorylation state. Orb2 and CPEB3 translational activity depends on their conformational state. In both cases, the monomer represses translation. But when activated and converted to its oligomeric state, these proteins become translational activators (Fioriti et al., 2015; Khan et al., 2015). Although CPEB2 oligomerizes, the role of CPEB2 oligomer has yet to be determined.

In all, if we consider that we did identify that a CPEB2 target is misregulated in the CPEB2 $PD^{-/-}$ model, we can presume that the full-length CPEB2 is required for CAMKIIa regulation. Further, the complete CPEB2 knockout is perinatally lethal due to translational repression of ChAT and likely other mRNAs. It should be noted that potentially many other genes are also dysregulated in this model. However, CPEB2 $PD^{-/-}$ mice are viable, thus we hypothesize that the truncated CPEB2 protein is sufficient to maintain translational regulation during development. Therefore, we propose that the different CPEB2 isoforms have distinct effects on translation.

CPEB2 localizes to the synapse

The final experiments in this chapter found that CPEB2 is present at the synapse. Using a synaptosome preparation, we show CPEB2 is expressed in the cytosolic, nuclear, light membrane, and synaptic fractions. Observing CPEB2 expression at the synapse is critical for understanding CPEB2's role in long-term memory and long-term potentiation. CPEB3 in mice and apCPEB in *Apylsia* regulate translation at the synapse. Like apCPEB and CPEB3, we

observed both the oligomer and monomer of CPEB2 at the synapse (Fig 3.4B). However, because CPEB2 is expressed in multiple compartments, we were unable to determine CPEB2's primary site of action. Localization of CPEB2 to the synapse established a potential site of action for the experiments in the next chapter testing whether the loss of CPEB2 disrupts LTP and long-term memory.

Chapter 4: CPEB2 is required for synaptic plasticity and long-term memory

CPEB2 as a regulator of synaptic plasticity

The results in Chapters 2 and 3 identified key features of CPEB2 that are characteristic of other proteins implicated in synaptic plasticity. Chapter 3 described how CPEB2 interacts with translating mRNA, affects levels of proteins required for LTP, and localizes to the synapse (the cellular "unit" of learning and memory). Chapter 2 provides evidence that CPEB2 is a putative prion-like protein, like CPEB3 or Orb2, both of which use activity-dependent prion-like conversions to regulate synaptic plasticity *in vivo*. Indeed, full-length CPEB2 oligomerizes, yet when the amino acid sequence encoded by exon 1 is removed in CPEB2 $PD^{-/-}$, this abrogates CPEB2's oligomeric features.

This chapter seeks to go beyond characterization of CPEB2 protein features and seeks to determine what role CPEB2 plays in synaptic plasticity and long-term memory in mice. That the full-length CPEB2 KO is early postnatal lethal, but CPEB2 $PD^{-/-}$ mouse, which still produces a truncated form of CPEB2, has normal development and lifespan hints at CPEB2 isoforms having different functions *in vivo*. At least a truncated form of CPEB2 is sufficient to support life. An initial clue was apparent in the model whereby removal of full-length CPEB2 is restricted to the forebrain and hippocampus yields viable, developmentally normal mice. In turn, as these mice survived into adulthood, it became clear that a lack of full-length CPEB2 in the hippocampus led to disruptions in the formation of LTP and memory (Lu et al., 2017). Having identified CPEB2 prion-like domain resides in exon 1, and CPEB2 $PD^{-/-}$ aging normally into adulthood, we sought to resolve whether CPEB2 isoform bearing the prion-like domain CPEB2 is required to support

LTP and memory *in vivo*. Thus, we inquired whether CPEB2 PD$^{-/-}$ mice exhibit disrupted synaptic plasticity and learning.

As a first step, we used electrophysiological hippocampal slice recordings to determine if synaptic plasticity in CPEB2 PD$^{-/-}$ mice. Historically, hippocampal slices are the most commonly used model system to study LTP *ex vivo* because the hippocampal circuitry is well described and clearly visualized. Moreover, perpendicular slices along the long axis of the hippocampus allows preservation of neuronal connections. Two essential components of the hippocampal circuitry studied here involve the CA1 and CA3 regions. Each of these host a layer of readily visible pyramidal neurons. CA3 pyramidal cells form synaptic connections with pyramidal neurons in CA1 stratum radiatum, via an axon bundle known as Schaffer collaterals. The simplicity of the hippocampal circuit allows researchers to provide isolated stimulation to CA3 axons and record the responses evoked in CA1 neurons (Fig 4-1A).

In these experiments, hippocampal slices were obtained from 1 month of age wild-type and CPEB2 PD$^{-/-}$ mice. The slices were kept alive by superfusing with gassed artificial cerebrospinal fluid (ACSF). For the recording phase, the slices were visualized under a microscope and the extracellular field excitatory postsynaptic potentials (fEPSPs) were monitored using a glass recording electrode in CA1 (Fig 4-1A). We first measured the baseline response and excitability of CA1 neurons by stimulating CA3 axons with an electrode placed in the Schaffer collaterals (Fig 4-1A). When stimulated, CA3 axons release glutamate at their synaptic connections with CA1 neurons. The amplitude of the fEPSP reflects the degree of activation of CA1 neurons (insets in Fig 4-1B). Both the slope of the fEPSP and the fiber volley in response to stimulation of the Schaffer collaterals are recorded. The fiber volley represents presynaptic action potentials in CA3 axons evoked by the stimulus. As the stimulation amplitude is increased, the fiber volley increases

as more axons are activated. Similarly, as more axons are recruited and release more glutamate, the fEPSP amplitude increases. To determine if there are differences in the Schaffer collateral–CA1 synaptic connectivity between wild-type and CPEB2 $PD^{-/-}$ mice, the slope of fEPSP and fiber volley amplitude in the CA1 are determined at increasing strengths of CA3 stimulation. The plots of fEPSP slope versus fiber volley amplitude are similar in wild-type and CPEB2 $PD^{-/-}$ mice and suggest there are no functional differences in the basic synaptic connectivity in these genotypes.

Next, two-types of synaptic plasticity at the Schaffer collateral-CA1 synapses were evaluated. The first experiment assessed short-term plasticity. When CA3 neurons are stimulated with two pulses (paired-pulses) of equal amplitude that are delivered at brief inter-pulse intervals, each pulse evokes a fEPSP that reflects the responses of the CA1 neurons. If a second stimulus is provided within a brief interval, a stronger fESPS is generated relative to the first pulse. This facilitation is measured as the ratio of the response amplitudes evoked by the second stimulus to the first stimulus, the "paired-pulse ratio". A positive paired-pulse ratio indicates pair-pulse facilitation (PPF) occurred, a form of short-term plasticity (Zucker & Regehr, 2002). We measured the paired-pulse ratio in hippocampal slices from both wild-type and CPEB2 $PD^{-/-}$ mice at one month of age. As expected, slices from wild-type mice demonstrate positive paired-pulse ratios at 25, 50, 75, 100, and 200ms inter-pulse intervals (Fig 4-1D). Strikingly, CPEB2 $PD^{-/-}$ slices fail to show positive pair-pulse ratios at any of the inter-pulse intervals tested (Fig 4-1D). Thus, PPF is absent at the Schaffer collateral-CA1 synapses in one month old CPEB2 $PD^{-/-}$ mice, which suggests a deficit in short term plasticity.

Figure 4.1

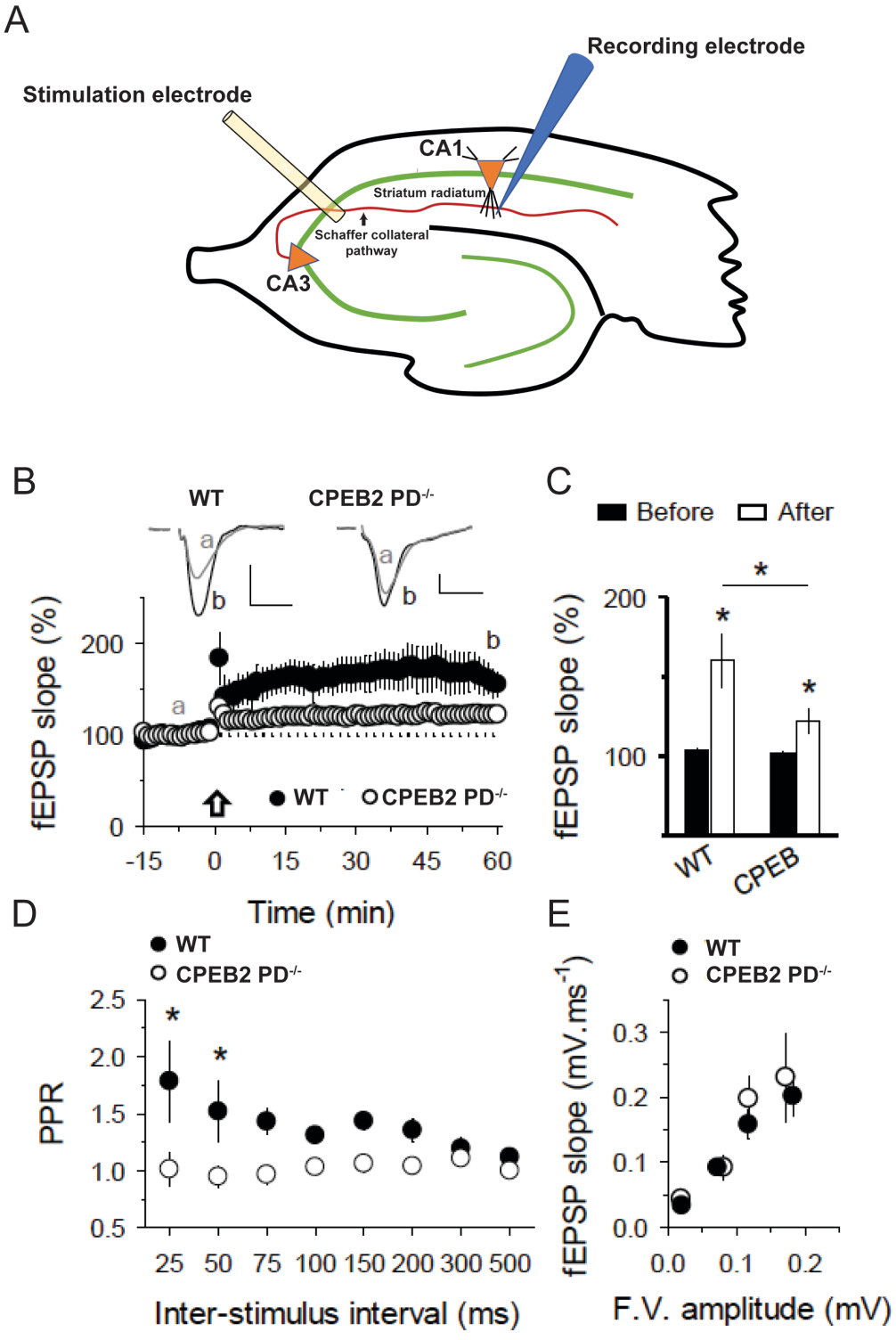
A
Recording electrode
Stimulation electrode
CA1
Striatum radiatum
Schaffer collateral pathway
CA3
B
WT
CPEB2 PD-/-
a
b
fEPSP slope (%)
200
100
0
-15
0
15
30
45
60
WT
CPEB2 PD-/-
C
Before
After
fEPSP slope (%)
200
100
WT
CPEB
D
Time (min)
WT
CPEB2 PD-/-
PPR
2.5
2.0
1.5
1.0
0.5
25
50
75
100
150
200
300
500
Inter-stimulus interval (ms)
E
WT
CPEB2 PD-/-
fEPSP slope (mV.ms-1)
0.3
0.2
0.1
0.0
0.0
0.1
0.2
F.V. amplitude (mV)

Figure 4.1 Young CPEB2 PD$^{-/-}$ mice show decreased LTP and PPF in the hippocampus. Hippocampal slices were prepared from p15-p30 wild-type and CPEB2 PD$^{-/-}$ mice. **(A)** Schematic representation of transverse hippocampal slice with electrodes to stimulate and record field excitatory postsynaptic potentials (fEPSP) from neurons in the stratum radiatum of the CA1 region. **(B)** LTP is reduced in CPEB2 PD$^{-/-}$ mice. fEPSP were recorded in the CA1 region after stimulation of Schaffer collaterals. Long-term potentiation was induced by 4 trains of 100-Hz high frequency stimulation (HFS) at time 0 min (black arrow). Graph is normalized fEPSP slope vs time. Sample traces represent average fEPSP 5 min before (grey) and last 5 mins after (black) HFS. Scale bars: 0.1 mV, 15 ms. **(C)** Magnitude of LTP is reduced in CPEB2 PD$^{-/-}$ mice. Graph of normalized fEPSP slope before and 60 min after HFS in wild-type and CPEB2 PD$^{-/-}$ mice (n=6 and n=9, respectively). **(D)** CPEB2 PD$^{-/-}$ have decreased paired pulse ratio (PPR) at 25ms and 50ms inter-stimulus intervals. PPR obtained induced by two consecutive stimuli delivered at different time intervals in wild-type and CPEB2 PD$^{-/-}$ mice (n=11 and n=12, respectively). **(E)** Basal synaptic transmission is intact in CPEB2 PD$^{-/-}$ mice. Input–output (I–O) curves of fiber volley (F.V.) amplitude vs fEPSP slope relationship in wild-type and CPEB2 PD$^{-/-}$ mice (n=11 and n=12, respectively). Data are represented as mean ± SEM. Normality was verified with a Shapiro-Wilk test. For LTP experiments results were compared using two-tailed Student's t-test (α=0.05). For PPR and input-output relationship, data were compared using a two-way ANOVA with Holm-Sidak post hoc. Statistical differences were established as $P<0.05$ (*).

Next, we examined whether LTP in CPEB2 PD$^{-/-}$ hippocampal slices is also impaired. To induce LTP, high-frequency stimulation (HFS) consisting of four 100 Hz stimulus trains lasting 1 second at 30 second intervals was applied to Schaffer collaterals. The synaptic response before (for 15 min) and after (for 60 min) the HFS was assessed by applying single stimulation pulses at 0.33 Hz to the Schaffer collaterals and recording the evoked fEPSP in the stratum radiatum region of the CA1 (Fig 4-1B, compare before and after black arrow). To determine if HFS induced long-lasting synaptic potentiation (L-LTP), the baseline fEPSP responses obtained from the last 5 minutes before HFS were compared to the responses obtained from the last 5 minutes after HFS. In wild-type slices, the baseline response increase to158% after HFS, indicating LTP was elicited (Fig 4-1B). In CPEB2 PD$^{-/-}$ slices, the response increased to 120% after HFS, but this increase is considerably smaller (P value) than in wild type (Fig 4-1B, C). These results demonstrate CPEB2 PD$^{-/-}$ mice have a significant LTP deficit in the CA3-CA1 synapse at one month of age.

Given the lack of LTP deficits in the global CPEB1$^{-/-}$ and CPEB4$^{-/-}$ mouse models, it has been conjectured that the CPEB1-4's function overlaps. Following this logic, if one member is removed, another might compensate for the loss of function over time. To address whether the LTP deficit in CPEB2 PD$^{-/-}$ mice is sustained over time, hippocampal CA3-CA1 plasticity was also assayed in aged CPEB2 PD$^{-/-}$ mice using hippocampal slices from six to eight-month-old mice.

The Shaffer collateral-CA1 input–output relationships were again indistinguishable in wild-type and CPEB2 PD$^{-/-}$ mice (Fig 4-2D). At six months of age, paired-pulse ratio was again significantly impaired in CPEB2 PD$^{-/-}$ slices at 25, 50, 75 inter-pulse intervals (Fig 4-2C). Interestingly, the paired-pulse ratio of CPEB2 PD$^{-/-}$ animals was significantly higher in six-month-old mice than was observed at one month (Fig 4-2C and Fig 4-1D). While the CPEB PD$^{-/-}$ paired-

pulse ratio is still reduced relative to the wild-type animals, the degree of the deficit decreased over time. This suggests short-term plasticity in the hippocampus likely improved with age in CPEB2 $PD^{-/-}$ mice.

LTP was also evaluated in aged animals. A normal LTP response was elicited in wild-type with HFS (Fig 4-2A). Strikingly, at this older age, a difference in LTP between wild type and CPEB2 $PD^{-/-}$ slices was no longer evident (Fig 4-2A, B). Thus, LTP was restored in the CPEB2 $PD^{-/-}$ aged mice. Together these results indicate oligomeric CPEB2 is necessary for mouse hippocampal synaptic plasticity in early life. With age, perhaps other synaptic regulatory proteins normally replace CPEB2 in this role, or in the case of CPEB2 $PD^{-/-}$, other protein(s) emerge to compensate for this deficit.

Figure 4.2

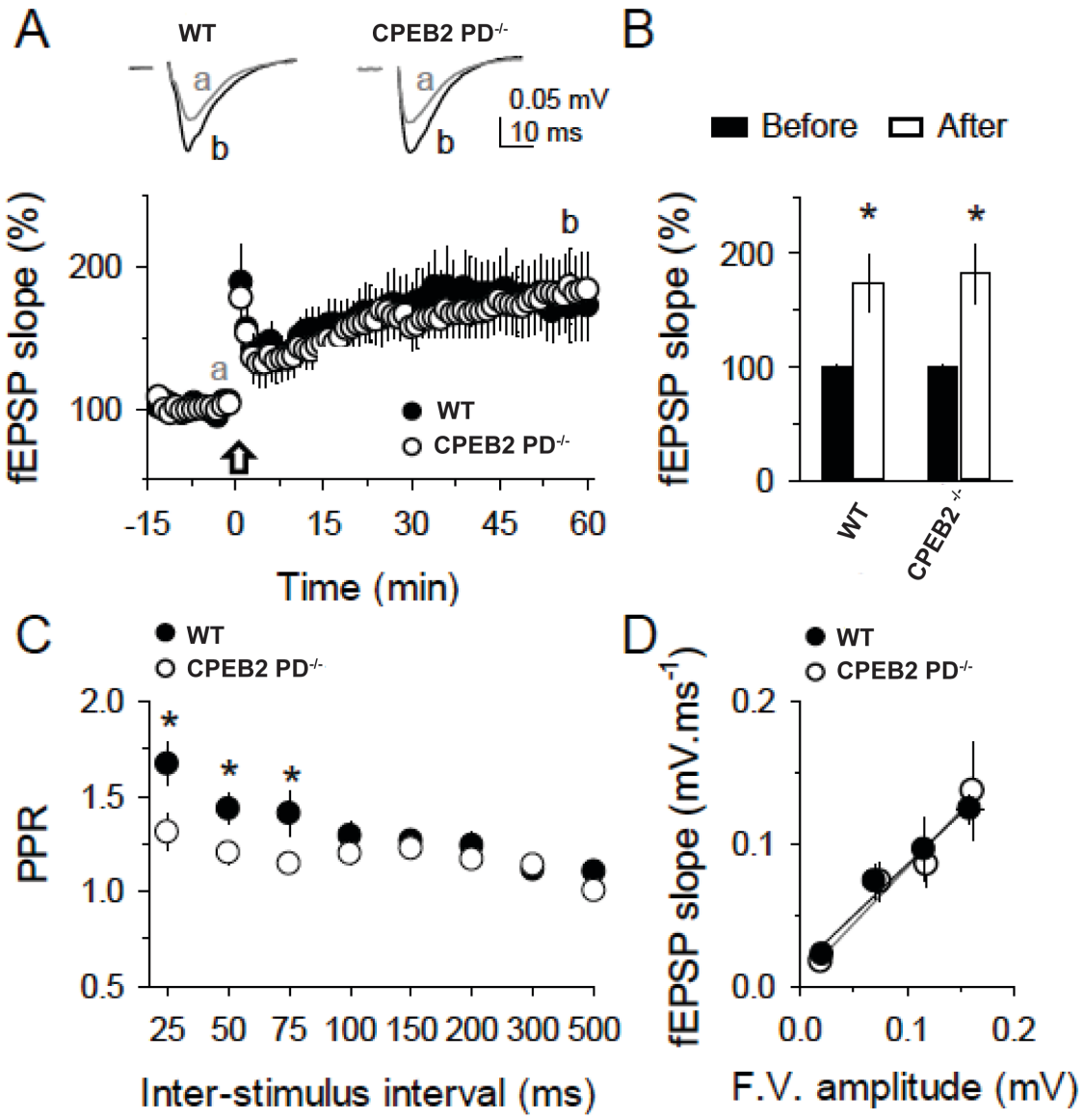
A
WT
CPEB2 PD-/-
a
b
0.05 mV
10 ms
fEPSP slope (%)
200
100
a
b
WT
CPEB2 PD-/-
-15
0
15
30
45
60
Time (min)
B
Before
After
fEPSP slope (%)
200
100
0
*
*
WT
CPEB2 -/-
C
WT
CPEB2 PD-/-
PPR
2.0
1.5
1.0
0.5
*
*
*
25
50
75
100
150
200
300
500
Inter-stimulus interval (ms)
D
WT
CPEB2 PD-/-
fEPSP slope (mV.ms-1)
0.2
0.1
0.0
0.0
0.1
0.2
F.V. amplitude (mV)

Figure 4.2 Aged CPEB2 PD$^{-/-}$ mice show intact LTP and impaired PPF in the hippocampus. Hippocampal slices were prepared from 6-8 months old wild-type and CPEB2 PD$^{-/-}$ mice. **(A)** fEPSP were recorded in the CA1 region after stimulation of Schaffer collaterals. Long-term potentiation was induced by 4 trains of 100-Hz high frequency stimulation (HFS) at time 0 min (black arrow). Graph of normalized fEPSP slope vs time. Samples traces represent average fEPSP at 5 min before (grey) and during last 5 mins after (black) HFS. **(B)** Intact LTP in aged CPEB2 PD$^{-/-}$ mice. Graph of normalized fEPSP slope before and 60 min after HFS in wild-type and CPEB2 PD$^{-/-}$ mice (n=8 and n=8, respectively). **(C)** CPEB2 PD$^{-/-}$ have decreased paired pulse ratio (PPR) at 25ms, 50ms, and 75ms inter-stimulus intervals. PPR obtained induced by two consecutive stimuli delivered at different time intervals in wild-type and aged CPEB2 PD$^{-/-}$ mice (n=12 and n=11, respectively). **(D)** Basal synaptic transmission is intact in aged CPEB2 PD$^{-/-}$ mice. Input–output (I–O) curve of fiber volley (F.V.) amplitude vs fEPSP slope relationship in wild-type and CPEB2 PD$^{-/-}$ mice (n=14 and n=13, respectively). Data are represented as mean ± SEM. For LTP experiments results were compared using a two-tailed, paired Student's t-test (α=0.05). For PPR and input-output relationships results were compared using a two-tailed Student's t-test (α=0.05). Statistical differences were established as $p<0.05$ (*).

CPEB2 PD$^{-/-}$ mice display impaired long-term memory

The electrophysiological results demonstrate that exon 1 of CPEB2 is required for synaptic plasticity in young mice. We hypothesized that young CPEB2 PD$^{-/-}$ mice should exhibit impairments in behavioral learning and memory tasks. Given that CPEB2 PD$^{-/-}$ synaptic plasticity deficits were identified in the hippocampus, we used two hippocampal-dependent behavioral paradigms that test long-term memory: 1) contextual inhibitory avoidance and 2) Morris water maze.

To correctly interpret these memory-dependent behavioral tests, we first determined whether knocking out the CPEB2 prion-like domain results in motor deficits or other behavioral changes. To this end, we used the open-field test (OFT) to assay general locomotor performance and anxiety levels in CPEB2 PD$^{-/-}$ mice. The open-field test consists of a large box apparatus with a brightly illuminated center field (Fig 4-3A). Mice are placed in the apparatus for ten minutes and their velocity and location relative to the center are recorded to assess for motor deficits (Fig 4-3A). Mice naturally avoid open and well-lit areas where they might be visible to predators. Therefore, when placed in the open field arena, mice display a balance between avoiding the open field and exploring a new environment (Crawley, 2008; Hitzemann, 2000; Post et al., 2011). In the OFT, mouse models with increased anxiety avoid exploring the open field near the center of the box and spend more time at the periphery.

Figure 4.3

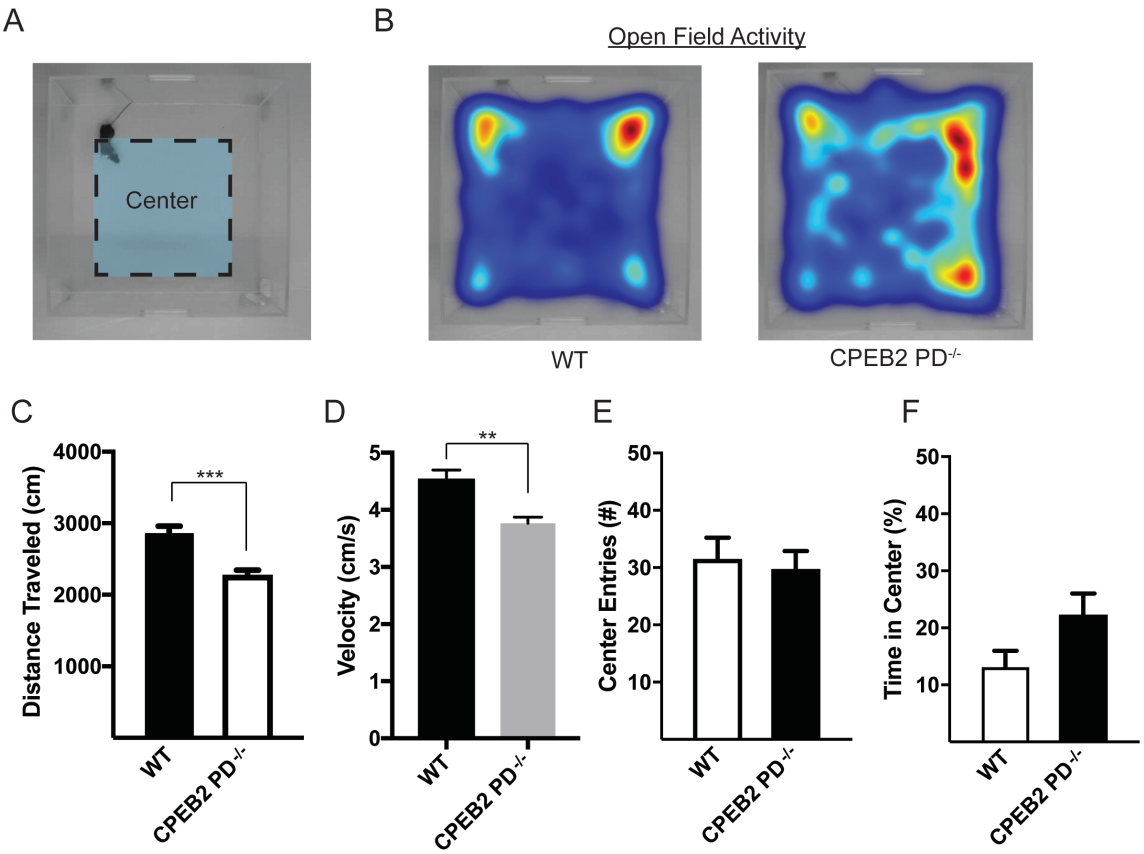

Figure 4.3 CPEB2 PD$^{-/-}$ mice exhibit motor deficit but do not display increased anxiety in open-field test. Open field test at 3 months of age for CPEB2 PD$^{-/-}$ and wild-type littermates (mice n=6 and n=8 respectively). **(A)** Schematic of zones in open field area. **(B)** Cumulative heat maps depict the time and movement spent in open field arena across all trials for wild-type and CPEB2 PD$^{-/-}$ mice. Color maps indicates mice spent increased time in a particular area, with red more and blue less time **(C)** CPEB2 PD$^{-/-}$ mice travel less than wild-type mice. **(D)** CPEB2 PD$^{-/-}$ mice have lower average velocity than wild-type mice. **(E and F)** CPEB2 PD$^{-/-}$ mice exhibit normal anxiety **(E)** CPEB2 PD$^{-/-}$ and wild-type mice enter the center zone with the same frequency. **(F)** CPEB2 PD$^{-/-}$ and wild-type mice spend similar amounts of time in the center zone. Data are represented as mean ± SEM. *p<0.05, unpaired Student's test.

In the OFT, both wild-type and CPEB PD$^{-/-}$ mice display preference for the edges of the box (Fig 4-3B, the red indicates the areas where mice were located the majority of the test). Interestingly, CPEB2 PD$^{-/-}$ mice travel significantly less than wild-type mice (Fig 4-3C) and this likely accounts for their reduced velocity (18%) (Fig 4-3D). Concerning the possibility of an anxiety phenotype, the number of times the mice entered the center of the box or the percent time spent inside the center was not statically significant between genotypes (Fig 4-3E, F). Given the animals similarly explore the center of the box (a novel area), the decrease in locomotion observed in CPEB2 PD$^{-/-}$ mice is less likely to be due to increased anxiety levels. However, the reduced travel distance suggests CPEB2 PD$^{-/-}$ mice may have a mild locomotor impairment.

The first test of long-term memory formation and persistence, we used a modified contextual fear conditioning paradigm (CFC). This involves learning contextual information and emotional information. The apparatus consists of a chamber with a brightly illuminated open field connected to a dark shock compartment (Fig 4-4A). The paradigm trains mice to form a stable association between the dark compartment (context) and a noxious stimulus (foot shock) (Curzon, Rustay, & Browman, 2009; Huff, Emmons, Narayanan, & LaLumiere, 2016; Wehner & Radcliffe, 2004). On the first day of training, the mouse is placed in the illuminated side of the apparatus. The mouse's natural behavior is to retreat into the dark compartment. When the mouse enters the dark compartment, the animal receives a mild foot shock and is immediately removed from the dark chamber. The foot shock establishes a negative relationship between the comforting (dark) space and a negative stimulus (shock). It has been well-established that contextual fear conditioning is a form of learning dependent on the hippocampus and amygdala (Phillips & LeDoux, 1992). To determine if the mouse has formed a long-term memory of the incident, the mouse is returned to the illuminated chamber 48 hours later, and the latency of the

mouse to cross into the dark compartment recorded. If the mouse has formed a strong association between the dark compartment and the shock stimulus, the animal avoids returning to the dark compartment, despite the instinctual unlearned drive to do so. The longer it takes for the animal to enter the dark compartment indicates a stronger memory. The "strength" of this memory can be reassessed over time, without additional training, by returning the mouse to the same illuminated chamber (Fig 4-4B).

Using this paradigm, we assessed long-term memory formation in 2-3 months of age CPEB2 $PD^{-/-}$ mice and their wild-type littermates. When returned to the illuminated chamber 48 hours after training, wild-type animals appropriately avoid re-entering the dark compartment (average latency of 560 ± 148s, SD) (Fig 4-4C). Strikingly, CPEB2 $PD^{-/-}$ mice more readily enter the dark chamber, with a significantly reduced latency-to-enter compared to wild-type controls (average latency of 342 ± 239s, SD) (Fig 4-4C). These results show that CPEB2 $PD^{-/-}$ mice have a decreased ability to form long-term memory compared to wild-type littermates. To test the stability of this memory, the latencies were also measured at one week, two weeks, one month, and two months after initial training. Across all additional time points, wild-type animals demonstrate greater latencies (>400s) than CPEB2 $PD^{-/-}$ mice (<280s) (Fig 4-4C). For a control, we undertook a mock training phase in which wild-type and CPEB2 $PD^{-/-}$ mice performed the task without receiving the foot shock when they entered the dark compartment. After the mock training, wild-type and CPEB2 $PD^{-/-}$ mice tested at 48 hours, one week, two weeks, and one month show no avoidance of the dark compartment (Fig 4-4D). Together these findings suggest CPEB2 $PD^{-/-}$ mice have impaired contextual long-term memory.

Figure 4.4

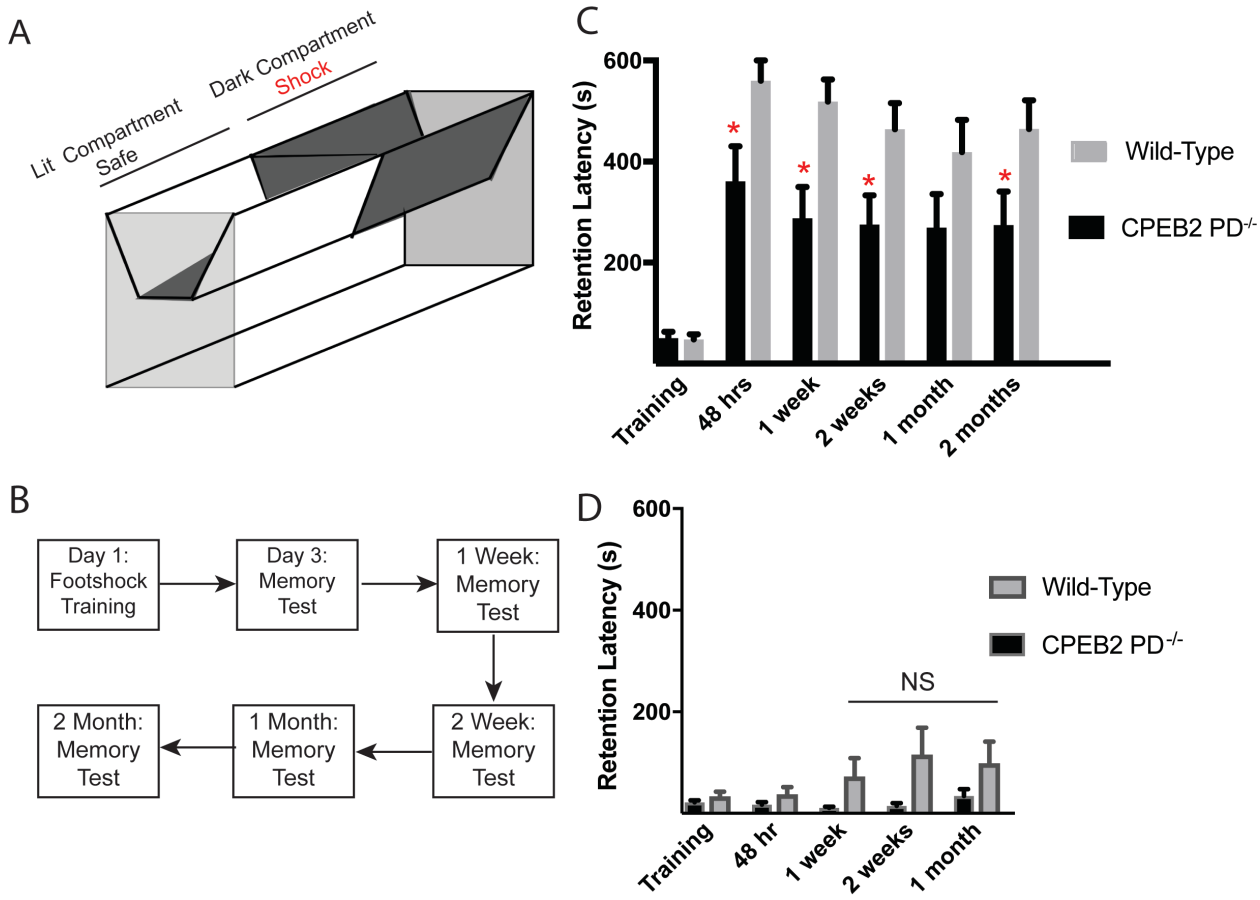

Figure 4.4 Long-term contextual memory deficit in CPEB2 PD$^{-/-}$ mice. Modified contextual fear conditioning (CF) test of CPEB2 PD$^{-/-}$ mice and wild-type littermates at 3 months of age (mice n=7 and n=8 respectively). **(A)** Diagram of inhibitory avoidance apparatus used in modified CFC. **(B)** Schematic of the training paradigm for behavior training and memory testing. **(C)** Retention impairment in CPEB2 PD$^{-/-}$ mice. Inhibitory avoidance behavior was assayed by recording the latency for each mouse to cross into the dark chamber. Graph of the latency for each group in which greater retention latencies indicate more stable memory. CPEB2 PD$^{-/-}$ mice exhibit decreased retention latencies at 48 hours, 1 week, 2 weeks, and 2 months after footshock training. **(D)** Mice received mock training on day 1 with no footshock. Neither genotype avoided entering into the dark compartment. Data are represented as mean ± SEM. Data were compared using a two-way ANOVA with Holm-Sidak post hoc. Statistical differences were established as $p<0.05$ (*).

The CFC paradigm uses a short one-day training period that produces a robust long-lasting memory. We next asked whether CPEB2 PD$^{-/-}$ mice could form long-term memory in another hippocampal based memory paradigm, the Morris water maze (MWM), which uses a longer and more robust training period (Morris, 1984). The MWM consists of circular pool of water surrounded on each axis by four large distal visual cues. An accessible submerged hidden platform is in one quadrant of the pool (called the platform zone) (Fig 4-5A). The MWM tests spatial learning by training the mice to use distal cues to form a hippocampal-dependent map of the location of the submerged platform (Vorhees & Williams, 2006). The spatial map is formed during repeated training trials when the mice are placed in different starting locations in the pool. During the three days of training a normal mouse learns the location of the hidden platform relative to the distal cues (Fig 4-5B). Each day, the mice are trained with four two-minute trials from predetermined starting positions. after three days of training, long-term spatial memory is assessed in a probe trial given 24 hours later. After the training period, the spatial learning is measured by removing the hidden platform. Mice that generated a strong spatial map will spend the majority of the probe time searching the target quadrant (TQ) that previously contained the platform.

Using this paradigm, we assessed the ability of 2-3 months of age CPEB2 PD$^{-/-}$ mice and their wild-type littermates to form-long term memory. As a measure of long-term memory, we first determined the escape latency, the time required for the mouse to reach the platform with training. Both genotypes demonstrate normal learning acquisition, with a daily improvement in the ability to locate the platform on each successive day of training (Fig 4-5C). On the first probe trial, wild-type mice have a moderate preference for the TQ, while the CPEB2 PD$^{-/-}$ mice do not. However, there was no statistical difference between the two genotypes for the duration

of the time spent in TQ (Fig 4-5D, comparing TQ duration of both genotypes). After three additional trainings, a second probe trial was given. The second probe trial show that both wild-type and CPEB2 PD$^{-/-}$ mice are able to form a statistically significant preference for the time spent in TQ (Fig 4-5E). Again, there was no difference between genotypes (Fig 4-5E). A more precise measure of hippocampal-dependent spatial map formation is based on analyzing the animals' searching patterns, quantifying the occupancy time in the area immediately above the platform, the platform zone (Nakazawa et al., 2002). During the first probe trial, CPEB2 PD$^{-/-}$ mice spend significantly less time searching in the platform zone compared to wild-type (Fig 4-5F, G). With additional training, wild-type and CPEB2 PD$^{-/-}$ mice spend the same amount of time searching for the platform zone (Fig 4-5G). The hippocampal memory-dependent special tasks presented here suggest CPEB2 PD$^{-/-}$ mice have moderately impaired memory recall in the MWM.

Figure 4.5

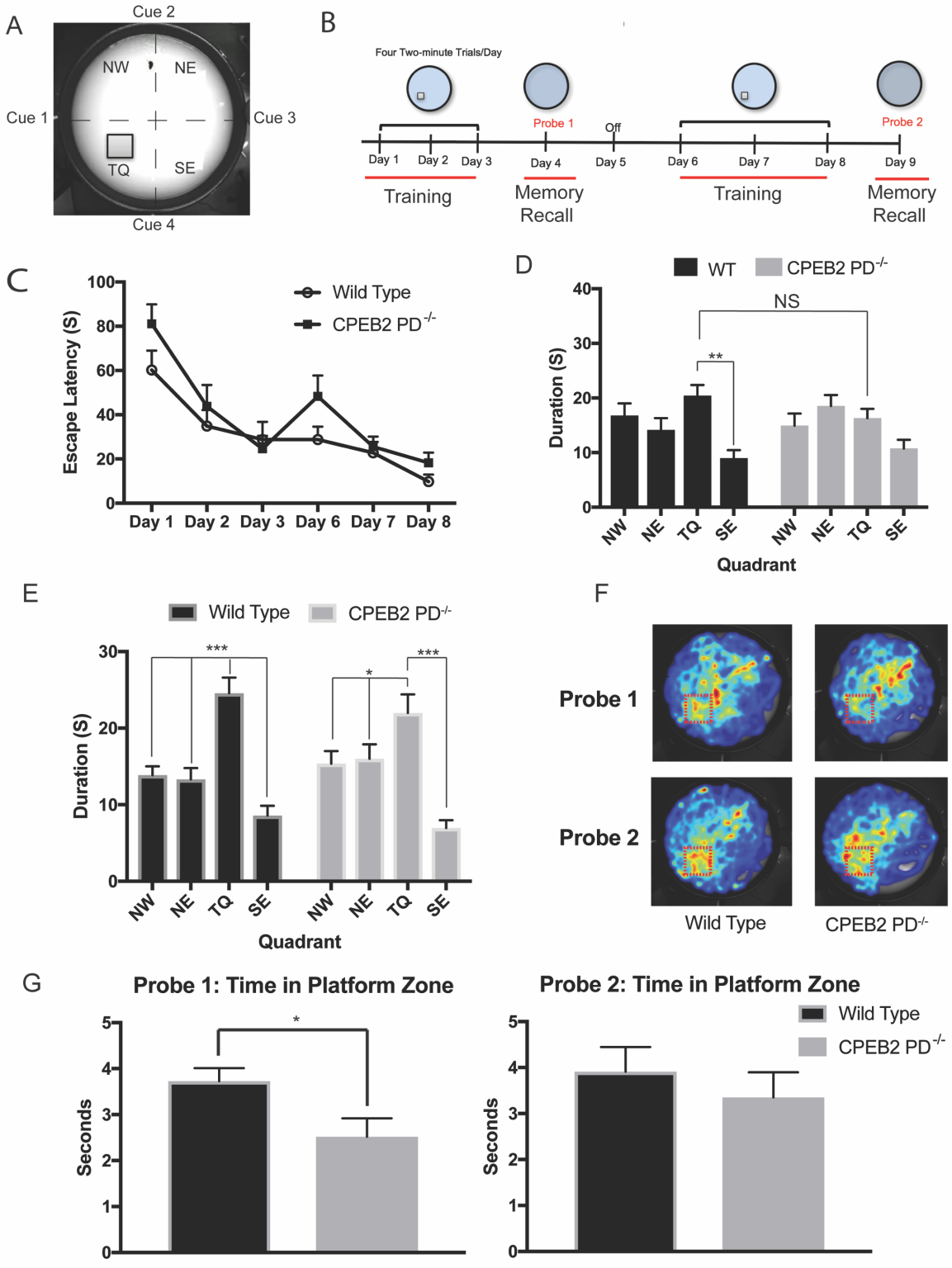
A
Cue 2
NW
NE
Cue 1
Cue 3
TQ
SE
Cue 4
B
Four Two-minute Trials/Day
Probe 1
Off
Probe 2
Day 1
Day 2
Day 3
Day 4
Day 5
Day 6
Day 7
Day 8
Day 9
Training
Memory Recall
Training
Memory Recall
C
Escape Latency (S)
Wild Type
CPEB2 PD-/-
Day 1
Day 2
Day 3
Day 6
Day 7
Day 8
D
WT
CPEB2 PD-/-
Duration (S)
NS
**
NW
NE
TQ
SE
Quadrant
E
Wild Type
CPEB2 PD-/-
Duration (S)
***
*
***
Quadrant
F
Probe 1
Probe 2
Wild Type
CPEB2 PD-/-
G
Probe 1: Time in Platform Zone
Seconds
*
Probe 2: Time in Platform Zone
Wild Type
CPEB2 PD-/-
Seconds

Figure 4.5 Intact learning and minor spatial memory deficit in CPEB2 PD$^{-/-}$ mice. Morris water maze (MWM) spatial memory task of CPEB2 PD$^{-/-}$ mice and wild-type littermates at 2-3 months of age (mice n=18 and n=17 respectively). **(A)** Image of MWM with labeled quadrants. Location of submerged platform is shown by grey square. **(B)** Diagram of MWM training and memory testing paradigm. Training days consisted of four two-minute trials per day with the platform place in the pool. Memory recall was assayed on days 4 and 9 by removing the platform and recording the mouse's position for 60 seconds. **(C)** Wild-type and CPEB2 PD$^{-/-}$ mice normally learned in the location of submerged platform within three days of training. Graphed is the average time each genotype took to find the platform on the first trial of each training day. **(D)** In the first probe trial, the platform was removed, and the percentage of time the mouse spent in each quadrant was recorded. Neither genotype showed a strong preference for the quadrant that previously contained the platform (TQ). **(E)** After three days of additional training, a second probe trial was performed. Both wild-type mice and CPEB2 PD$^{-/-}$ mice spent increased time searching the TQ where the platform was previously placed. **(F)** Cumulative heat maps from all trials of the searching patterns during both probe trials. Red box depicts exact location of previous platform (platform zona), as opposed to the quadrant with the platform (TQ). Quantified in G. **(G)** During probe, CPEB2 PD$^{-/-}$ mice search longer directly over the previous platform zone. Graphed is the average number of seconds the mice spend in platform zone for both genotype during probe 1 and 2. Data were compared using a two-way ANOVA with Bonferroni post hoc. Statistical differences were established as $P<0.05$ (*), $P<0.01$ (**) and $P<0.001$ (***).

Discussion

This chapter describes two important phenotypes resulting from the loss of CPEB2 PD in mice. At the circuit level, CPEB2 PD$^{-/-}$ mice exhibit a severe age-dependent LTP deficit. In behavioral testing, CPEB2 PD$^{-/-}$ mice display a pronounced long-term memory impairment in contextual fear conditioning and a moderate memory recall impairment in the Morris water maze.

CPEB2 is required for early age synaptic plasticity

Electrophysiological experiments using mouse hippocampal slices show that at 1 month of age, CPEB2 PD$^{-/-}$ lack both PPF and LTP. Paired pulse facilitation (PPF) is a form of activity-dependent synaptic plasticity that results when residual calcium in the axon terminal produced by the first pulse augments the response generated by the second pulse (L. G. Wu & Saggau, 1994). PPF is thought to serve as a mechanism for simple learning and rapid information processing (Fisher, Fischer, & Carew, 1997; Fortune & Rose, 2001). Originally, it was proposed that two key presynaptic factors regulate paired-pulse plasticity: the ready releasable pool of presynaptic vesicles (Rizzoli & Betz, 2005) and the calcium levels in the presynaptic terminal (Fioravante & Regehr, 2011). However, other studies argue that PPF also involves post-synaptic changes consisting of alterations in the number of available AMPA receptors at the post-synaptic site (Rozov & Burnashev, 1999; Rozov, Zilberter, Wollmuth, & Burnashev, 1998). Intriguingly, activated CAMKIIa works to stimulates AMPA receptor tracking to the post-synaptic membrane (Maletic-Savatic, Koothan, & Malinow, 1998). In Chapter 3, we demonstrate that CPEB2 PD KO$^{-/-}$ mice have increased levels of CAMKIIa, but do

not have altered levels of the AMPA receptor subunit, GluR1. Overall, we show that the CPEB2 containing amino acid sequence encoded by exon 1 is required to generate PPF in both young and aged mice and this is not rescued by production of truncated CPEB2.

Young CPEB2 $PD^{-/-}$ mice show a deficit in LTP. High frequency stimulation in 1 month old CPEB2 $PD^{-/-}$ mice results in a dramatic reduction in L-LTP compared to wild-type controls. These findings indicate CPEB2 is required for early-age LTP. Curiously, synaptic plasticity was restored in older CPEB2 $PD^{-/-}$ mice. At six months, CPEB2 $PD^{-/-}$ mice exhibit normal LTP and only moderately reduced PPF. The loss of early-age LTP may be due to changes in protein expression in neurons. We found increased levels of CAMKIIa protein in the CPEB2 $PD^{-/-}$ hippocampus. CAMKIIa is critical for LTP in young and adult animals (Wang et al., 2003). We also find that the recovery of LTP correlates with a recovery in CAMKIIa levels in the CPEB2 $PD^{-/-}$ adult mice (Appendix 2 A, B). The formation of LTP requires local translation of CAMKIIa mRNA in dendrites and synapses (Aakalu, Smith, Nguyen, Jiang, & Schuman, 2001; Miller et al., 2002) and CAMKIIa mRNA binds CPEB2 protein *in-vitro* (Turimella et al., 2015). Therefore, we propose that the alteration of CAMKIIa in CPEB2 $PD^{-/-}$, possibly through translational dysregulation, contributes to the LTP deficit in young mice.

To our knowledge, the CPEB2 $PD^{-/-}$ is the only mouse model that displays an age-dependent loss of LTP, being deficient in early life and restored later in adulthood. There are two possible explanations, 1) CPEB2 is required for synaptic plasticity in young mice, but not at six months of age or 2) other CPEB family members compensate for the loss of CPEB2 protein. One way to differentiate these two explanations is by examining the levels of CPEB2 expression. For example, normal loss of CPEB2 expression in aged wild-type mice would suggest CPEB2 is not required for adult LTP. However, we did not observe explicit differences in CPEB2

monomeric or oligomeric protein levels between young and aged wild-type mice, implying that other mechanisms are responsible for LTP recovery. An alternative mechanism is compensation by other CPEB family members with aging. In support of this possibility, the RNA binding domains of CPEB2-4 are 96% similar (Tsai et al., 2013), and the distinct CPEB family members bind the same mRNAs (Turimella et al., 2015). Global CPEB1 knockout mice display a LTP deficit with a weak stimulation protocol but normal LTP with strong stimulation protocols (Alarcon et al., 2004). The authors speculated that with stronger stimulation, other readily available CPEB proteins are recruited and compensate for the missing CPEB1. Regarding CPEB3, when it was knocked out from all tissues, the investigators found no LTP deficits (Chao et al., 2013). Yet when CPEB3 is selectively knocked out from the hippocampus, cortex, amygdala, LTP deficits were reported (Fioriti et al., 2015). Either through developmental changes or with greater activation, it appears that loss of CPEB function can be compensated for. As we do not find an increase in CPEB3 levels with age in the CPEB2 $PD^{-/-}$ mice (Fig 2-5A), we suggest that other CPEB family members compensate for the loss of CPEB2 with age.

These findings demonstrate the longest CPEB2 isoform is required for both PPF and LTP in young mice. It is notable that while the PPF does improve in aged CPEB2 $PD^{-/-}$ mice, it remains significantly reduced relative to wild-type. Homozygous knockout models of the RNA-binding protein, Ataxin-1, and heterozygous knockouts of CAMKII also demonstrate deficits in PPF with intact LTP (Matilla et al., 1998; Silva et al., 1996). These studies suggest that proper PPF is not required for the formation of LTP. However, our findings suggest that CPEB2 is capable of disrupting pathways required for both PPF and LTP in an age-dependent manner. Therefore, with further study, the CPEB2 $PD^{-/-}$ model could provide additional insights into understanding how these distinct forms of plasticity are regulated.

CPEB2 is required for long-term memory

We inquired whether disrupted PPF and LTP in CPEB2 $PD^{-/-}$ mice was reflected in behavioral correlates using two long-term memory paradigms. In the contextual fear condition paradigm, we found that CPEB2 $PD^{-/-}$ mice do not form a strong memory between a contextual conditioned stimulus and an unconditioned (learned) noxious stimulus and this memory deficit persists up to two months after training. Hippocampal-dependent long-term memory can be subdivided into two subcategories: spatial and contextual. These findings suggest that CPEB2 $PD^{-/-}$ mice are unable to form context-based long-term memories. Interestingly, in CPEB2 $PD^{-/-}$ mice although there is significant reduction in memory, the memory that was formed persisted for at least two months. These results suggest there are CPEB2 independent pathway that are sufficient to form some low level but stable memory. We speculate that in aged animals, similar pathways may also explain the lack of memory phenotype.

A less robust phenotype was observed in the Morris water maze. Wild-type animals performed better early in the task (probe 1), but with additional training the performance of CPEB2 $PD^{-/-}$ mice became virtually indistinguishable from wild-type controls (probe 2). This indicates long-term spatial memory formation was delayed in the CPEB2 $PD^{-/-}$ mice. However, given that CPEB2 $PD^{-/-}$ mice perform close to wild-type levels on all but one of the MWM measures, we speculate that spatial tasks are less dependent on CPEB2. These seemingly contradictory findings are intriguing, as CPEB2 $PD^{-/-}$ mice exhibit a strong deficit in the CFC task. While the MWM is thought to be strongly dependent upon the hippocampus, several reports have demonstrated impaired or absent CA1 LTP with normal spatial learning (Meiri, Sun, Segal, & Alkon, 1998; Montkowski & Holsboer, 1997; Zamanillo et al., 1999). However,

CFC requires both the amygdala and hippocampus (Phillips & LeDoux, 1992; Tayler, Tanaka, Reijmers, & Wiltgen, 2013). The differences in performance between these two tasks suggests the role of CPEB2 in CFC may involve the amygdala. In CPEB2 $PD^{-/-}$ mice, CPEB2 was removed from all tissues and CPEB2 function is likely critical in other brain regions, including the amygdala. In summary, the results presented in this chapter demonstrate that the CPEB2 containing the prion-like domain is required for synaptic plasticity and contextual long-term memory formation.

Chapter 5: Conclusions and future directions

Major findings

The body of work presented in this thesis suggest that CPEB2 is a putative prion-like protein and an essential molecule required for both synaptic plasticity and some form of long-term memory. This thesis project began by asking whether the four different CPEB genes contain the sequences found in a novel class of yeast prion-like proteins. We found that relative to the entire proteome, CPEB2-4 are rich in prion-like sequences. CPEB2 stood out with the highest degree of similarity to other known prion-like proteins. Further, the CPEB2 prion-like domain is encoded by exon 1, and the CPEB2-204 isoform contains this sequence. In the initial biochemical and immunofluorescent experiments we show that CPEB2 forms SDS-resistant higher order structures and aggregates in both cultured tissue cells and primary neuronal cultures.

Based on these findings, we generated an isoform specific CPEB2 knockout model that specifically lacked the exon 1 containing the putative prion-domain (CPEB2 $PD^{-/-}$). Our biochemical studies reveal that the CPEB2 PD-/- mice produce a truncated *CPEB2* transcript and protein. Indeed, using CPEB2 $PD^{-/-}$ P5 brain samples, we observed a protein band that likely corresponds to the smallest endogenous CPEB2 isoform (CPEB2-202). The presence of both CPEB2 mRNA transcripts and proteins suggests the CPEB2 $PD^{-/-}$ is a specific isoform knockout. Despite previous observations that a global knockout of all CPEB2 isoforms is lethal in the perinatal period, global CPEB2 PD knockout mice are viable and healthy (Lai et al., 2016). We conclude that the sequence encoded by CPEB2 exon 1 is not required for CPEB2 functions critical for development.

An inadvertent finding is that this smallest CPEB2 isoform is likely required to sustain life in early development, via an unknown mechanism. Death of complete CPEB2 knockout mice is attributed to severe bronchoconstriction due to hyper-activation of parasympathetic neurons (Lai et al., 2016). As discussed in more detail in Chapter 1, these investigators provided evidence to support a mechanism whereby CPEB2 represses the translation of choline acetyltransferase (ChAT), and hyper-activation of parasympathetic neurons ensues. Our results suggest that CPEB2-dependent life-sustaining pathways depend on the shorter CPEB2-202, not the full-length CPEB2-204 removed in the CPEB2 PD KO model.

To date, removal of CPEB2 alters the level of at least three different proteins studied: 1) global CPEB2 knockout increases the ChAT expression, 2) forebrain restricted CPEB2 removal activates GRASP1 expression, and 3) removal of CPEB-204 (exon 1 and the prion-like domain) increases CAMKIIa expression. Furthermore, CPEB2 binds to each of the mRNAs transcripts of ChAT, GRASP1, and CAMKIIa. However, because we have not demonstrated *in-vitro* that CPEB2 directly regulates CAMKIIa, we cannot exclude the possibility that CAMKIIa expression is dysregulated due to other changes inside the neuron. It should be noted that the forebrain restricted CPEB2 knockouts do not have changes in CAMKIIa expression (Lu et al., 2017). In our model, increased CAMKIIa expression seems to ensue from the absence of the CPEB2-204, not GRASP1 loss.

It has been proposed CPE-mediated translation is regulated by the number of CPEs in the 3'UTR. In *Xenopus*, CPEB1-dependent translation of cyclin B is modulated by altering the position and number of CPEs (Pique, Lopez, Foissac, Guigo, & Mendez, 2008). The findings presented in this thesis introduces another layer of translational regulation in the nervous system by these regulatory proteins, whereby distinct CPEB2 isoforms modulate translation of different

target mRNAs. Because CaMKIIa expression is enhanced in the CPEB2 PD$^{-/-}$, we conclude that the full-length CPEB2-204 isoform containing exon 1 is necessary at least for the regulation of CamKIIa expression. Correspondingly, CPEB2-202 is required for survival during the neonatal period. These findings suggest a model in which individual CPEB2 isoforms differentially regulate translation either by binding different targets or by differential time expression or cell specific expression.

It is intriguing to consider our findings in conjunction with results demonstrating that alternative-splicing regulates the expression of protein isoforms in a tissue specific manner (Jensen et al., 2000). One possible mechanism to account for differential expression of CPEB2 isoforms is by the splicing regulatory protein, Nova-1. CPEB2 contains a Nova-1 binding motif in the sequence encoded by exon 1. Nova-1 is an RNA-binding protein that is developmentally expressed in a subset of neurons in the brainstem, hypothalamus, and spinal cord (Buckanovich, Posner, & Darnell, 1993). It has been shown that Nova-1 is a splicing factor that promotes alternative splicing by binding to the pre-mRNA's containing a Nova binding site and recruiting the spliceosomal complex (Ule et al., 2006). It remains to be determined whether CPEB2 is regulated by Nova-1. However, the possibility is consistent with the observation that juvenile and adult neurons and glia in the hippocampus express different combinations of the CPEB2 isoforms (Turimella et al., 2015). Considering that many genes contain binding sites for CPEB2 in their 3' UTRs and that CPEB2 is required for different functions, it is likely that CPEB2 expression is highly regulated (Chen & Huang, 2012; Chen et al., 2015; Lai et al., 2016; Lu et al., 2017). Future experiments *in-vivo* are needed to determine if CPEB2 cell-specific expression is a mechanism by which districted isoform expression of CPEB2 works to mediate translational regulation.

Our findings also demonstrate that CPEB2-204 is critical for synaptic plasticity and long-term memory. While it was previous established that forebrain restricted removal of CPEB2 is required for LTP and long-term memory, the results in this thesis provide the novel insight that the CPEB2-204 isoform containing exon 1 and its prion-like domain are critical for this phenotype. The CPEB2 $PD^{-/-}$ model has severely disrupted PPF and LTP in organotypic hippocampal slices isolated from young mice. In line with the loss of PPF and reduction in LTP, CPEB2 $PD^{-/-}$ mice show contextual and spatial learning disruptions at a young age. Therefore, we conclude that full-length, oligomeric, CPEB2 plays a critical functional role in the regulation synaptic plasticity and the formation of long-term memory.

A primary objective of this thesis was to explore whether other CPEB family members use prion-like mechanisms for their function as observed with CPEB3. We performed experiments to determine if CPEB2-204 is a putative prion-like protein. Using SDS-AGE shows that full-length CPEB2 forms SDS-resistant oligomers that are resistant to reduction by DTT. The oligomers are present throughout the lifespan and localize to the synapse. In contrast, when the prion-like domain of CPEB2 encoded within exon 1 is removed, the oligomers are no longer evident. This implies that the protein sequence encoded by exon 1 is required for the formation of CPEB2 high-order assemblies. Following these observations, we propose that CPEB2 is putative-prion like protein. While further study is required, we show clearly that, paralleling prion-like proteins, CPEB2 forms higher order structures *in-vivo*.

What is the function of CPEB2 oligomers? It has been proposed similar structures serve as synaptic tags that are induced with neuronal activity. Best studied for the synaptic protein CPEB/Orb2 in *Drosophila*, in its monomeric state Orb2 acts to repress genes required for synaptic growth. Upon stimulation Orb2 converts into its prion-like oligomer conformation and

switches from a translational repressor to a translational activator (Khan et al., 2015; L. Li et al., 2016; Majumdar et al., 2012). The prion-like conformation of Orb2 induces the conversion of other monomeric Orb2 protein into prion-like states, leading to the model in which the amyloidogenic Orb2 functions as a synaptic tag at activated synapses due to oligomers ability to self-perpetuate and maintain synapses for long period of time. The significance of this oligomeric conversion becomes clear when Orb2, a protein whose function is required for long-term memory, is restricted to its monomeric state. Several experiments show that flies cannot form long term memories if Orb2 cannot form oligomers either by reducing its rate of oligomeric conversion, selectively cleaving the oligomeric protein, or by removing the prion-like domain from the endogenous locus, (Keleman et al., 2007; Majumdar et al., 2012). Given these findings, it was concluded that prion-like oligomers are critical for Orb2's role in memory.

Our results demonstrate CPEB2 meets several criteria shared with other established prion-like proteins, 1) CPEB2 forms SDS-resistant oligomers, 2) CPEB2 oligomers are present at the synapse, 3) CPEB2 oligomers associate with Q/N rich sequences, and 4) CPEB2 depends on the prion-like domain to fulfill its role in synaptic plasticity and long-term memory. An important limitation in our experiments is they did not discern whether the prion-domain is specifically required for LTP and memory, since exon 1 may be involved in other necessary functions. Intriguingly, the role of full-length CPEB2 in memory is clearly different from those of CPEB3 and Orb2. Despite that CPEB3 and Orb2 are required for the maintenance of memory, our results show CPEB2 $PD^{-/-}$ mice form as stable a memory as wild-type mice in contextual fear conditioning experiments. Conversely, in this task CPEB2 PD $KO^{-/-}$ mice do not form as strong of a memory as wild-type mice. This suggests CPEB2 and CPEB3 are required at different phases of memory formation. In summary, we present that CPEB2-204 is an essential

isoform required for the formation of LTP and long-term contextual memory in young mice, and CPEB2-204 is a strong candidate for further study as a functional prion-like protein in memory.

Future directions

Uncovering new gene pathways associated with CPEB2

One of our ongoing studies is analyzing the effect of removing CPEB2 from the nervous system on the translatome. The thesis demonstrates CPEB2 associates with translating mRNAs. To determine which RNAs CPEB2 regulates, we plan to isolate the polysome bound mRNAs from both wild-type and CPEB2 $PD^{-/-}$ mice. The RNAs found in these fractions will be evaluated by next-generation RNA sequencing (Hitzemann et al., 2014). These experiments will provide additional insights on the translational changes that emerge as a consequence of loss of full-length CPEB2. We expect that comparing these two genotypes will reveal which changes in gene expression or pathways associated with synaptic plasticity and long-term memory, with the potential to uncover new translation changes not previously associated with synaptic plasticity.

Because synaptic plasticity the CPEB2 $PD^{-/-}$ synaptic deficits are restricted to young mice, we will compare these results with RNA-sequencing analysis of polysome mRNA on six-month-old wild-type and CPEB2 mice. This additional analysis is designed to uncover changes between the young and adult CPEB2 $PD^{-/-}$ mice without LTP deficits. The goal is to identify if particular translational changes are associated with the recovery of LTP. One caveat of this experiment is that translational changes associated with normal aging, which will need to be discerned. However, with inclusion of the wild-type mice dataset, we hope to isolate the aging induced translational changes from the CPEB2-dependent changes.

CPEB2's role in memory

Our initial studies establish that CPEB2 is required for the formation of long-term memory. Moving forward there are two important questions to answer, 1) does long-term memory recover with age and, 2) during which phase of memory formation is CPEB2 necessary? Due to the fact that LTP and PPF recover by six months in CPEB2 $PD^{-/-}$ mice, we will assay the ability of aged CPEB2 $PD^{-/-}$ mice to form long-term memory using the CFC. Our hypothesis is that CFC memory will recover. Establishing this will allow us to make better comparisons between the transcriptional pathways observed in the CPEB2 $PD^{-/-}$ mice. Second, we plan to evaluate when CPEB2 expression is necessary for long-term memory formation. The approach will build on our previous genetic manipulation of removing exon 1 from CPEB2 by using a conditional CPEB2 knockout mouse model with LoxP sites in the intronic regions flanking exon 1. This model has been established by our laboratory. Using this model, we can test when CPEB2 expression is necessary for memory by selectively removing CPEB2, either during or after training. Results from the CPEB2 $PD^{-/-}$ model suggest CPEB2 is required for the initial memory formation. However, CPEB2 might be necessary for memory recall as well. To test this, we will remove CPEB2 expression by viral transduction in the hippocampus, either before or immediately after training. After the induction, memory paradigms can be used to test when CPEB2 expression is necessary for long-term memory formation. A potential confounds to this experiment is it that viral transduction requires days or weeks to occur, thus limiting to assaying the effect of removing only to the later time points. These experiments would help clarify the phases of memory CPEB2 is required.

CHAPTER 6: Materials and methods

PLAAC and SEQ analysis

PLAAC analysis of CPEB proteins and mouse proteome protein and was performed using the web based application (http://plaac.wi.mit.edu/). The PLAAC application scans the input protein sequence for amino acid compositions found in previously identified prion-like domains. Each amino acid is ranked for two states: prion-like or background using a hidden Markov model (Alberti et al., 2009). The states are based upon the amino acid frequencies found in the prion-like domains of yeast prion proteins. For our analysis, we set the minimum core length of the prion-like domain to 100 and scanned for prion-like sequence similarity using the S.Cerevisiae background frequencies. We input the mouse reference protein (UP000000589), containing all protein isoforms (including CPEB1-4) into the PLAAC application. From the output generated, we collected the LLR score (prion-like score) for each isoform, which is the log-likelihood ratios that the sequence is present in the prion-like state. Thus, the prion-like score indicates the degree to which the protein sequence is found in the prion-like state of the algorithm. The LLR score was used for further analysis. For identifying the particular sequence which contained a predicted prion-like domain in the different CPEB genes, PLAAC analysis was also used.

SEQ analysis was performed using SEQ plug-in filter of NCBI BLAST web based application (https://blast.ncbi.nlm.nih.gov/Blast.cgi). Using this approach, low-complexity sequence is identified based on the algorithm by Wootton and Federhen (Wootton and Federhen., 1993). The application identifies low-complexity sequence in the input sequence and scores the amount of lox-complexity sequence relative to total sequence length. For our analysis, we input the mouse

reference protein (UP000000589), containing all protein isoforms (including CPEB1-4) into the SEQ plug-in of NCBI BLAST. Each protein isoform was scored for the amount of lox-complexity sequence. The low-complexity score was used for further analysis.

Mice

The Institutional Animal Care and Use Committee approved all animal use protocols. All mice were housed and managed by Research Animal Resources under SPF conditions in an AAALAC-approved facility. CPEB2 PD mice were genotyped using the following primers: forward: ctgctgacgcacgttcc, reverse: caaactccagaagggaacaac. For behavioral experiments, CPEB2 $PD^{-/-}$ and wild-type littermates were obtained using heterozygous CPEB2 $PD^{+/-}$ crosses. For hippocampal cultures and slices, wild-type controls were obtained from crosses of CPEB2 $PD^{+/+}$, and experimental groups were obtained from crosses of CPEB2 $PD^{-/-}$.

Generation of CPEB $PD^{-/-}$ model

Guide RNAs were targeted against the 3' and 5' intronic regions of *CPEB2* exon 1. Guide RNA sequence was designed using CRISPR Design online tool (http://crispr.mit.edu/). The guide RNA sequences that were used are as follows: 5' –acggggtgcgtctcctgccg; 3' –ggagcgcccggggcgttcga. To ensure proper targeting to the CPEB2 introns, we first PCR amplified (Q5 Hotstart HiFi, New England Biosciences Cat No. M0493L, Ipswich, Massachusetts) the region surrounding each of the guide sites using the following primers pairs 5' ctgctgacgcacgttcc and 3' caaactccagaagggaacaac. The PCR product was cleaned and sequenced using the same primers that were used in the amplification. The guide sites were confirmed in the sequence, and there was no evidence of endogenous SNPs that would prevent target binding. The guide

sequences where then ordered as synthesized oligonucleotides (IDT) and cloned into the pSpCas9 plasmid (Addgene: px330) and sequence verified. The guide plasmids were then injected at (3ng/ul) into single cell F1c embryos, implanted into pseudo pregnant females (strain: CBA/CaJ x C57BL/10), and allowed to develop to term. Once mice were born and weaned tail samples were taken. Genomic DNA from tail samples were purified in a Promega Maxwell 16 using the Tissue DNA Kit (Promega Cat No. AS1030, Madison, Wisconsin). PCR was performed using primer pairs 5' ctgctgacgcacgttcc and 3' gcccagctcaggacaaa to identify founders with a deletion of exon 1. Two mice were positive for a deletion that occurred from the cut site of the 5` guide to the cut site of the 3` guide (1690bp deletion). One of these founders transmitted the deletion to germline and produced positive F1 pups. This line established the CPEB2 PD mouse model.

RNA isolation

Total RNA was isolated from the whole brains using TRIzol reagent (Life Technologies Cat No.15596-018, Carlsbad, California). Brains were homogenized in 1ml TRIzol using motorized pestles for 1 minute each. RNA isolation was completed following manufacturers protocol. RNA pellet was resuspending in 50ul of RNAse-free water and used in the following cDNA synthesis protocol.

cDNA synthesis

cDNA synthesis was performed using PrimeScript First Strand cDNA Synthesis Kit (Takara Bio USA Cat no. 6110A, Mountain View, California) using random hexamers following manufacturers protocol. 1ug total RNA input was used in each cDNA synthesis reaction(50uM).

Reverse transcriptase coupled PCR (RT-PCR)

RT-PCR experiments were performed using cDNA synthesized from total brain mRNA. PCR was performed using Q5 Hotstart HiFi (New England Biosciences Cat no. M0493L, Ipswich, Massachusetts) following the manufactures protocol. To assay the presence of each exon in the CPEB2 $PD^{-/-}$ mice, PCR paired each of the following primer sequences: 5' cgcccgccatgaatttac, ccgccatgaatttacctcaac, gccgttctcgggtaatgttat, with 3' ctgcagtgcaccaactatct, cccataactccttgcatttaacatt, and gcttcacctccacacgttta.

Primary hippocampal cultures

Hippocampal cultures were generated by dissecting the hippocampus from E17.5 embryos in wild-type and CPEB2 $PD^{-/-}$ mice. Neurons were plated at 4-6 x 10^5 cells in 6 well plates with 25mm glass coverslips pretreated with poly-l-lysine. Neurons were grown in Neurobasal Media containing B27 supplement in a 37 °C, 5% CO_2 incubator. Fresh medium was supplemented every 2 days after plating. For transfection, wild-type neurons at DIV7-8 were transfected CPEB2-EGFP tagged contract or EGFP alone using CalPhos Mammalian Transfection Kit following manufactures protocol (Takara USA Biosciences cat. No 631313, Ipswich, Massachusetts). After 24 hours, neurons were immunostaining detailed below.

Immunostaining

Coverslips with hippocampal neurons were fixed in a 4% paraformaldehyde solution for 10 minutes at room temperature. Coverslips were washed with PBS and blocked using 10% goat serum in 0.1% Triton PBS. Following blocking coverslips were incubated with the primary

antibody against MAP2K (EMD Millipore Cat No. AB5622) in 0.1% Triton PBS containing 10% goat serum for overnight. Following incubation, coverslips were washed three times in PBS and incubated with secondary antibody (Alexa Fluor 568 anti-rabbit, Abcam Cat No. ab175471) for 24 hours. Coverslips were washed three times in PBS and mount onto charged slides (Colorfrost Plus, Fisher). Fluorescently labeled tissue was imaged using a confocal Zeiss inverted microscope.

Western blotting

Brain or tissue culture samples used for western blotting were flash frozen in liquid nitrogen. Samples were homogenized with a motorized pestle for 30 seconds using 1mL of TSM lysis buffer (10mm Tris-Cl, 100mm NaCl, 30mg MgCl) supplemented with Protease Inhibitor Cocktail (Complete Mini, EDTA-Free, Roche Cat No. 1183617001). All samples and solutions were kept on ice. Unless otherwise noted, lysates were centrifuged at 12,500 rpm for 10 minutes at 4ºC, and the supernatant was collected. The supernatant protein concentration was measured using BCA assay (Pierce Biotechnology, Waltham, MA). 4-12% SDS-PAGE gels (Invitrogen Cat No. NP0322BOX, Carlsbad, CA) were loaded with 10µg of protein and run in the ThermoFisher Scientific XCell Surelock Mini-cell (ThermoFisher Scientific Cat No. EI0002). Gels were transferred on PVDF membrane using Trans Blot Turbo transfer apparatus. Membranes were blocked with 5% milk in PBS+0.1% Tween-20 at 4ºC. Primary antibody incubation was always performed overnight and secondary antibody incubation was for 1 hour. Proteins were assayed by chemiluminescent detection using ECL Western Blotting Substrate (Pierce Cat No. 32106).

Semi-denaturing detergent-agarose gel electrophoresis (SDD-AGE)

For SDD-AGE analysis, the lysates were prepared using western blot protocol above. Differently, after determining protein concertation, the lysates the lysates were loaded onto a 1.5% agarose gel containing 1xTris base, acetic acid (TAE) and 0.1 % SDS. The gel was run in 1 x TAE with .1% SDS buffer at 100V, and by gravity transfer, blotted onto PDVF membrane.

Synaptic plasma membrane purification

Synaptic Plasma Membrane were purified from entire mouse brains from wild-type and CPEB2 $PD^{-/-}$ mice at 30 days of age (Bermejo, Milenkovic, Salahpour, & Ramsey, 2014). All of the following centrifugations were performed at 4ºC. Lysates were prepared by homogenizing 2 grams of fresh brain tissue in .32 M HEPES-buffered sucrose solution. The homogenized sample was centrifuged at 900 x g for 10 min and the supernatant was collected (S1). The pellet (P1) contained the nuclear fraction and was collected and stored. S1 was then centrifuged at 10,000 x G for 15 minutes and supernatant (S2) was collected and stored. The remaining pellet (P2) contained the crude synaptosomal fraction, and was resuspended in 4 ml of 0.32 M HEPE-buffer sucrose solution. After an additional 10,000 x g centrifugation for 10 minutes, the supernatant was removed (S2') and the remaining pellet (P2') was subjected to hypotonic shock by adding 4ml of ddH_20 and rotating for 30 minutes at 4ºC. After hypo-osmotic shock, the P2' fraction was centrifuge at 25,000 x g for 20 minutes at 4 °C. The crude vesicular fraction (S3) was removed and the synaptosomal membrane fraction (P3) was resuspended in 1ml of .32M HEPES-buffer sucrose solution. To enrich for the synaptic plasma membrane, the resuspended P3 was layered on top of a 1.2M/1.0M/0.8M discontinuous sucrose gradient and ultracentrifuged in a swinging bucket rotor SW41 at 150,000 x g for 2 hours. The interphase between 1.0 M and

1.2 M layers was collected and centrifuged again at 150,000 x g for 30 minutes. The final pellet (SPM) contained the synaptic plasma membrane and was resuspended in 300µl of 50 mM HEPES / 2 mM EDTA solution and collected for analysis.

Polysome profiling

For analysis of CPEB2 polysome association, lysates were prepared from brains collected from 3 months of age wild-type mice. Brains were homogenized with a motorized pestle for 30 seconds using 1mL of TSM lysis buffer (10mm Tris-Cl, 100mm NaCl, 30mg MgCl) supplemented with 1mm DTT, 200ug/mL cycloheximide, 5ul RNasin, 1% NP40, and Protease Inhibitor Cocktail (Complete Mini, EDTA-Free, Roche Cat No. 1183617001). For the EDTA treated lysates, EDTA was added to a final concentration of 10mM. Both control and EDTA treated lysates were then centrifuged at 12,500 rpm for 10 minutes at 4ºC, and the supernatant was collected. Using a Nanodrop, the total RNA in each lysate was measured by 260nm absorbance (OD_{260}). Each lysate was adjusted to a 20.0 OD_{260} and 1ml of lysate was layered onto a 7-47% sucrose gradient. The control sucrose gradients contained 15mM Tris-Hcl, 140mM NH_4Cl_4, and 10mM MgOAc. The EDTA sucrose gradients contained 15mM Tris-Hcl, 140mM NH_4Cl_4, 10mM EDTA. The gradients were ultracentrifuged in a swinging bucket rotor at 35,000 x g for 2 hours at 4ºC.

For fractionation and polysome profiling, the gradients were fractioned into 500ul fractions by bottom displacement using a Isco fractionator. The ribosomal profile was continuously monitored at OD_{260} during fractionation. The fractions were then TCA precipitated and used in subsequent SDS-PAGE analysis.

Antibodies used for western and SDD-AGE

Primary antibody: GRASP1 antibody polyclonal rabbit IgG (GeneTex Cat No. GTX122295, Irvine, California), Fragile X antibody monoclonal mouse IgG (EDM Millipore Cat No. MAB2160), SNAP25 antibody monoclonal mouse IgG (BD Biosciences Cat No. 610366), CaMKIIa antibody monoclonal mouse IgG (ThermoFisher Cat No. 13-7300), Synaptotagmin antibody monoclonal mouse IgG (BD Biosciences Cat No. 610433), phospho-CREB (Ser133) Antibody polyclonal rabbit IgG (EDM Millipore Cat No. 06-519), MAP2 antibody polyclonal rabbit IgG (EMD Millipore Cat No. AB5622), Actin antibody monoclonal mouse IgG (EMD Millipore Cat No. MAB1501), PSD95 antibody monoclonal mouse IgG (ThermoFisher Cat No. MA1-046), alpha-tubulin antibody monoclonal mouse (Sigma Cat no. T5168), GluR1 antibody monoclonal rabbit IgG (EDM Millipore Cat No. 04-855), rS6 antibody monoclonal mouse (Sigma Cat no. 74459). CPEB2 Antibody polyclonal guinea pig affinity purified was raised against the purified smallest CPEB2 isoform (CPEB2-204). CPEB2-204 was induced via IPTG induction in pLysS Singles™ Competent Cells. The antibody was affinity purified using the purified CPEB2 protein.

Secondary Antibody: Anti-Mouse IgG secondary antibody, HRP conjugated (ThermoFisher Cat No. 32430), Anti-Guinea Pig IgG secondary antibody, HRP conjugated (Sigma Cat No. A7289), Anti-rabbit IgG secondary antibody, HRP-conjugated (Cell Signaling Technologies Cat No. 7074).

Hippocampal electrophysiology

Hippocampal slice preparation: Coronal hippocampal slices (350 μm thick) were obtained from both males and females p15-30 and 6-8 months of age WT and CPEB2 $PD^{-/-}$ mice. Mice were decapitated and the brain was rapidly extracted and placed in ice-cold artificial cerebrospinal fluid (ACSF) that contained (in mM): NaCl 124, KCl 5, NaH_2PO_4 1.25, $MgSO_4$ 2, $NaHCO_3$ 26, $CaCl_2$ 2 and glucose 10, and was gassed with 95% O_2 / 5% CO_2 (pH = 7.3-7.4). Slices were obtained with a vibratome (leica VT1200S) and incubated in ACSF at room temperature for at least 1 h before use. Then, slices were transferred to an immersion recording chamber, superfused at 2 ml/min with gassed ACSF and visualized under an Olympus BX50WI microscope (Olympus Optical, Japan). Picrotoxin (50 μM) and CGP54626 (1 μM) were added to the bath solution to block $GABA_A$ and $GABA_B$ receptors, respectively.

Electrophysiology: Field excitatory postsynaptic potentials (fEPSP) were recorded from a recording pipette placed in the stratum radiatum and filled with ACSF. Signals were obtained with a EX-1 amplifier (Dagan Instruments, MN, US) with a 10 KHz sampling rate and filtered with a 3 Hz low pass filter and a 300 Hz high pass filter. The pCLAMP 10.4 (Axon instruments) software was used for stimulus generation, data display, acquisition and storage. fEPSPs were evoked at 0.33 Hz by stimulating the Schaffer collaterals with a bipolar stimulation electrode placed in the stratum radiatum. Input–output relatioships of fEPSPs were made by increasing stimulus intensities from 0 to 100 μA. Paired pulses (0.2 ms duration) were applied in the Schaffer collaterals with 25, 50, 75, 100, 200, 300 and 500 ms interpulse intervals and the paired-pulse ratio was calculated (PPR = 2^{nd} fEPSC slope/ 1^{st} fEPSC slope). For LTP induction a tetanic stimulation (4 trains at 100 Hz for 1 s; 30 s intervals) was applied in the Schaffer collaterals. fEPSC slope was

normalized to 10 min of baseline recording. The presence of LTP was determined by comparing the last 5 min of baseline with the last 5 min of recording.

Open field testing

For open field testing, mice were housed in their home cages and brought into the testing room 24 hours prior to the test. The chamber consisted of a 50cm x 50cm x 50 cm box made of transparent plastic. For the test, a single mouse was placed into the middle of the open field arena and allowed to freely roam for 30 minutes. During the test, a video camera recorded the entire duration of the test. After the trial, the mouse was removed from the arena and the apparatus was cleaned with 95% ethanol prior to adding the next subject. The mouse's position and movement was analyzed using the mouse behavioral software EthoVision XT (Noldus, Wageningen, The Netherlands).

Contextual fear conditioning

For the contextual fear conditioning test mice were housed in their home cages and brought into the testing room 24 hours prior to the test. For this assay 3 months of age wild-type and CPEB2 $PD^{-/-}$ mice were used. On day 1, mice were placed into the fear conditioning apparatus (a trough-shaped alley divided between a dark compartment and a light compartment) and permitted to explore the apparatus freely. Upon crossing into the dark compartment, a door is inserted to confine the mouse to that compartment and inescapable footshocks are delivered (up to two footshocks, 1.0 mA intensity, 1 s duration). After the shock, the mouse is removed from the apparatus and returned to their home cage. Retention was tested at the indicated time points by returning the mouse to the light compartment with free access to the entire apparatus. The mouse

was allowed to freely roam the apparatus for 10 minutes. The time it took for the mouse to first enter to the dark compartment (latency) was recorded by the experimenter.

Morris water maze

For the contextual fear conditioning test mice were housed in their home cages and brought into the testing room 24 hours prior to the test. For this assay 2-3 months of age wild-type and CPEB2 $PD^{-/-}$ mice were used. For the training days, the platform was accessible but submerged. A training trial consisted of placing a mouse into the water maze at one of the 4 different starting locations (randomized for each day). The mouse was allowed to freely explore the pool for two minutes, when the mouse reached the platform it was removed after 15 seconds. Each training phase consisted of 4 trials per day for 3 days. The probe trial was performed on the 4^{th} and 9^{th} day in the water maze with the platform removed. During the probe trial, the mouse was allowed to freely search the pool for 1 minute. During both the training and probe trials the mouse's positions and movement was recorded by video. The video was analyzed by using the mouse behavioral software EthoVision XT (Noldus).

Statistical analysis

Data are represented as mean ± standard error of the mean (SEM). Unless otherwise noted: data were compared using a two-way ANOVA with Bonferroni post hoc. Statistical differences were established as $P<0.05$ (*), $P<0.01$ (**) and $P<0.001$ (***).

APPENDIX 1

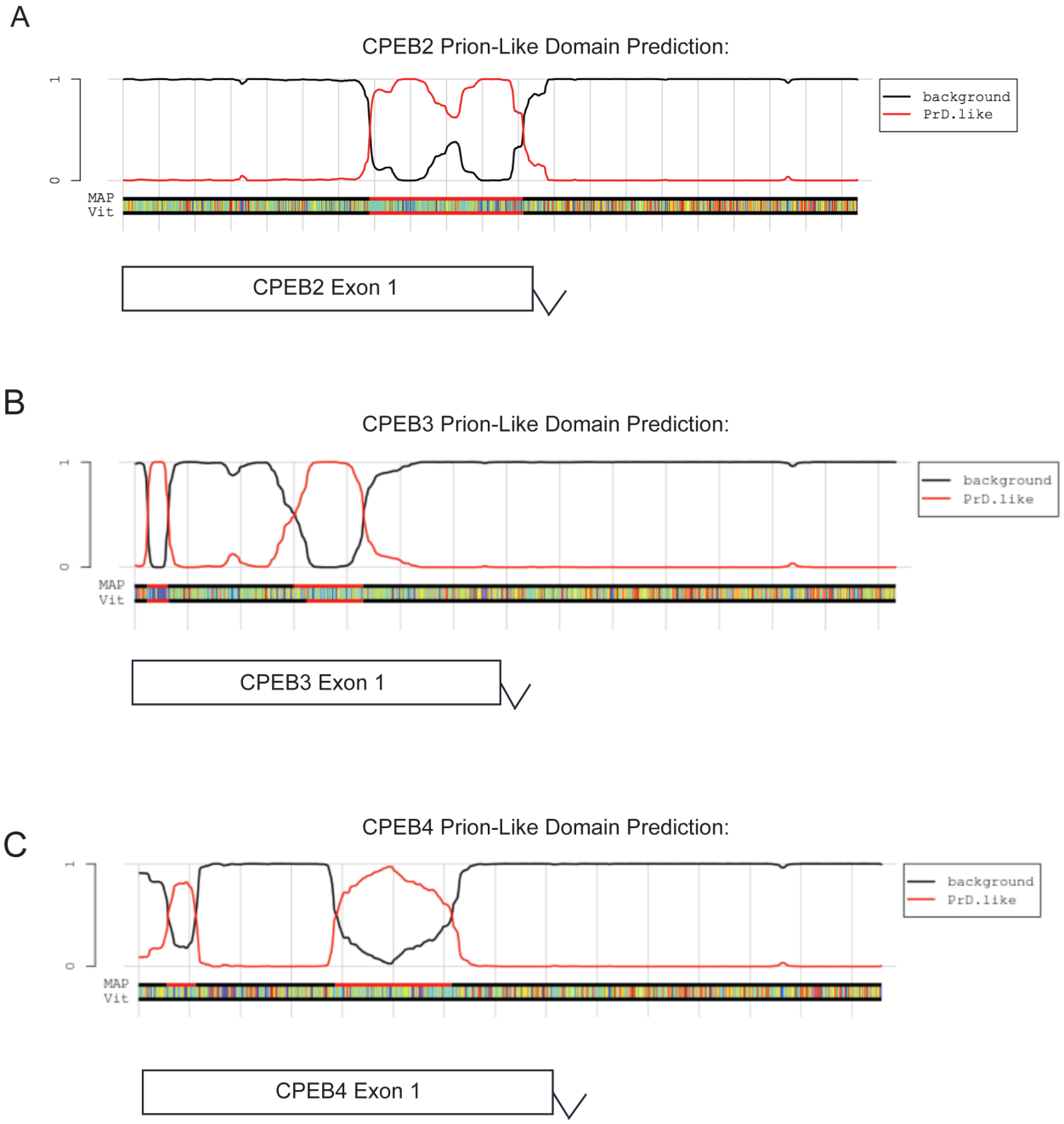

Appendix 1. PLAAC analysis of *CPEB*2-4. (A-C) Top: PLAAC output of longest Cpeb2-4 isoforms. Bottom: exon 1 of corresponding gene is aligned to PLAAC output. **(A)** *Cpeb2-204* analysis. (**B)** *Cpeb3-201* PLAAC analysis. **(C)** *Cpeb4-201* PLAAC analysis.

APPENDIX 2

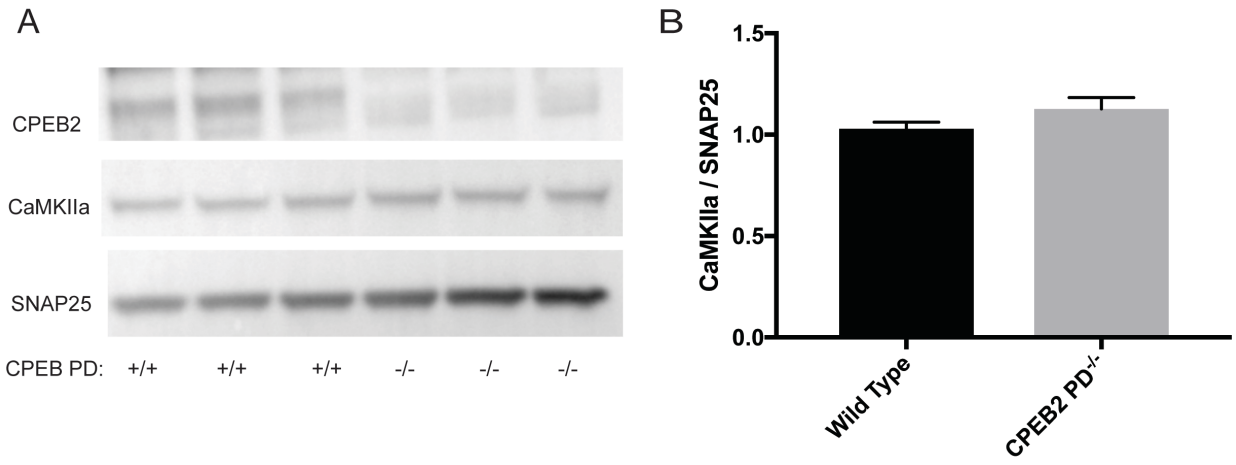

Appendix 2. No change in CaMKIIa expression in 6 - 7 months of age CPEB2 PD$^{-/-}$ mice. Whole brain lysates were used in western blots to evaluate levels of CPEB2 target proteins (n=3 for each target in wild-type and CPEB2 PD$^{-/-}$. **(A)** Western blot densitometry analysis shows no change in the expression CaMKIIa, between wild-type and CPEB2 PD$^{-/-}$ animals at 6-7 months of age (quantified in **B**). Data are represented as mean ± SEM. Student's t-test, * $p < 0.05$.

Bibliography

Aakalu, G., Smith, W. B., Nguyen, N., Jiang, C., & Schuman, E. M. (2001). Dynamic visualization of local protein synthesis in hippocampal neurons. *Neuron, 30*(2), 489-502.

Alarcon, J. M., Hodgman, R., Theis, M., Huang, Y. S., Kandel, E. R., & Richter, J. D. (2004). Selective modulation of some forms of schaffer collateral-CA1 synaptic plasticity in mice with a disruption of the CPEB-1 gene. *Learn Mem, 11*(3), 318-327. doi:10.1101/lm.72704

Alberini, C. M., & Kandel, E. R. (2014). The regulation of transcription in memory consolidation. *Cold Spring Harb Perspect Biol, 7*(1), a021741. doi:10.1101/cshperspect.a021741

Alberti, S., Halfmann, R., King, O., Kapila, A., & Lindquist, S. (2009). A systematic survey identifies prions and illuminates sequence features of prionogenic proteins. *Cell, 137*(1), 146-158. doi:10.1016/j.cell.2009.02.044

Anderson, P., & Kedersha, N. (2008). Stress granules: the Tao of RNA triage. *Trends Biochem Sci, 33*(3), 141-150. doi:10.1016/j.tibs.2007.12.003

Bacskai, B. J., Hochner, B., Mahaut-Smith, M., Adams, S. R., Kaang, B. K., Kandel, E. R., & Tsien, R. Y. (1993). Spatially resolved dynamics of cAMP and protein kinase A subunits in Aplysia sensory neurons. *Science, 260*(5105), 222-226.

Bagriantsev, S. N., Kushnirov, V. V., & Liebman, S. W. (2006). Analysis of amyloid aggregates using agarose gel electrophoresis. *Methods Enzymol, 412*, 33-48. doi:10.1016/S0076-6879(06)12003-0

Barnard, D. C., Ryan, K., Manley, J. L., & Richter, J. D. (2004). Symplekin and xGLD-2 are required for CPEB-mediated cytoplasmic polyadenylation. *Cell, 119*(5), 641-651. doi:10.1016/j.cell.2004.10.029

Berger-Sweeney, J., Zearfoss, N. R., & Richter, J. D. (2006). Reduced extinction of hippocampal-dependent memories in CPEB knockout mice. *Learn Mem, 13*(1), 4-7. doi:10.1101/lm.73706

Bermejo, M. K., Milenkovic, M., Salahpour, A., & Ramsey, A. J. (2014). Preparation of synaptic plasma membrane and postsynaptic density proteins using a discontinuous sucrose gradient. *J Vis Exp*(91), e51896. doi:10.3791/51896

Boehm, J., Ehrlich, I., Hsieh, H., & Malinow, R. (2006). Two mutations preventing PDZ-protein interactions of GluR1 have opposite effects on synaptic plasticity. *Learn Mem, 13*(5), 562-565. doi:10.1101/lm.253506

Buckanovich, R. J., Posner, J. B., & Darnell, R. B. (1993). Nova, the paraneoplastic Ri antigen, is homologous to an RNA-binding protein and is specifically expressed in the developing motor system. *Neuron, 11*(4), 657-672.

Cao, Q., & Richter, J. D. (2002). Dissolution of the maskin-eIF4E complex by cytoplasmic polyadenylation and poly(A)-binding protein controls cyclin B1 mRNA translation and oocyte maturation. *EMBO J, 21*(14), 3852-3862. doi:10.1093/emboj/cdf353

Casadio, A., Martin, K. C., Giustetto, M., Zhu, H., Chen, M., Bartsch, D., . . . Kandel, E. R. (1999). A transient, neuron-wide form of CREB-mediated long-term facilitation can be stabilized at specific synapses by local protein synthesis. *Cell, 99*(2), 221-237.

Chao, H. W., Tsai, L. Y., Lu, Y. L., Lin, P. Y., Huang, W. H., Chou, H. J., . . . Huang, Y. S. (2013). Deletion of CPEB3 enhances hippocampus-dependent memory via increasing

expressions of PSD95 and NMDA receptors. *J Neurosci, 33*(43), 17008-17022. doi:10.1523/JNEUROSCI.3043-13.2013
Chasse, H., Boulben, S., Costache, V., Cormier, P., & Morales, J. (2017). Analysis of translation using polysome profiling. *Nucleic Acids Res, 45*(3), e15. doi:10.1093/nar/gkw907
Chen, P. J., & Huang, Y. S. (2012). CPEB2-eEF2 interaction impedes HIF-1alpha RNA translation. *EMBO J, 31*(4), 959-971. doi:10.1038/emboj.2011.448
Chen, P. J., Weng, J. Y., Hsu, P. H., Shew, J. Y., Huang, Y. S., & Lee, W. H. (2015). NPGPx modulates CPEB2-controlled HIF-1alpha RNA translation in response to oxidative stress. *Nucleic Acids Res, 43*(19), 9393-9404. doi:10.1093/nar/gkv1010
Crawley, J. N. (2008). Behavioral phenotyping strategies for mutant mice. *Neuron, 57*(6), 809-818. doi:10.1016/j.neuron.2008.03.001
Curzon, P., Rustay, N. R., & Browman, K. E. (2009). Cued and Contextual Fear Conditioning for Rodents. In nd & J. J. Buccafusco (Eds.), *Methods of Behavior Analysis in Neuroscience*. Boca Raton (FL).
Darnell, J. C., Van Driesche, S. J., Zhang, C., Hung, K. Y., Mele, A., Fraser, C. E., . . . Darnell, R. B. (2011). FMRP stalls ribosomal translocation on mRNAs linked to synaptic function and autism. *Cell, 146*(2), 247-261. doi:10.1016/j.cell.2011.06.013
Derkatch, I. L., Bradley, M. E., Zhou, P., Chernoff, Y. O., & Liebman, S. W. (1997). Genetic and environmental factors affecting the de novo appearance of the [PSI+] prion in Saccharomyces cerevisiae. *Genetics, 147*(2), 507-519.
Derkatch, I. L., Chernoff, Y. O., Kushnirov, V. V., Inge-Vechtomov, S. G., & Liebman, S. W. (1996). Genesis and variability of [PSI] prion factors in Saccharomyces cerevisiae. *Genetics, 144*(4), 1375-1386.
Drisaldi, B., Colnaghi, L., Fioriti, L., Rao, N., Myers, C., Snyder, A. M., . . . Kandel, E. R. (2015). SUMOylation Is an Inhibitory Constraint that Regulates the Prion-like Aggregation and Activity of CPEB3. *Cell Rep, 11*(11), 1694-1702. doi:10.1016/j.celrep.2015.04.061
Ebbinghaus, H. (1885). *Über das Gedächtnis. Untersuchungen zur experimentellen Psychologie*. Leipzig,: Duncker & Humblot.
Fass, B., & Steward, O. (1983). Increases in protein-precursor incorporation in the denervated neuropil of the dentate gyrus during reinnervation. *Neuroscience, 9*(3), 653-664.
Fioravante, D., & Regehr, W. G. (2011). Short-term forms of presynaptic plasticity. *Curr Opin Neurobiol, 21*(2), 269-274. doi:10.1016/j.conb.2011.02.003
Fioriti, L., Myers, C., Huang, Y. Y., Li, X., Stephan, J. S., Trifilieff, P., . . . Kandel, E. R. (2015). The Persistence of Hippocampal-Based Memory Requires Protein Synthesis Mediated by the Prion-like Protein CPEB3. *Neuron, 86*(6), 1433-1448. doi:10.1016/j.neuron.2015.05.021
Fisher, S. A., Fischer, T. M., & Carew, T. J. (1997). Multiple overlapping processes underlying short-term synaptic enhancement. *Trends Neurosci, 20*(4), 170-177.
Flexner, J. B., Flexner, L. B., & Stellar, E. (1963). Memory in mice as affected by intracerebral puromycin. *Science, 141*(3575), 57-59.
Fortune, E. S., & Rose, G. J. (2001). Short-term synaptic plasticity as a temporal filter. *Trends Neurosci, 24*(7), 381-385.
Frey, S., Morris, R., & Petrides, M. (1997). A neuroanatomical method to assess the integrity of fibers of passage following ibotenate-induced damage to the central nervous system. *Neurosci Res, 28*(3), 285-288.

Frey, U., Krug, M., Reymann, K. G., & Matthies, H. (1988). Anisomycin, an inhibitor of protein synthesis, blocks late phases of LTP phenomena in the hippocampal CA1 region in vitro. *Brain Res, 452*(1-2), 57-65.

Frey, U., & Morris, R. G. (1997). Synaptic tagging and long-term potentiation. *Nature, 385*(6616), 533-536. doi:10.1038/385533a0

Ganusova, E. E., Ozolins, L. N., Bhagat, S., Newnam, G. P., Wegrzyn, R. D., Sherman, M. Y., & Chernoff, Y. O. (2006). Modulation of prion formation, aggregation, and toxicity by the actin cytoskeleton in yeast. *Mol Cell Biol, 26*(2), 617-629. doi:10.1128/MCB.26.2.617-629.2006

Giese, K. P., Fedorov, N. B., Filipkowski, R. K., & Silva, A. J. (1998). Autophosphorylation at Thr286 of the alpha calcium-calmodulin kinase II in LTP and learning. *Science, 279*(5352), 870-873.

Golding, G. B. (1999). Simple sequence is abundant in eukaryotic proteins. *Protein Sci, 8*(6), 1358-1361. doi:10.1110/ps.8.6.1358

Hagele, S., Kuhn, U., Boning, M., & Katschinski, D. M. (2009). Cytoplasmic polyadenylation-element-binding protein (CPEB)1 and 2 bind to the HIF-1alpha mRNA 3'-UTR and modulate HIF-1alpha protein expression. *Biochem J, 417*(1), 235-246. doi:10.1042/BJ20081353

Harrison, A. F., & Shorter, J. (2017). RNA-binding proteins with prion-like domains in health and disease. *Biochem J, 474*(8), 1417-1438. doi:10.1042/BCJ20160499

Hitzemann, R. (2000). Animal models of psychiatric disorders and their relevance to alcoholism. *Alcohol Res Health, 24*(3), 149-158.

Hitzemann, R., Darakjian, P., Walter, N., Iancu, O. D., Searles, R., & McWeeney, S. (2014). Introduction to sequencing the brain transcriptome. *Int Rev Neurobiol, 116*, 1-19. doi:10.1016/B978-0-12-801105-8.00001-1

Hoogenraad, C. C., Popa, I., Futai, K., Martinez-Sanchez, E., Wulf, P. S., van Vlijmen, T., . . . van der Sluijs, P. (2010). Neuron specific Rab4 effector GRASP-1 coordinates membrane specialization and maturation of recycling endosomes. *PLoS Biol, 8*(1), e1000283. doi:10.1371/journal.pbio.1000283

Huang, Y. S., Jung, M. Y., Sarkissian, M., & Richter, J. D. (2002). N-methyl-D-aspartate receptor signaling results in Aurora kinase-catalyzed CPEB phosphorylation and alpha CaMKII mRNA polyadenylation at synapses. *EMBO J, 21*(9), 2139-2148. doi:10.1093/emboj/21.9.2139

Huang, Y. S., Kan, M. C., Lin, C. L., & Richter, J. D. (2006). CPEB3 and CPEB4 in neurons: analysis of RNA-binding specificity and translational control of AMPA receptor GluR2 mRNA. *EMBO J, 25*(20), 4865-4876. doi:10.1038/sj.emboj.7601322

Huff, M. L., Emmons, E. B., Narayanan, N. S., & LaLumiere, R. T. (2016). Basolateral amygdala projections to ventral hippocampus modulate the consolidation of footshock, but not contextual, learning in rats. *Learn Mem, 23*(2), 51-60. doi:10.1101/lm.039909.115

Jensen, K. B., Dredge, B. K., Stefani, G., Zhong, R., Buckanovich, R. J., Okano, H. J., . . . Darnell, R. B. (2000). Nova-1 regulates neuron-specific alternative splicing and is essential for neuronal viability. *Neuron, 25*(2), 359-371.

Kaech, S., & Banker, G. (2006). Culturing hippocampal neurons. *Nat Protoc, 1*(5), 2406-2415. doi:10.1038/nprot.2006.356

Kandel, E. R., Dudai, Y., & Mayford, M. R. (2014). The molecular and systems biology of memory. *Cell, 157*(1), 163-186. doi:10.1016/j.cell.2014.03.001

Kang, H., & Schuman, E. M. (1996). A requirement for local protein synthesis in neurotrophin-induced hippocampal synaptic plasticity. *Science, 273*(5280), 1402-1406.
Keleman, K., Kruttner, S., Alenius, M., & Dickson, B. J. (2007). Function of the Drosophila CPEB protein Orb2 in long-term courtship memory. *Nat Neurosci, 10*(12), 1587-1593. doi:10.1038/nn1996
Kelleher, R. J., 3rd, Govindarajan, A., & Tonegawa, S. (2004). Translational regulatory mechanisms in persistent forms of synaptic plasticity. *Neuron, 44*(1), 59-73. doi:10.1016/j.neuron.2004.09.013
Khan, M. R., Li, L., Perez-Sanchez, C., Saraf, A., Florens, L., Slaughter, B. D., . . . Si, K. (2015). Amyloidogenic Oligomerization Transforms Drosophila Orb2 from a Translation Repressor to an Activator. *Cell, 163*(6), 1468-1483. doi:10.1016/j.cell.2015.11.020
Kim, H. J., Kim, N. C., Wang, Y. D., Scarborough, E. A., Moore, J., Diaz, Z., . . . Taylor, J. P. (2013). Mutations in prion-like domains in hnRNPA2B1 and hnRNPA1 cause multisystem proteinopathy and ALS. *Nature, 495*(7442), 467-473. doi:10.1038/nature11922
Kim, J. H., & Richter, J. D. (2006). Opposing polymerase-deadenylase activities regulate cytoplasmic polyadenylation. *Mol Cell, 24*(2), 173-183. doi:10.1016/j.molcel.2006.08.016
King, O. D., Gitler, A. D., & Shorter, J. (2012). The tip of the iceberg: RNA-binding proteins with prion-like domains in neurodegenerative disease. *Brain Res, 1462*, 61-80. doi:10.1016/j.brainres.2012.01.016
Krug, M., Lossner, B., & Ott, T. (1984). Anisomycin blocks the late phase of long-term potentiation in the dentate gyrus of freely moving rats. *Brain Res Bull, 13*(1), 39-42.
Kruttner, S., Stepien, B., Noordermeer, J. N., Mommaas, M. A., Mechtler, K., Dickson, B. J., & Keleman, K. (2012). Drosophila CPEB Orb2A mediates memory independent of Its RNA-binding domain. *Neuron, 76*(2), 383-395. doi:10.1016/j.neuron.2012.08.028
Kryndushkin, D. S., Alexandrov, I. M., Ter-Avanesyan, M. D., & Kushnirov, V. V. (2003). Yeast [PSI+] prion aggregates are formed by small Sup35 polymers fragmented by Hsp104. *J Biol Chem, 278*(49), 49636-49643. doi:10.1074/jbc.M307996200
Kumar, A. (2011). Long-Term Potentiation at CA3-CA1 Hippocampal Synapses with Special Emphasis on Aging, Disease, and Stress. *Front Aging Neurosci, 3*, 7. doi:10.3389/fnagi.2011.00007
Kurihara, Y., Tokuriki, M., Myojin, R., Hori, T., Kuroiwa, A., Matsuda, Y., . . . Uesugi, S. (2003). CPEB2, a novel putative translational regulator in mouse haploid germ cells. *Biol Reprod, 69*(1), 261-268. doi:10.1095/biolreprod.103.015677
Lai, Y. T., Su, C. K., Jiang, S. T., Chang, Y. J., Lai, A. C., & Huang, Y. S. (2016). Deficiency of CPEB2-Confined Choline Acetyltransferase Expression in the Dorsal Motor Nucleus of Vagus Causes Hyperactivated Parasympathetic Signaling-Associated Bronchoconstriction. *J Neurosci, 36*(50), 12661-12676. doi:10.1523/JNEUROSCI.0557-16.2016
Lancaster, A. K., Nutter-Upham, A., Lindquist, S., & King, O. D. (2014). PLAAC: a web and command-line application to identify proteins with prion-like amino acid composition. *Bioinformatics, 30*(17), 2501-2502. doi:10.1093/bioinformatics/btu310
Li, L., & Lindquist, S. (2000). Creating a protein-based element of inheritance. *Science, 287*(5453), 661-664.

Li, L., Sanchez, C. P., Slaughter, B. D., Zhao, Y., Khan, M. R., Unruh, J. R., . . . Si, K. (2016). A Putative Biochemical Engram of Long-Term Memory. *Curr Biol, 26*(23), 3143-3156. doi:10.1016/j.cub.2016.09.054

Li, Y. R., King, O. D., Shorter, J., & Gitler, A. D. (2013). Stress granules as crucibles of ALS pathogenesis. *J Cell Biol, 201*(3), 361-372. doi:10.1083/jcb.201302044

Lin, C. L., Evans, V., Shen, S., Xing, Y., & Richter, J. D. (2010). The nuclear experience of CPEB: implications for RNA processing and translational control. *RNA, 16*(2), 338-348. doi:10.1261/rna.1779810

Lisman, J., Malenka, R. C., Nicoll, R. A., & Malinow, R. (1997). Learning mechanisms: the case for CaM-KII. *Science, 276*(5321), 2001-2002.

Lu, W. H., Yeh, N. H., & Huang, Y. S. (2017). CPEB2 Activates GRASP1 mRNA Translation and Promotes AMPA Receptor Surface Expression, Long-Term Potentiation, and Memory. *Cell Rep, 21*(7), 1783-1794. doi:10.1016/j.celrep.2017.10.073

Mahmoud, G. S., & Grover, L. M. (2006). Growth hormone enhances excitatory synaptic transmission in area CA1 of rat hippocampus. *J Neurophysiol, 95*(5), 2962-2974. doi:10.1152/jn.00947.2005

Majumdar, A., Cesario, W. C., White-Grindley, E., Jiang, H., Ren, F., Khan, M. R., . . . Si, K. (2012). Critical role of amyloid-like oligomers of Drosophila Orb2 in the persistence of memory. *Cell, 148*(3), 515-529. doi:10.1016/j.cell.2012.01.004

Maletic-Savatic, M., Koothan, T., & Malinow, R. (1998). Calcium-evoked dendritic exocytosis in cultured hippocampal neurons. Part II: mediation by calcium/calmodulin-dependent protein kinase II. *J Neurosci, 18*(17), 6814-6821.

Martin, K. C., Casadio, A., Zhu, H., Yaping, E., Rose, J. C., Chen, M., . . . Kandel, E. R. (1997). Synapse-specific, long-term facilitation of aplysia sensory to motor synapses: a function for local protein synthesis in memory storage. *Cell, 91*(7), 927-938.

Martin, K. C., Michael, D., Rose, J. C., Barad, M., Casadio, A., Zhu, H., & Kandel, E. R. (1997). MAP kinase translocates into the nucleus of the presynaptic cell and is required for long-term facilitation in Aplysia. *Neuron, 18*(6), 899-912.

Mastushita-Sakai, T., White-Grindley, E., Samuelson, J., Seidel, C., & Si, K. (2010). Drosophila Orb2 targets genes involved in neuronal growth, synapse formation, and protein turnover. *Proc Natl Acad Sci U S A, 107*(26), 11987-11992. doi:10.1073/pnas.1004433107

Mathur, V., Taneja, V., Sun, Y., & Liebman, S. W. (2010). Analyzing the birth and propagation of two distinct prions, [PSI+] and [Het-s](y), in yeast. *Mol Biol Cell, 21*(9), 1449-1461. doi:10.1091/mbc.E09-11-0927

Matilla, A., Roberson, E. D., Banfi, S., Morales, J., Armstrong, D. L., Burright, E. N., . . . Matzuk, M. M. (1998). Mice lacking ataxin-1 display learning deficits and decreased hippocampal paired-pulse facilitation. *J Neurosci, 18*(14), 5508-5516.

Mayford, M., Siegelbaum, S. A., & Kandel, E. R. (2012). Synapses and memory storage. *Cold Spring Harb Perspect Biol, 4*(6). doi:10.1101/cshperspect.a005751

McGrew, L. L., Dworkin-Rastl, E., Dworkin, M. B., & Richter, J. D. (1989). Poly(A) elongation during Xenopus oocyte maturation is required for translational recruitment and is mediated by a short sequence element. *Genes Dev, 3*(6), 803-815.

Meiri, N., Sun, M. K., Segal, Z., & Alkon, D. L. (1998). Memory and long-term potentiation (LTP) dissociated: normal spatial memory despite CA1 LTP elimination with Kv1.4 antisense. *Proc Natl Acad Sci U S A, 95*(25), 15037-15042.

Mendez, R., Murthy, K. G., Ryan, K., Manley, J. L., & Richter, J. D. (2000). Phosphorylation of CPEB by Eg2 mediates the recruitment of CPSF into an active cytoplasmic polyadenylation complex. *Mol Cell, 6*(5), 1253-1259.

Michelitsch, M. D., & Weissman, J. S. (2000). A census of glutamine/asparagine-rich regions: implications for their conserved function and the prediction of novel prions. *Proc Natl Acad Sci U S A, 97*(22), 11910-11915. doi:10.1073/pnas.97.22.11910

Miller, S., Yasuda, M., Coats, J. K., Jones, Y., Martone, M. E., & Mayford, M. (2002). Disruption of dendritic translation of CaMKIIalpha impairs stabilization of synaptic plasticity and memory consolidation. *Neuron, 36*(3), 507-519.

Miniaci, M. C., Kim, J. H., Puthanveettil, S. V., Si, K., Zhu, H., Kandel, E. R., & Bailey, C. H. (2008). Sustained CPEB-dependent local protein synthesis is required to stabilize synaptic growth for persistence of long-term facilitation in Aplysia. *Neuron, 59*(6), 1024-1036. doi:10.1016/j.neuron.2008.07.036

Minshall, N., Reiter, M. H., Weil, D., & Standart, N. (2007). CPEB interacts with an ovary-specific eIF4E and 4E-T in early Xenopus oocytes. *J Biol Chem, 282*(52), 37389-37401. doi:10.1074/jbc.M704629200

Miyamoto, E. (2006). Molecular mechanism of neuronal plasticity: induction and maintenance of long-term potentiation in the hippocampus. *J Pharmacol Sci, 100*(5), 433-442.

Montkowski, A., & Holsboer, F. (1997). Intact spatial learning and memory in transgenic mice with reduced BDNF. *Neuroreport, 8*(3), 779-782.

Morris, R. (1984). Developments of a water-maze procedure for studying spatial learning in the rat. *J Neurosci Methods, 11*(1), 47-60.

Nakazawa, K., Quirk, M. C., Chitwood, R. A., Watanabe, M., Yeckel, M. F., Sun, L. D., . . . Tonegawa, S. (2002). Requirement for hippocampal CA3 NMDA receptors in associative memory recall. *Science, 297*(5579), 211-218. doi:10.1126/science.1071795

Novoa, I., Gallego, J., Ferreira, P. G., & Mendez, R. (2010). Mitotic cell-cycle progression is regulated by CPEB1 and CPEB4-dependent translational control. *Nat Cell Biol, 12*(5), 447-456. doi:10.1038/ncb2046

Oesch, B., Westaway, D., Walchli, M., McKinley, M. P., Kent, S. B., Aebersold, R., . . . et al. (1985). A cellular gene encodes scrapie PrP 27-30 protein. *Cell, 40*(4), 735-746.

Pan, K. M., Baldwin, M., Nguyen, J., Gasset, M., Serban, A., Groth, D., . . . et al. (1993). Conversion of alpha-helices into beta-sheets features in the formation of the scrapie prion proteins. *Proc Natl Acad Sci U S A, 90*(23), 10962-10966.

Pavlopoulos, E., Trifilieff, P., Chevaleyre, V., Fioriti, L., Zairis, S., Pagano, A., . . . Kandel, E. R. (2011). Neuralized1 activates CPEB3: a function for nonproteolytic ubiquitin in synaptic plasticity and memory storage. *Cell, 147*(6), 1369-1383. doi:10.1016/j.cell.2011.09.056

Phillips, R. G., & LeDoux, J. E. (1992). Differential contribution of amygdala and hippocampus to cued and contextual fear conditioning. *Behav Neurosci, 106*(2), 274-285.

Pique, M., Lopez, J. M., Foissac, S., Guigo, R., & Mendez, R. (2008). A combinatorial code for CPE-mediated translational control. *Cell, 132*(3), 434-448. doi:10.1016/j.cell.2007.12.038

Post, A. M., Weyers, P., Holzer, P., Painsipp, E., Pauli, P., Wultsch, T., . . . Lesch, K. P. (2011). Gene-environment interaction influences anxiety-like behavior in ethologically based mouse models. *Behav Brain Res, 218*(1), 99-105. doi:10.1016/j.bbr.2010.11.031

Prusiner, S. B. (1982). Novel proteinaceous infectious particles cause scrapie. *Science, 216*(4542), 136-144.

Prusiner, S. B. (1998). Prions. *Proc Natl Acad Sci U S A, 95*(23), 13363-13383.
Raveendra, B. L., Siemer, A. B., Puthanveettil, S. V., Hendrickson, W. A., Kandel, E. R., & McDermott, A. E. (2013). Characterization of prion-like conformational changes of the neuronal isoform of Aplysia CPEB. *Nat Struct Mol Biol, 20*(4), 495-501. doi:10.1038/nsmb.2503
Richter, J. D. (1999). Cytoplasmic polyadenylation in development and beyond. *Microbiol Mol Biol Rev, 63*(2), 446-456.
Rizzoli, S. O., & Betz, W. J. (2005). Synaptic vesicle pools. *Nat Rev Neurosci, 6*(1), 57-69. doi:10.1038/nrn1583
Rozov, A., & Burnashev, N. (1999). Polyamine-dependent facilitation of postsynaptic AMPA receptors counteracts paired-pulse depression. *Nature, 401*(6753), 594-598. doi:10.1038/44151
Rozov, A., Zilberter, Y., Wollmuth, L. P., & Burnashev, N. (1998). Facilitation of currents through rat Ca2+-permeable AMPA receptor channels by activity-dependent relief from polyamine block. *J Physiol, 511 (Pt 2)*, 361-377.
Sachs, A. B., Sarnow, P., & Hentze, M. W. (1997). Starting at the beginning, middle, and end: translation initiation in eukaryotes. *Cell, 89*(6), 831-838.
Salles, F. J., Lieberfarb, M. E., Wreden, C., Gergen, J. P., & Strickland, S. (1994). Coordinate initiation of Drosophila development by regulated polyadenylation of maternal messenger RNAs. *Science, 266*(5193), 1996-1999.
Shin, J., Salameh, J. S., & Richter, J. D. (2016). Impaired neurodevelopment by the low complexity domain of CPEB4 reveals a convergent pathway with neurodegeneration. *Sci Rep, 6*, 29395. doi:10.1038/srep29395
Si, K., Choi, Y. B., White-Grindley, E., Majumdar, A., & Kandel, E. R. (2010). Aplysia CPEB can form prion-like multimers in sensory neurons that contribute to long-term facilitation. *Cell, 140*(3), 421-435. doi:10.1016/j.cell.2010.01.008
Si, K., Giustetto, M., Etkin, A., Hsu, R., Janisiewicz, A. M., Miniaci, M. C., . . . Kandel, E. R. (2003). A neuronal isoform of CPEB regulates local protein synthesis and stabilizes synapse-specific long-term facilitation in aplysia. *Cell, 115*(7), 893-904.
Si, K., Lindquist, S., & Kandel, E. R. (2003). A neuronal isoform of the aplysia CPEB has prion-like properties. *Cell, 115*(7), 879-891.
Silva, A. J., Rosahl, T. W., Chapman, P. F., Marowitz, Z., Friedman, E., Frankland, P. W., . . . Bourtchuladze, R. (1996). Impaired learning in mice with abnormal short-lived plasticity. *Curr Biol, 6*(11), 1509-1518.
Silva, A. J., Stevens, C. F., Tonegawa, S., & Wang, Y. (1992). Deficient hippocampal long-term potentiation in alpha-calcium-calmodulin kinase II mutant mice. *Science, 257*(5067), 201-206.
Stebbins-Boaz, B., Cao, Q., de Moor, C. H., Mendez, R., & Richter, J. D. (1999). Maskin is a CPEB-associated factor that transiently interacts with elF-4E. *Mol Cell, 4*(6), 1017-1027.
Stephan, J. S., Fioriti, L., Lamba, N., Colnaghi, L., Karl, K., Derkatch, I. L., & Kandel, E. R. (2015). The CPEB3 Protein Is a Functional Prion that Interacts with the Actin Cytoskeleton. *Cell Rep, 11*(11), 1772-1785. doi:10.1016/j.celrep.2015.04.060
Steward, O., & Fass, B. (1983). Polyribosomes associated with dendritic spines in the denervated dentate gyrus: evidence for local regulation of protein synthesis during reinnervation. *Prog Brain Res, 58*, 131-136. doi:10.1016/S0079-6123(08)60013-8

Steward, O., & Levy, W. B. (1982). Preferential localization of polyribosomes under the base of dendritic spines in granule cells of the dentate gyrus. *J Neurosci, 2*(3), 284-291.
Tayler, K. K., Tanaka, K. Z., Reijmers, L. G., & Wiltgen, B. J. (2013). Reactivation of neural ensembles during the retrieval of recent and remote memory. *Curr Biol, 23*(2), 99-106. doi:10.1016/j.cub.2012.11.019
Telling, G. C., Parchi, P., DeArmond, S. J., Cortelli, P., Montagna, P., Gabizon, R., . . . Prusiner, S. B. (1996). Evidence for the conformation of the pathologic isoform of the prion protein enciphering and propagating prion diversity. *Science, 274*(5295), 2079-2082.
Theis, M., Si, K., & Kandel, E. R. (2003). Two previously undescribed members of the mouse CPEB family of genes and their inducible expression in the principal cell layers of the hippocampus. *Proc Natl Acad Sci U S A, 100*(16), 9602-9607. doi:10.1073/pnas.1133424100
Tsai, L. Y., Chang, Y. W., Lin, P. Y., Chou, H. J., Liu, T. J., Lee, P. T., . . . Huang, Y. S. (2013). CPEB4 knockout mice exhibit normal hippocampus-related synaptic plasticity and memory. *PLoS One, 8*(12), e84978. doi:10.1371/journal.pone.0084978
Turimella, S. L., Bedner, P., Skubal, M., Vangoor, V. R., Kaczmarczyk, L., Karl, K., . . . Theis, M. (2015). Characterization of cytoplasmic polyadenylation element binding 2 protein expression and its RNA binding activity. *Hippocampus, 25*(5), 630-642. doi:10.1002/hipo.22399
Ule, J., Stefani, G., Mele, A., Ruggiu, M., Wang, X., Taneri, B., . . . Darnell, R. B. (2006). An RNA map predicting Nova-dependent splicing regulation. *Nature, 444*(7119), 580-586. doi:10.1038/nature05304
Villalba, A., Coll, O., & Gebauer, F. (2011). Cytoplasmic polyadenylation and translational control. *Curr Opin Genet Dev, 21*(4), 452-457. doi:10.1016/j.gde.2011.04.006
Vorhees, C. V., & Williams, M. T. (2006). Morris water maze: procedures for assessing spatial and related forms of learning and memory. *Nat Protoc, 1*(2), 848-858. doi:10.1038/nprot.2006.116
Wang, H., Shimizu, E., Tang, Y. P., Cho, M., Kyin, M., Zuo, W., . . . Tsien, J. Z. (2003). Inducible protein knockout reveals temporal requirement of CaMKII reactivation for memory consolidation in the brain. *Proc Natl Acad Sci U S A, 100*(7), 4287-4292. doi:10.1073/pnas.0636870100
Wehner, J. M., & Radcliffe, R. A. (2004). Cued and contextual fear conditioning in mice. *Curr Protoc Neurosci, Chapter 8*, Unit 8 5C. doi:10.1002/0471142301.ns0805cs27
West, A. E., Griffith, E. C., & Greenberg, M. E. (2002). Regulation of transcription factors by neuronal activity. *Nat Rev Neurosci, 3*(12), 921-931. doi:10.1038/nrn987
Whittaker, V. P. (1993). Thirty years of synaptosome research. *J Neurocytol, 22*(9), 735-742.
Whittaker, V. P., Michaelson, I. A., & Kirkland, R. J. (1964). The separation of synaptic vesicles from nerve-ending particles ('synaptosomes'). *Biochem J, 90*(2), 293-303.
Wootton, J. C., & Federhen, S. (1996). Analysis of compositionally biased regions in sequence databases. *Methods Enzymol, 266*, 554-571.
Wu, L., Wells, D., Tay, J., Mendis, D., Abbott, M. A., Barnitt, A., . . . Richter, J. D. (1998). CPEB-mediated cytoplasmic polyadenylation and the regulation of experience-dependent translation of alpha-CaMKII mRNA at synapses. *Neuron, 21*(5), 1129-1139.
Wu, L. G., & Saggau, P. (1994). Presynaptic calcium is increased during normal synaptic transmission and paired-pulse facilitation, but not in long-term potentiation in area CA1 of hippocampus. *J Neurosci, 14*(2), 645-654.

Zamanillo, D., Sprengel, R., Hvalby, O., Jensen, V., Burnashev, N., Rozov, A., . . . Sakmann, B. (1999). Importance of AMPA receptors for hippocampal synaptic plasticity but not for spatial learning. *Science, 284*(5421), 1805-1811.

Zearfoss, N. R., Alarcon, J. M., Trifilieff, P., Kandel, E., & Richter, J. D. (2008). A molecular circuit composed of CPEB-1 and c-Jun controls growth hormone-mediated synaptic plasticity in the mouse hippocampus. *J Neurosci, 28*(34), 8502-8509. doi:10.1523/JNEUROSCI.1756-08.2008

Zucker, R. S., & Regehr, W. G. (2002). Short-term synaptic plasticity. *Annu Rev Physiol, 64*, 355-405. doi:10.1146/annurev.physiol.64.092501.114547